Supporting Information

Anion Recognition Using meta-Substituted Ureidocalix[4]arene Receptors

A. Surina,[a] J. Čejka,[b] K. Salvadori,[c,d] and P. Lhoták[a*]

[a] *Department of Organic Chemistry, University of Chemistry and Technology, Prague (UCTP), Technicka 5, 166 28 Prague 6, Czech Republic. E-mail: lhotakp@vscht.cz; Fax: +420-220444288; Tel: +420-220445055.*
[b] *Department of Solid State Chemistry, UCTP, 166 28 Prague 6, Czech Republic.*
[c] *Institute of chemical process fundamentals of Czech Academy of Sciences v.v.i., Rozvojová 135, Prague 6, 16502, Czech Republic.*
[d] *J. Heyrovský Institute of Physical Chemistry of Czech Academy of Sciences v.v.i., Dolejškova 2155/3, 182 23 Prague 8, Czech Republic.*

Table of Contents

1. Spectral characterization of compounds

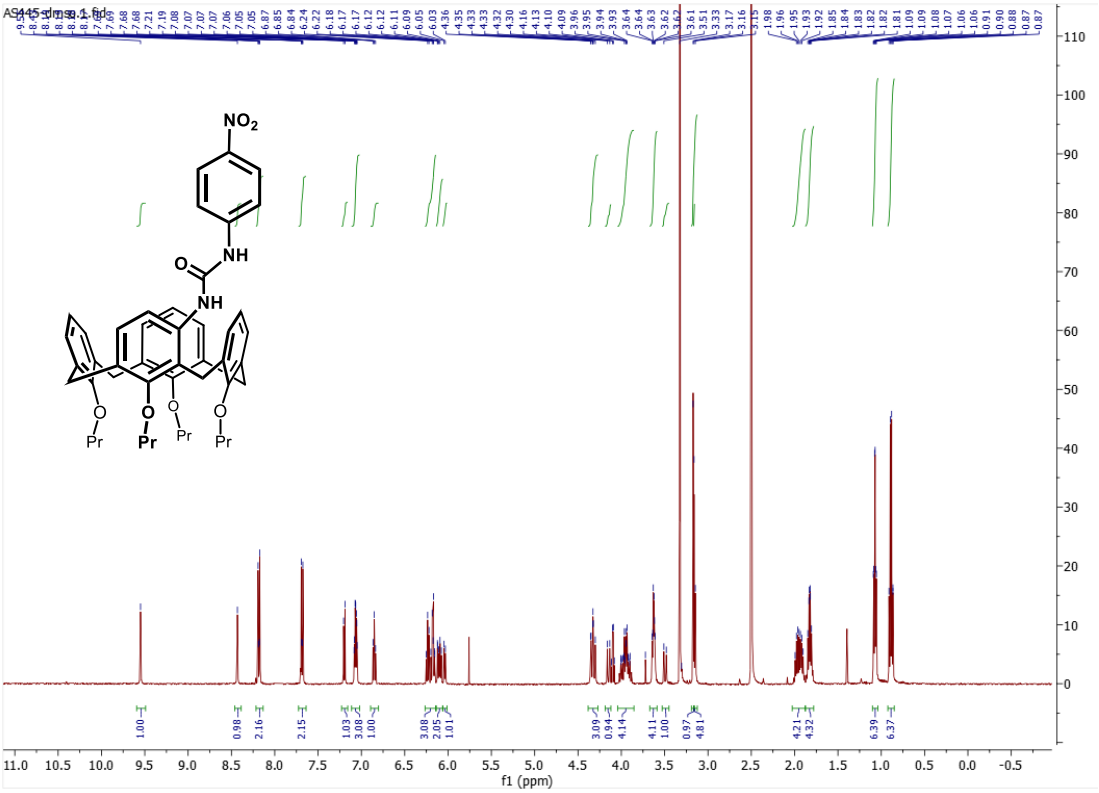

Fig. S1: ^{1}H NMR of compound **3a** (DMSO, 500 MHz, 298 K)

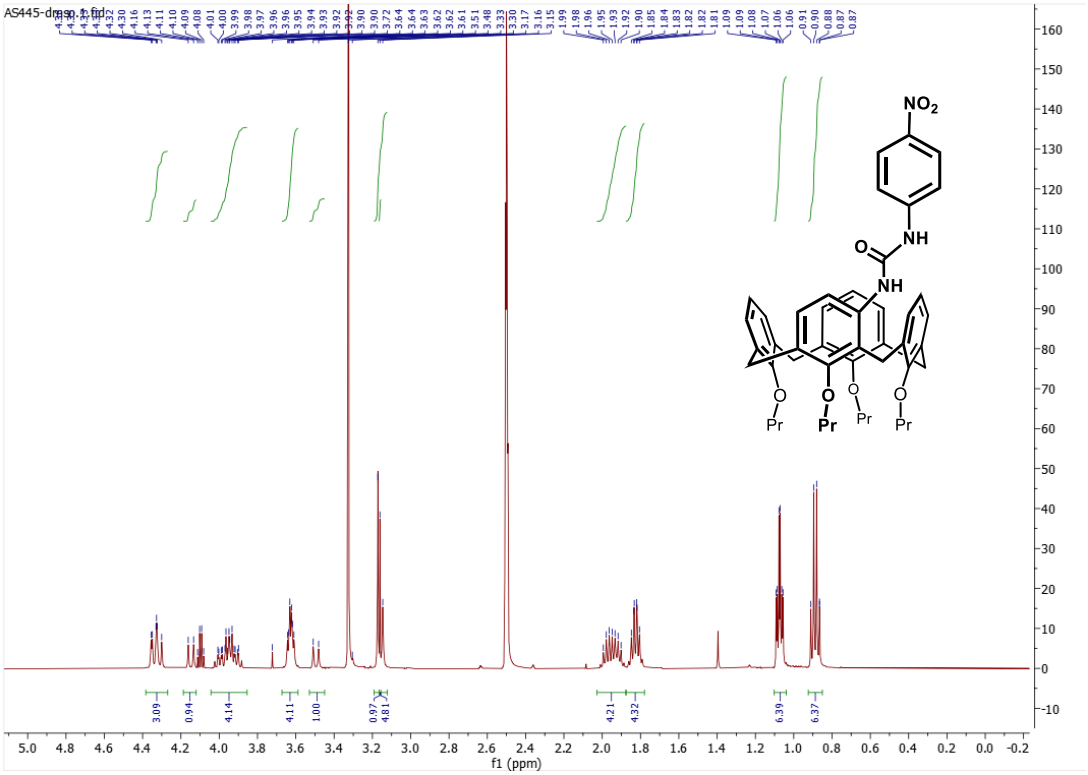

Fig. S2: ^{1}H NMR of compound **3a**, aliphatic region (DMSO, 500 MHz, 298 K)

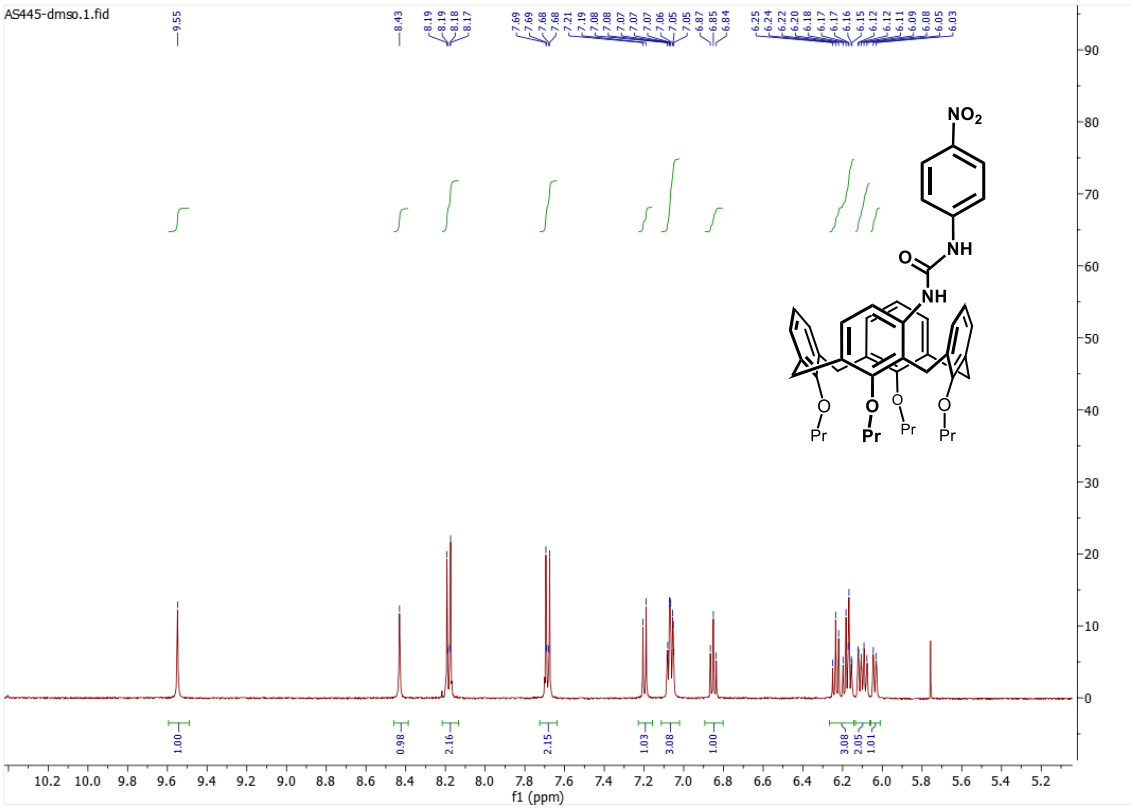

Fig. S3: ^{1}H NMR of compound **3a**, aromatic region (DMSO, 500 MHz, 298 K)

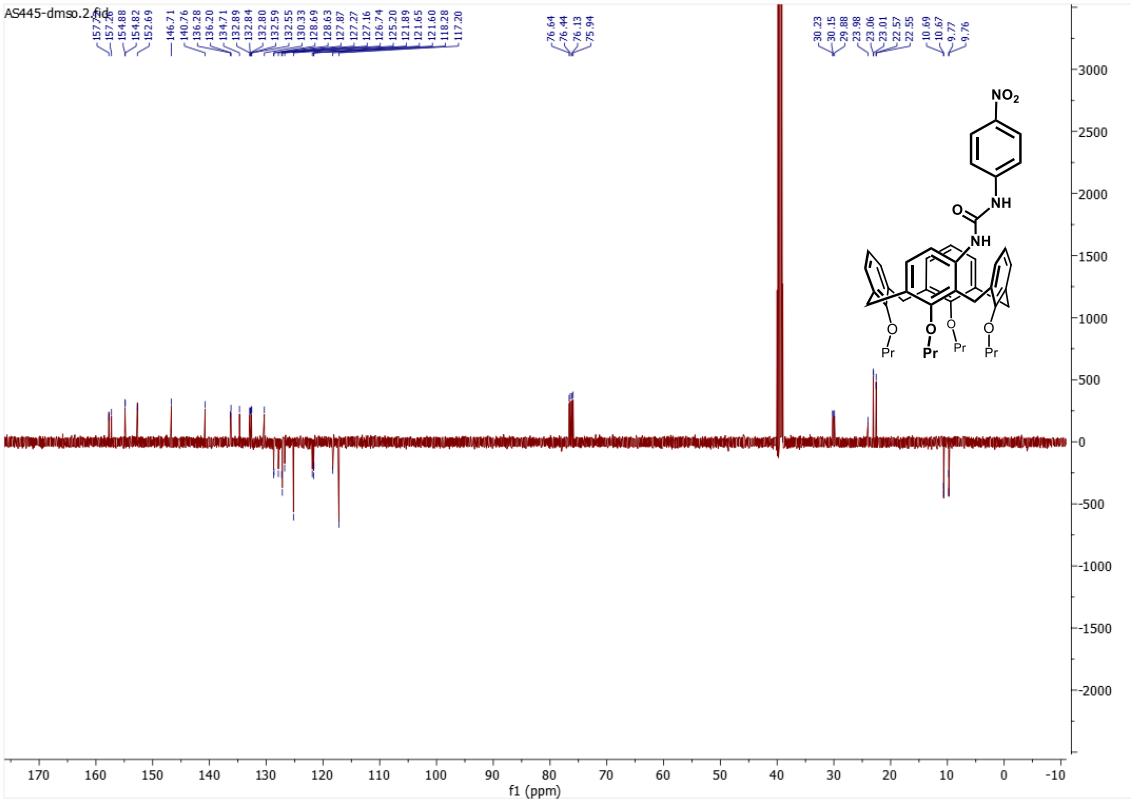

Fig. S4: ^{13}C(APT) NMR of compound **3a** (DMSO, 125 MHz, 298 K)

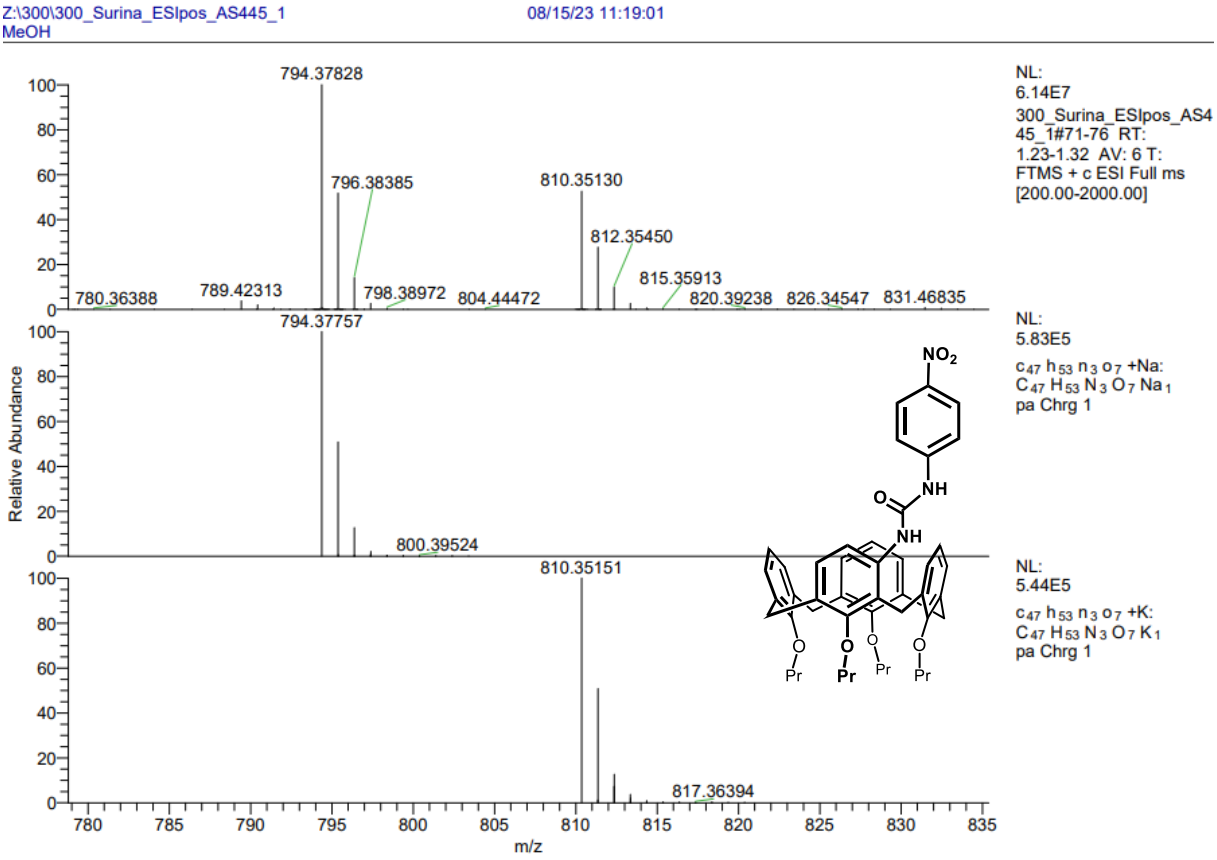

Fig. S5: HRMS (ESI) of compound **3a** calcd for $C_{47}H_{53}N_3O_7$ 794.3776 $[M+Na]^+$, found m/z 794.3783 $[M+Na]^+$.

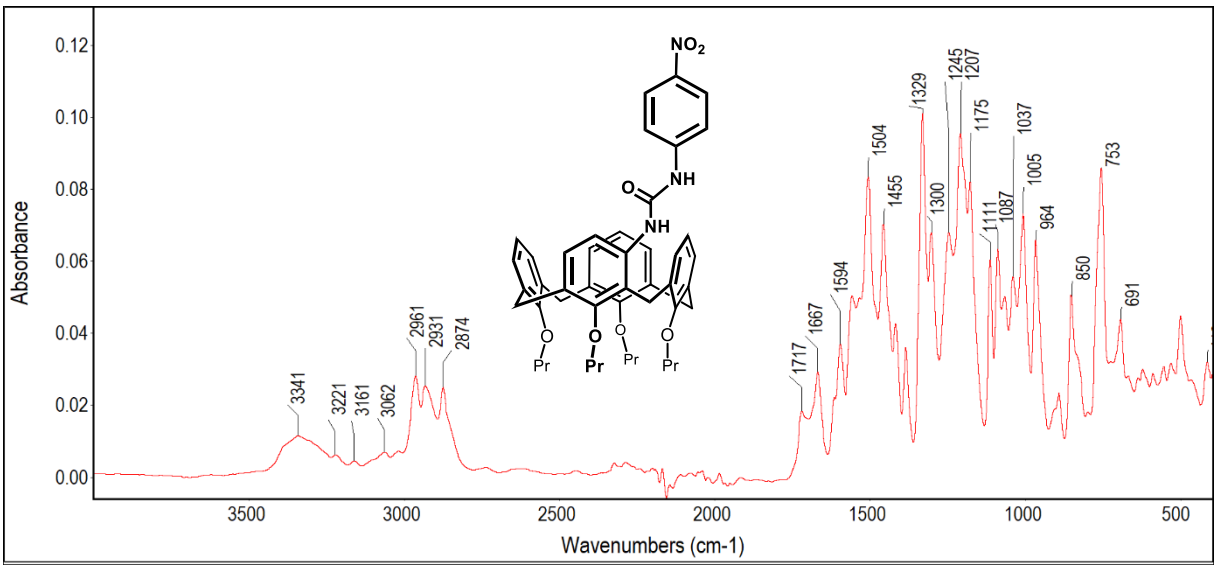

Fig. S6: IR spectrum of compound **3a** (ATR).

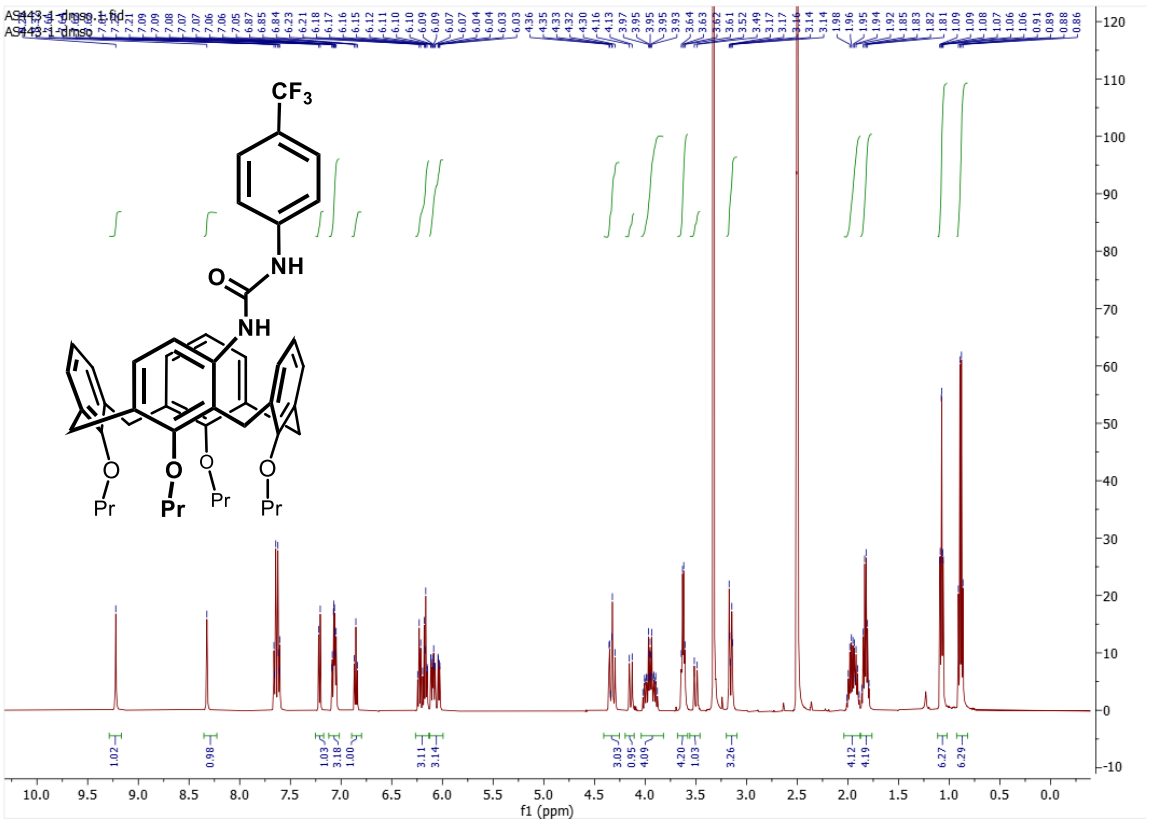

Fig. S7: ^{1}H NMR of compound **3b** (DMSO, 500 MHz, 298 K)

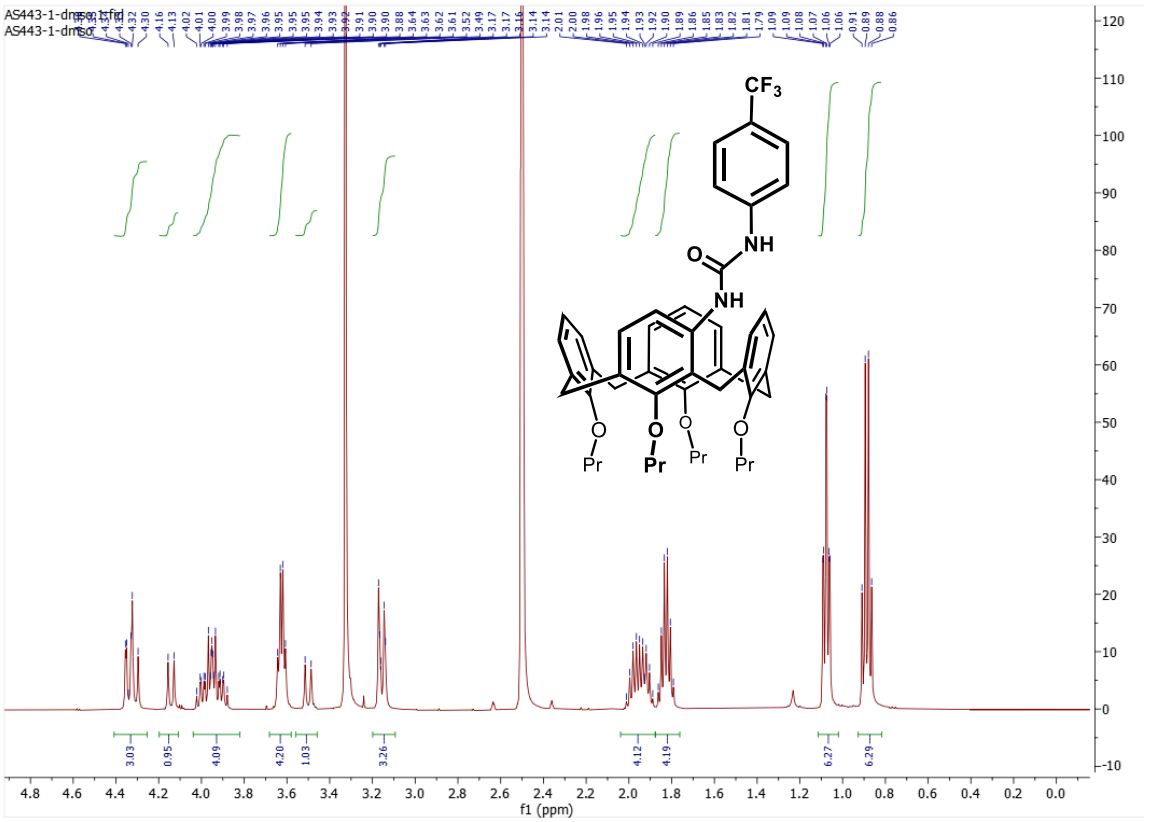

Fig. S8: ^{1}H NMR of compound **3b**, aliphatic region (DMSO, 500 MHz, 298 K)

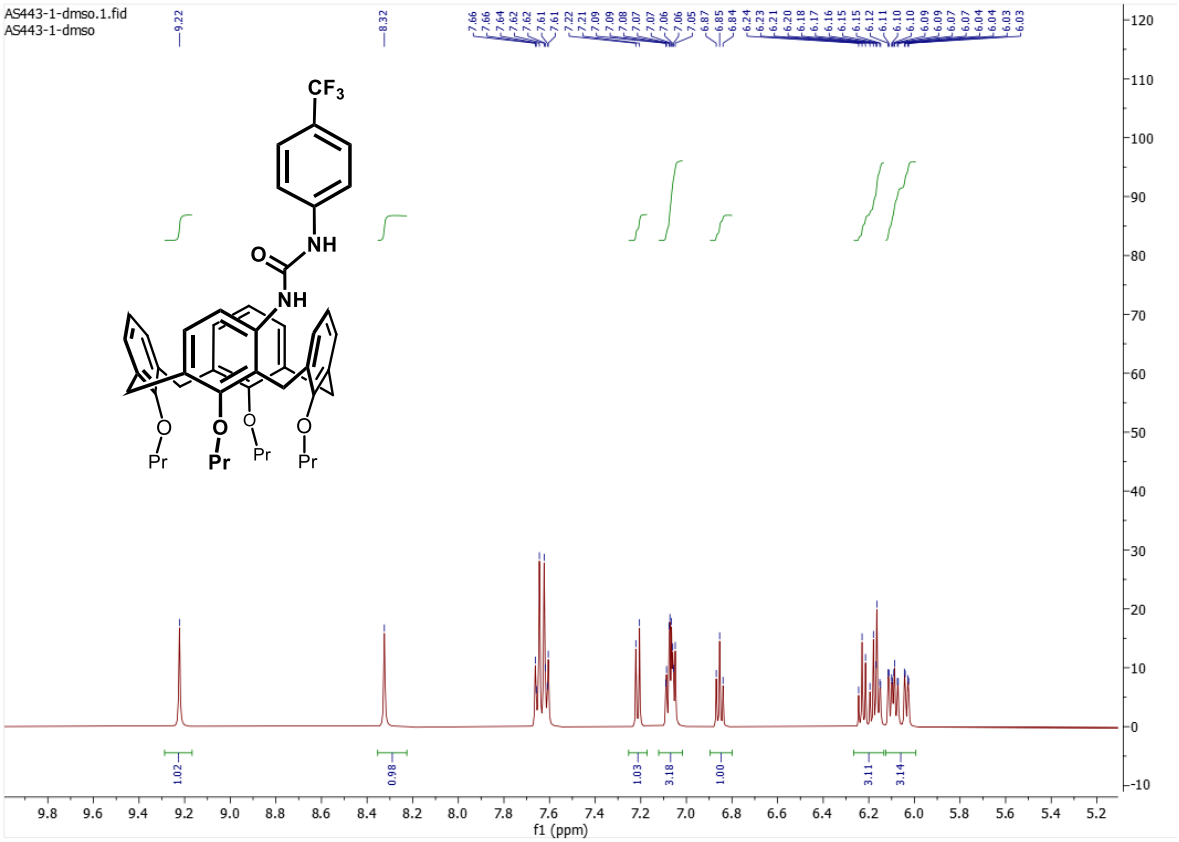

Fig. S9: [1]H NMR of compound **3b**, aromatic region (DMSO, 500 MHz, 298 K)

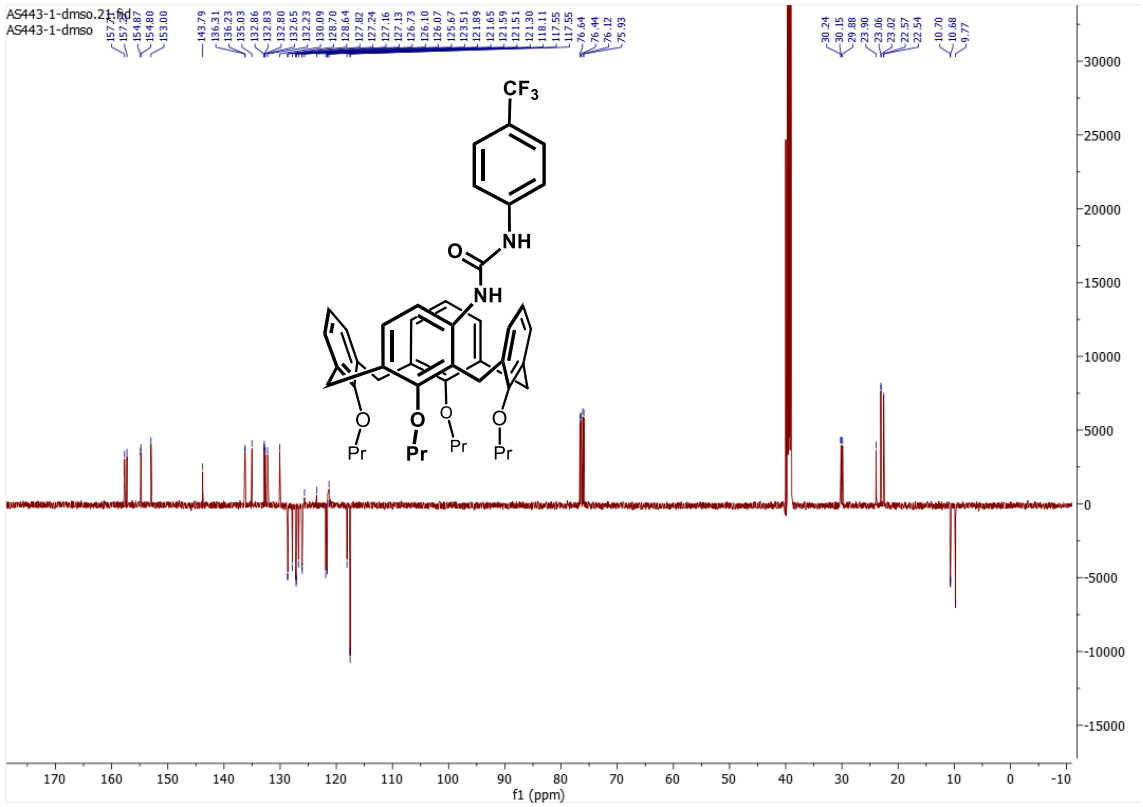

Fig. S10: [13]C(APT) NMR of compound **3b** (DMSO, 125 MHz, 298 K)

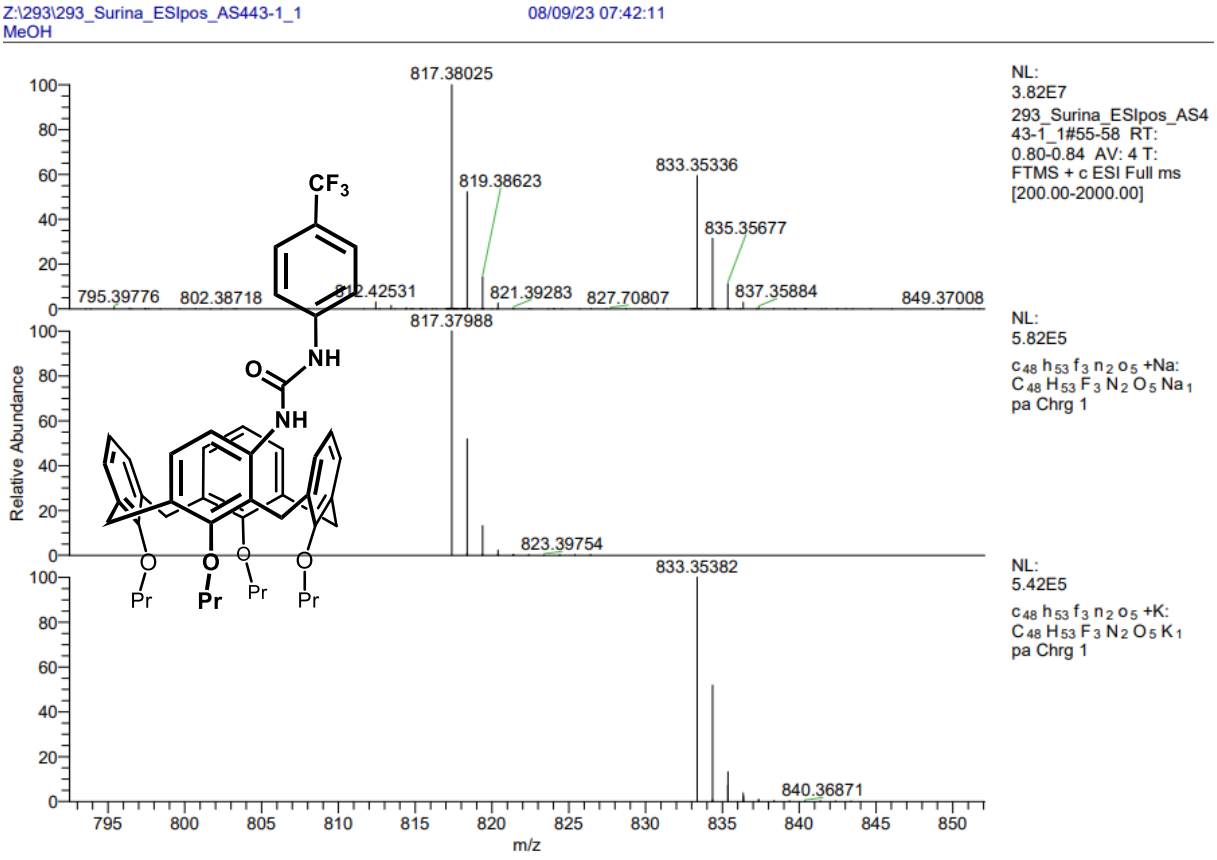

Fig. S11: HRMS (ESI) of compound **3b** calcd for $C_{47}H_{53}N_3O_7$ 794.3776 $[M+Na]^+$, found m/z 794.3783 $[M+Na]^+$.

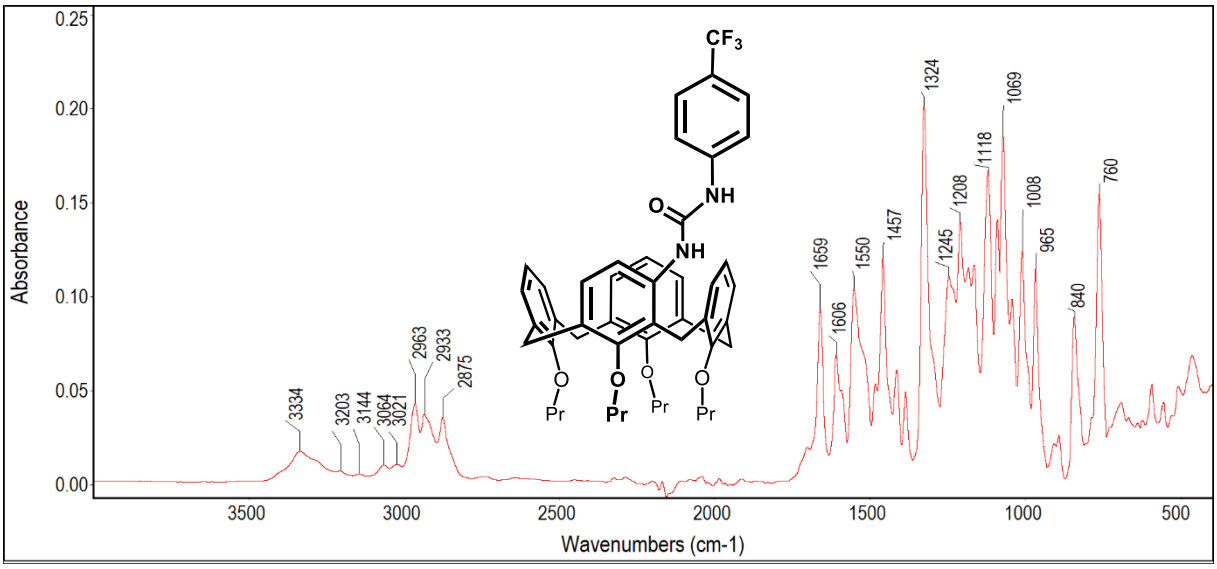

Fig. S12: IR spectrum of compound **3b** (ATR).

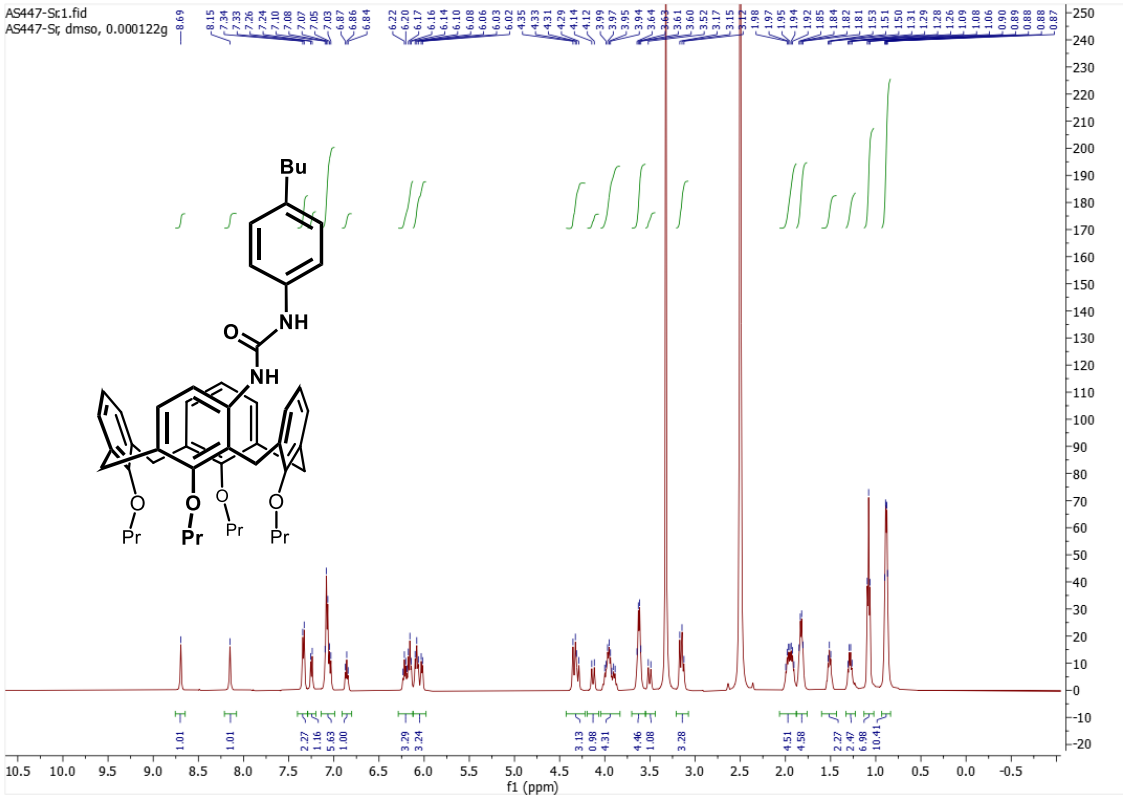

Fig. S13: [1]H NMR of compound **3c** (DMSO, 500 MHz, 298 K)

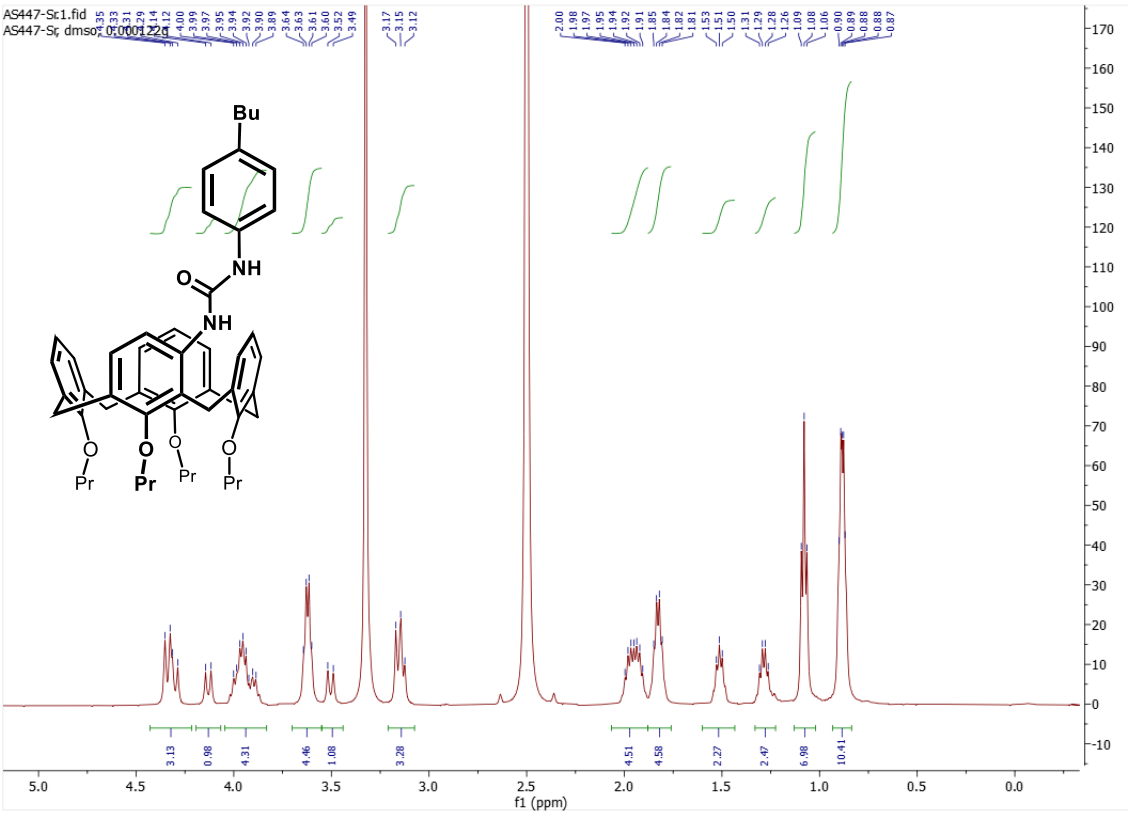

Fig. S14: [1]H NMR of compound **3c**, aliphatic region (DMSO, 500 MHz, 298 K)

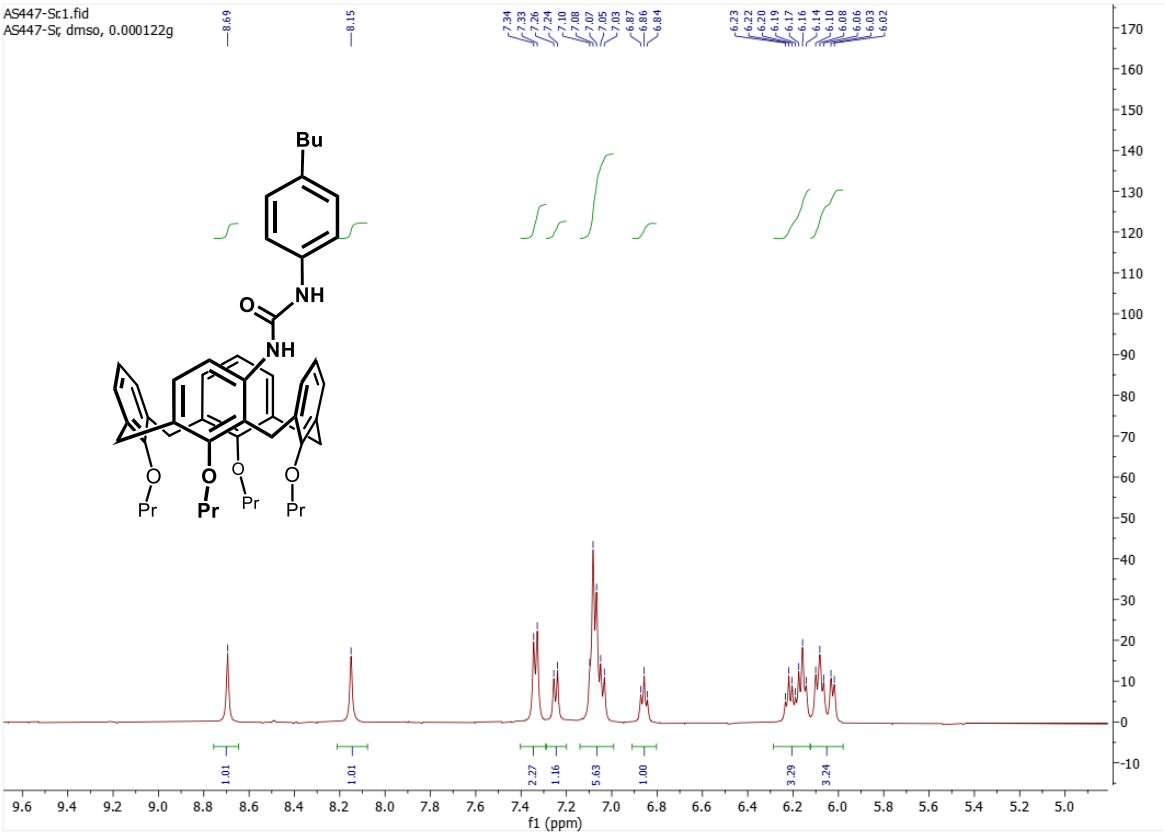

Fig. S15: ^{1}H NMR of compound **3c**, aromatic region (DMSO, 500 MHz, 298 K)

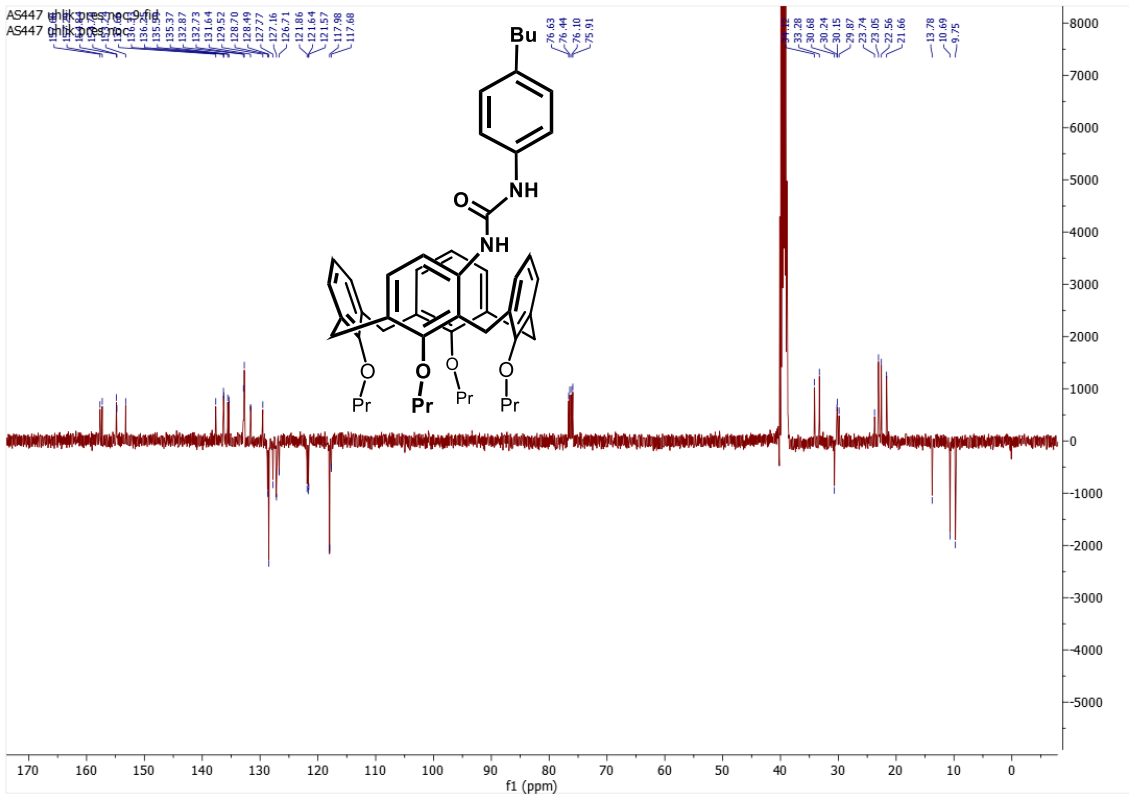

Fig. S16: ^{13}C(APT) NMR of compound **3c** (DMSO, 125 MHz, 298 K)

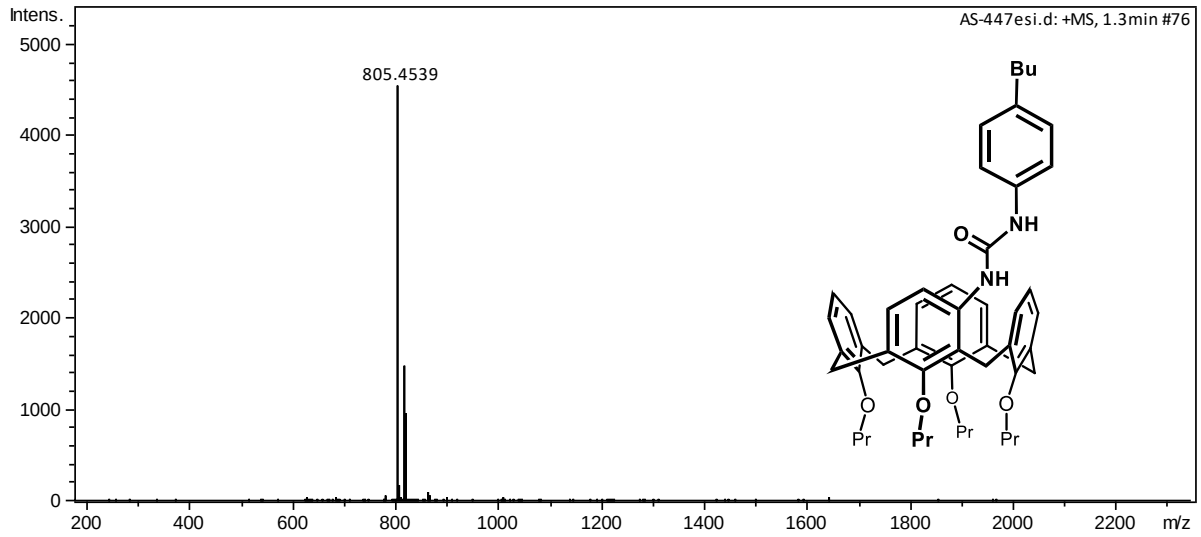

Fig. S17: HRMS (ESI) of compound **3c** calcld. $[C_{51}H_{62}N_2O_5+Na]^+$ 805.4551; found *m/z* 805.4539 $[M+Na]^+$.

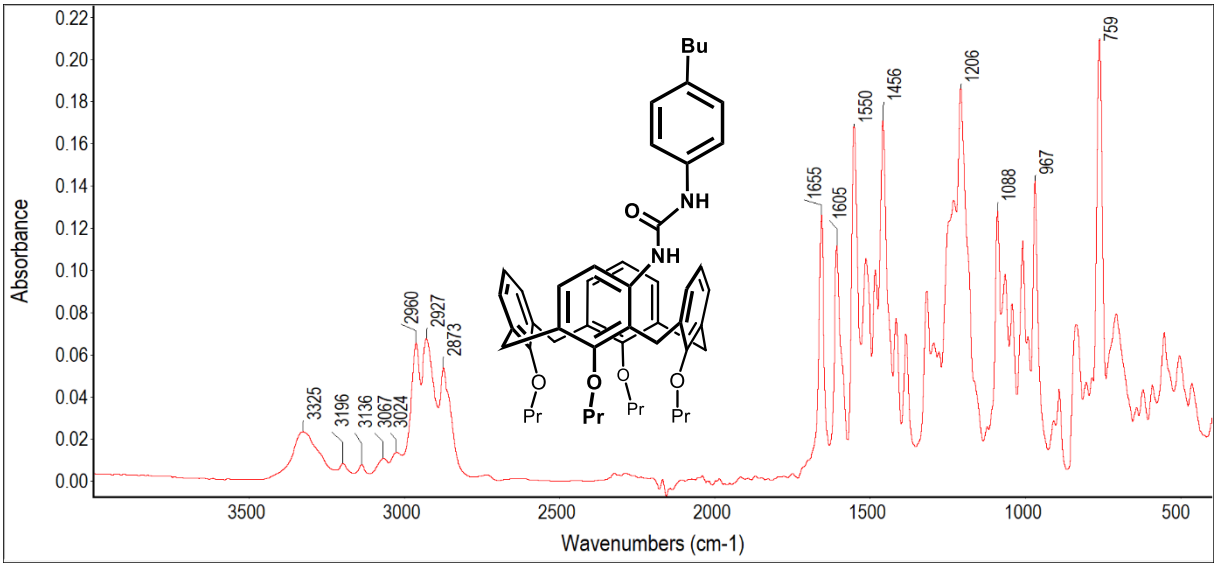

Fig. S18: IR spectrum of compound **3c** (ATR).

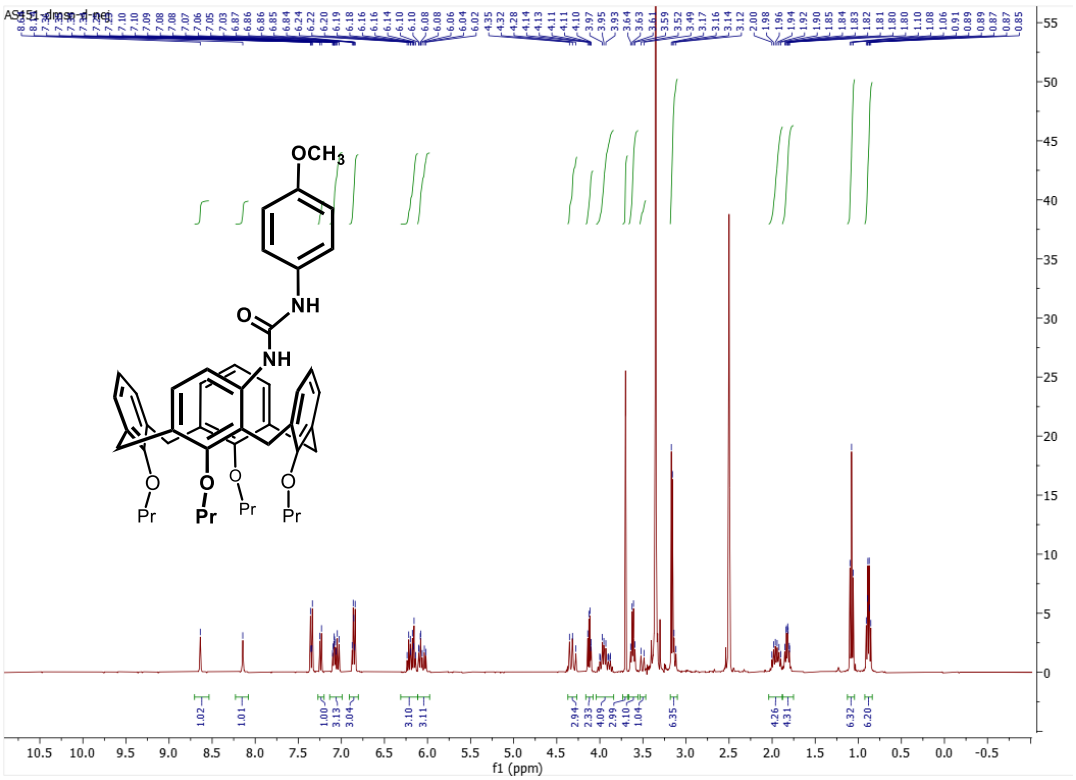

Fig. S19: ^{1}H NMR of compound **3d** (DMSO, 500 MHz, 298 K)

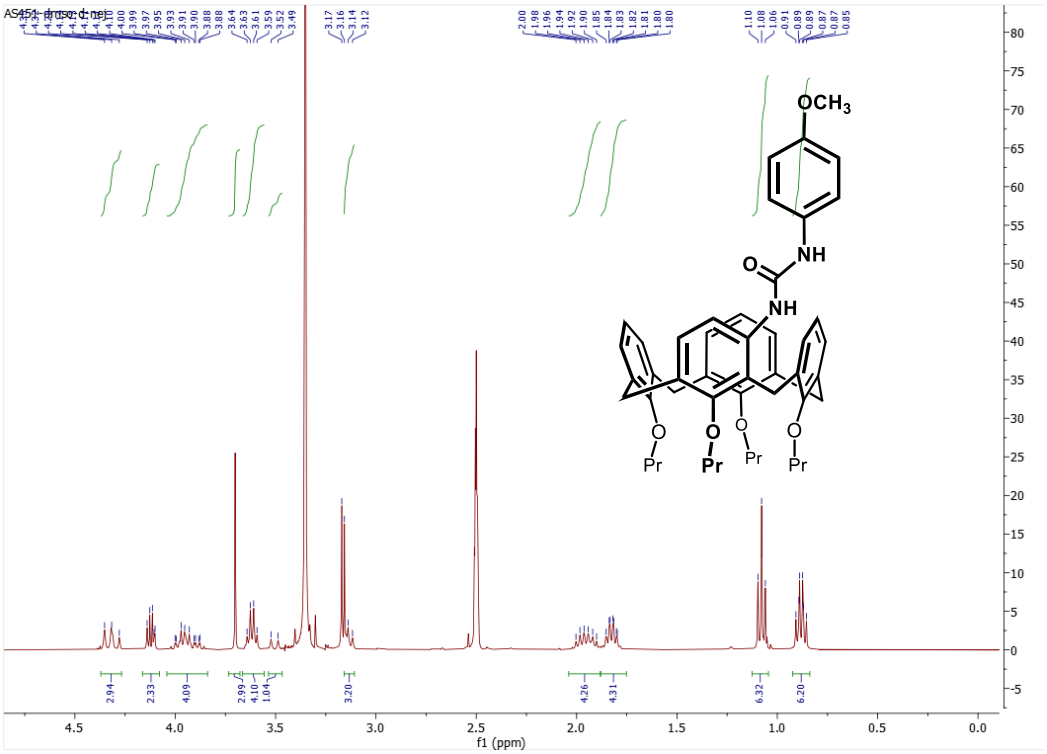

Fig. S20: ^{1}H NMR of compound **3d**, aliphatic region (DMSO, 500 MHz, 298 K)

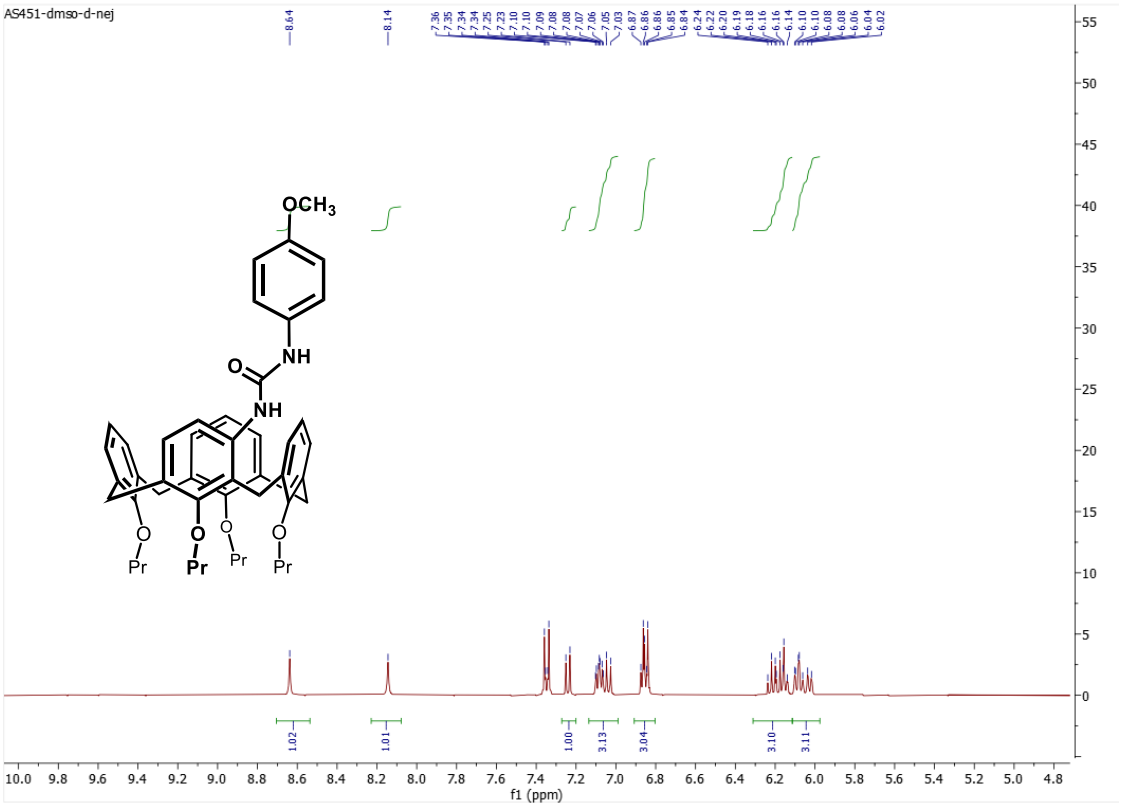

Fig. S21: ^{1}H NMR of compound **3d**, aromatic region (DMSO, 500 MHz, 298 K)

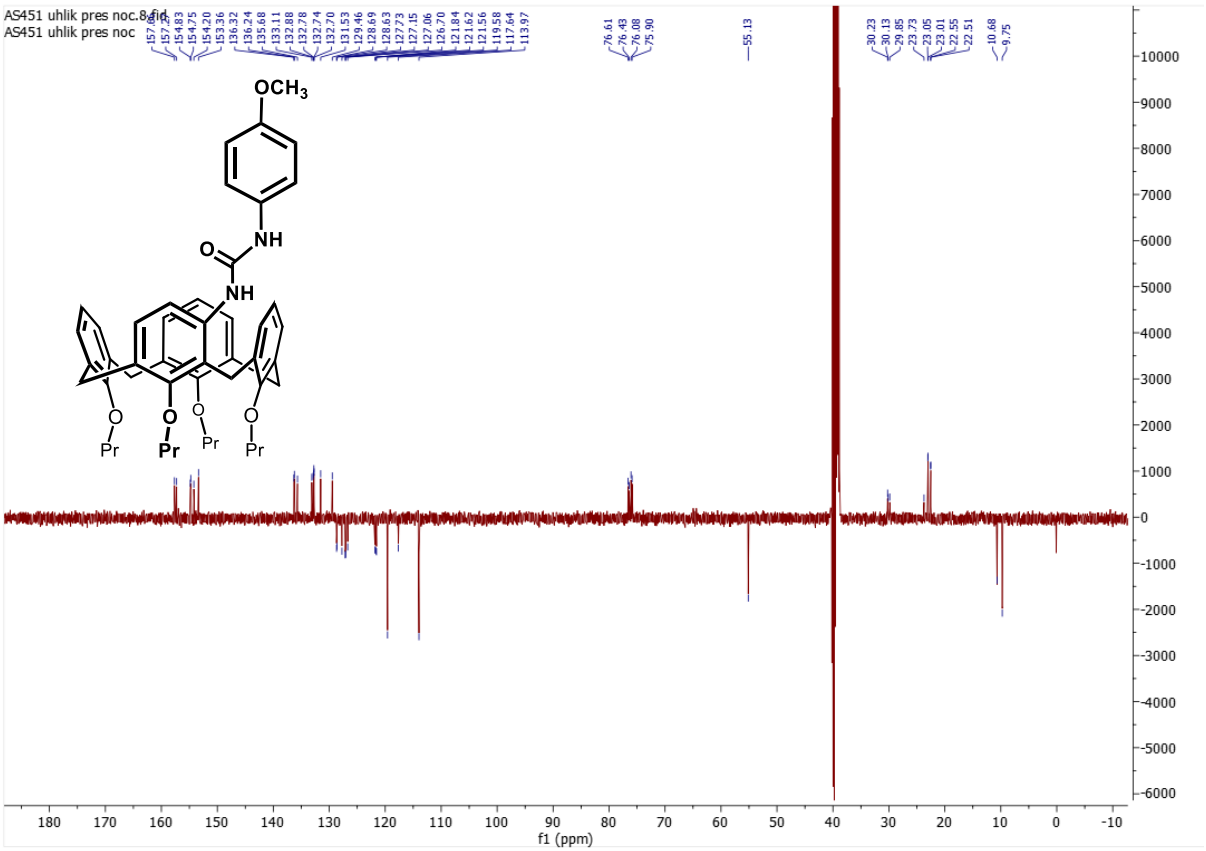

Fig. S22: ^{13}C(APT) NMR of compound **3d** (DMSO, 125 MHz, 298 K)

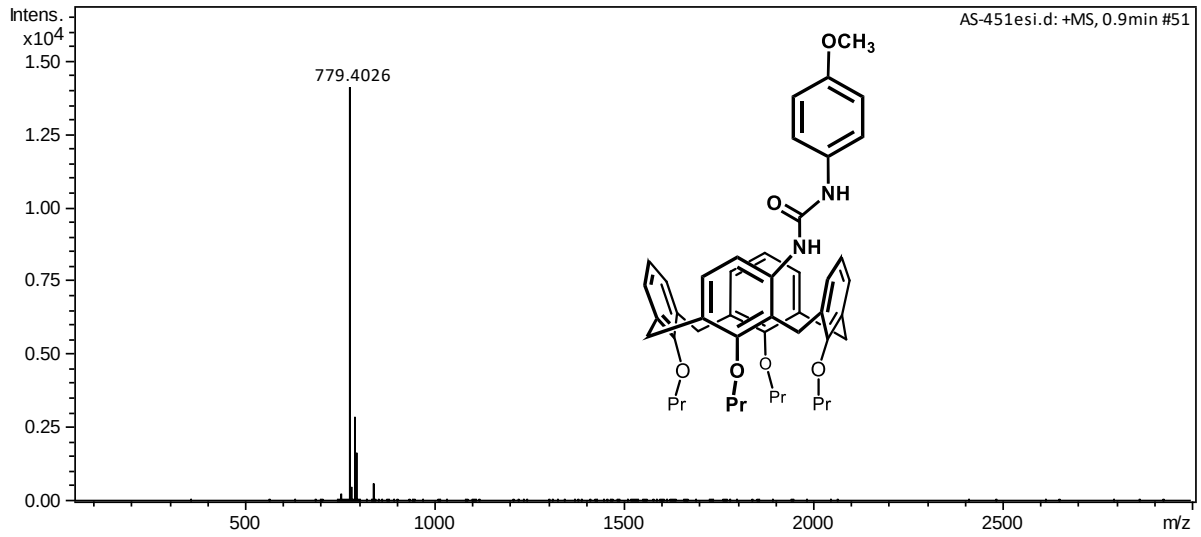

Fig. S23: HRMS (ESI) of compound **3d** calcld. $[C_{48}H_{56}N_2O_6+Na]^+$ 779.4030; found *m/z* 779.4026 [M+Na]+.

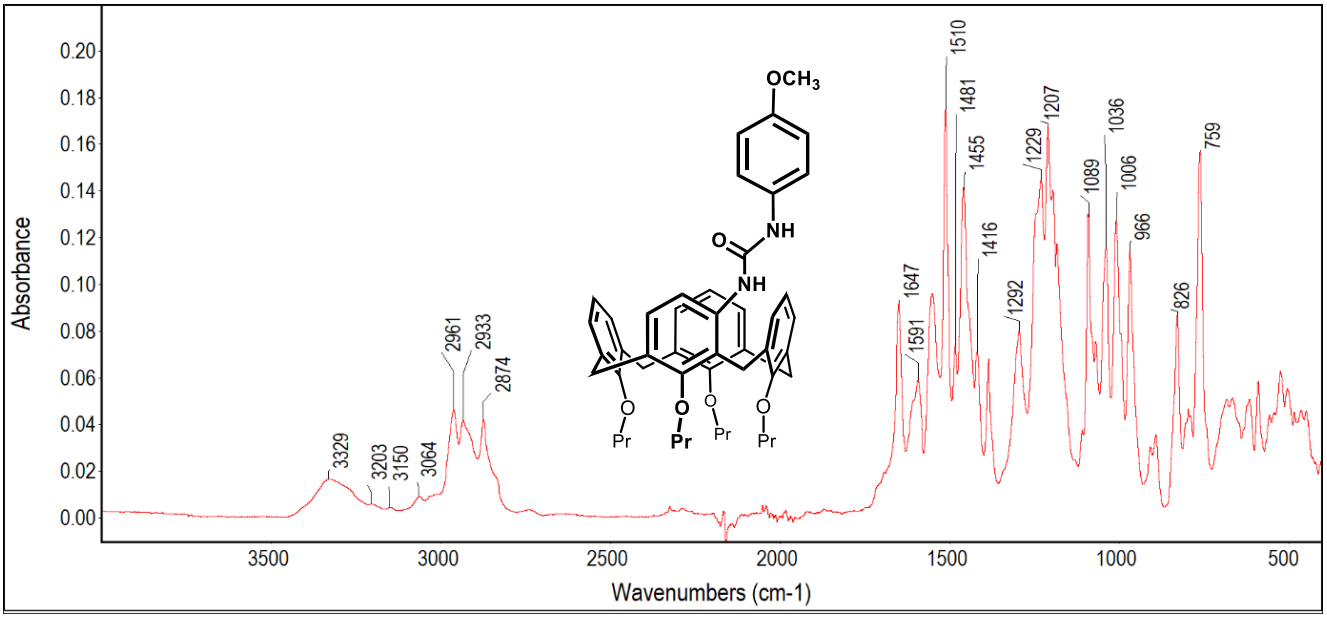

Fig. S24: IR spectrum of compound **3d** (ATR).

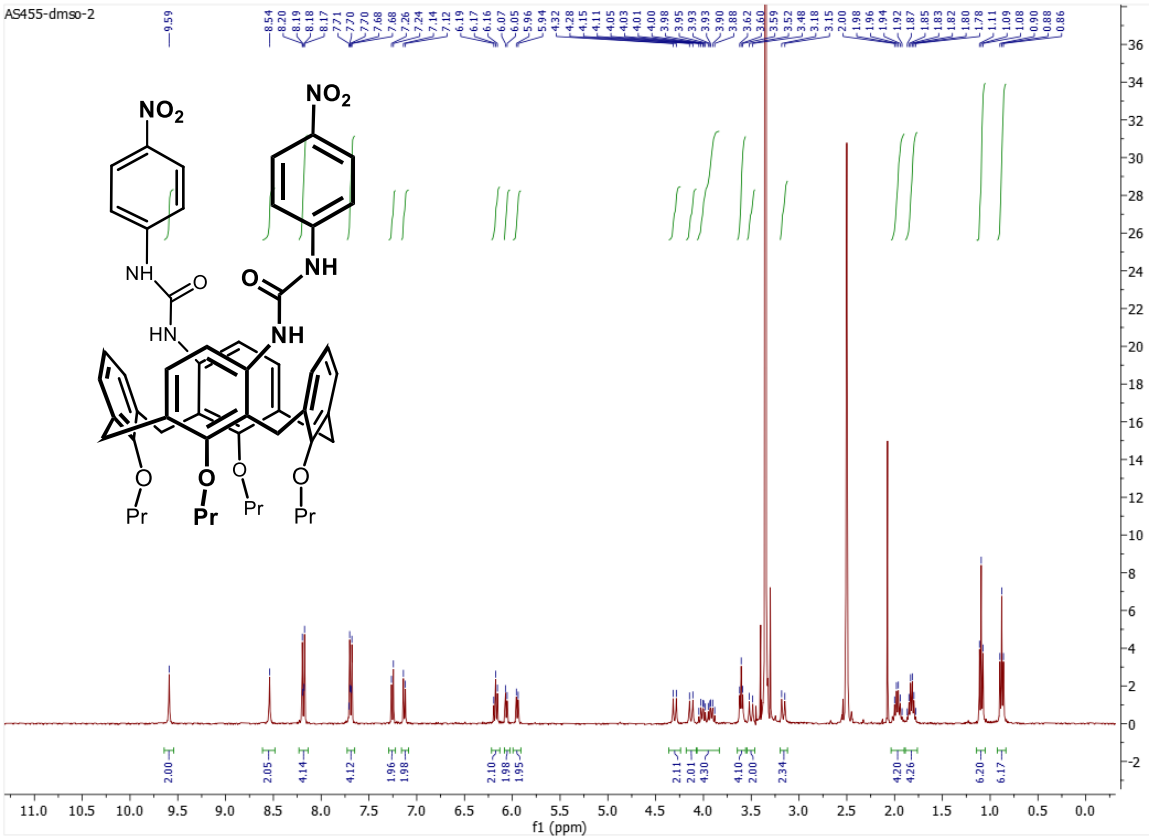

Fig. S25: ^{1}H NMR of compound **7a** (DMSO, 500 MHz, 298 K)

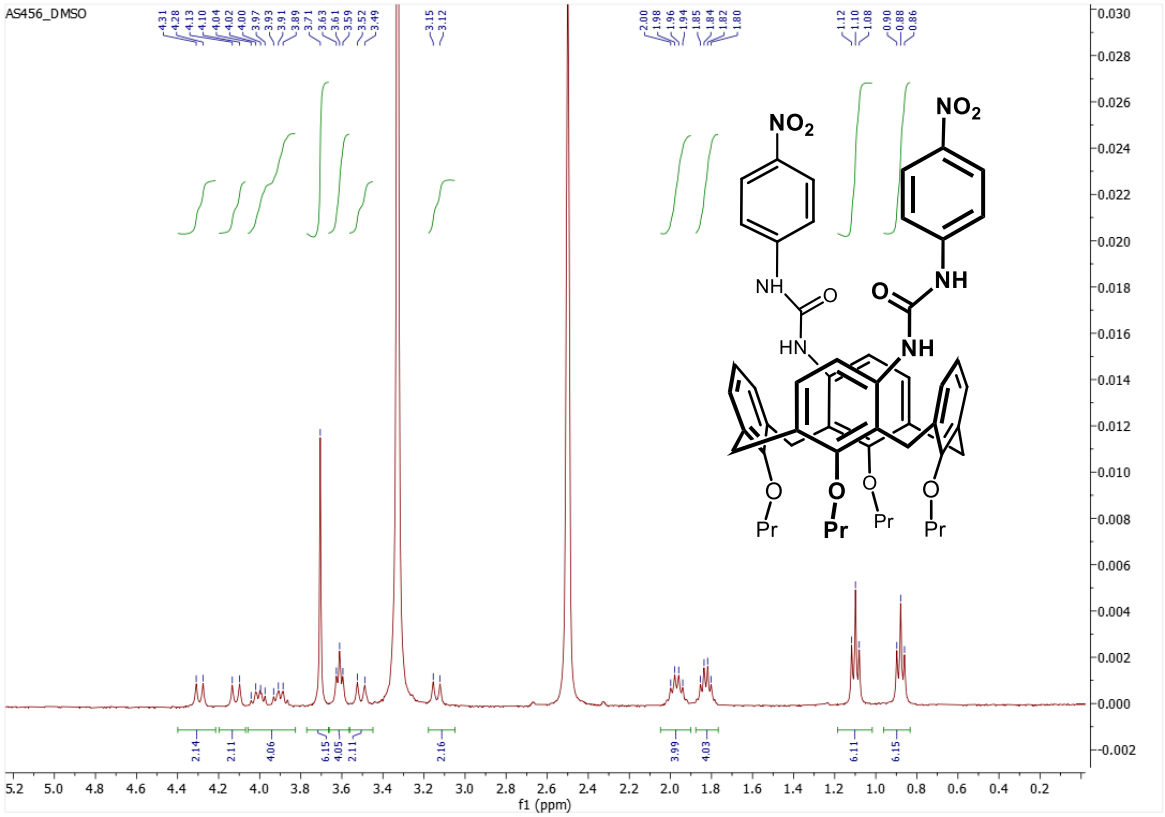

Fig. S26: ^{1}H NMR of compound **7a**, aliphatic region (DMSO, 500 MHz, 298 K)

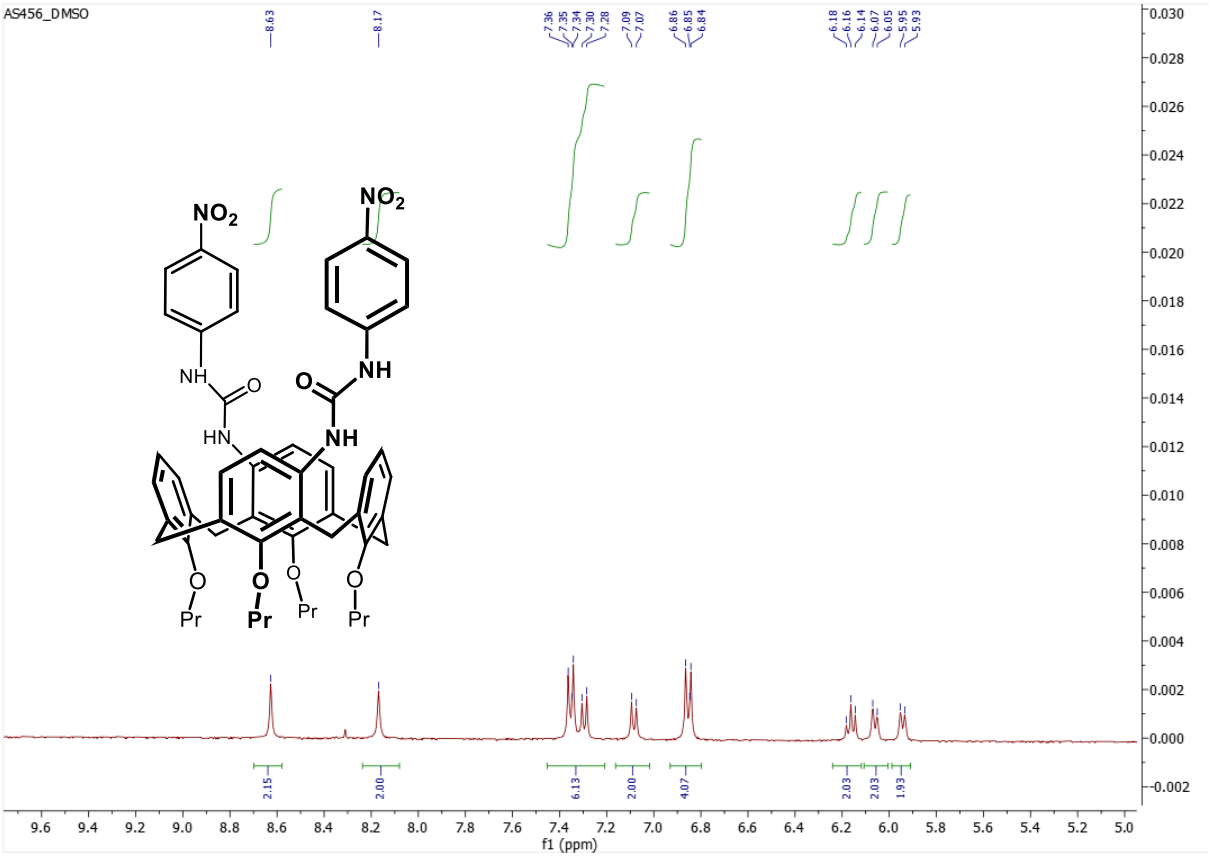

Fig. S27: ^{1}H NMR of compound **7a**, aromatic region (DMSO, 500 MHz, 298 K)

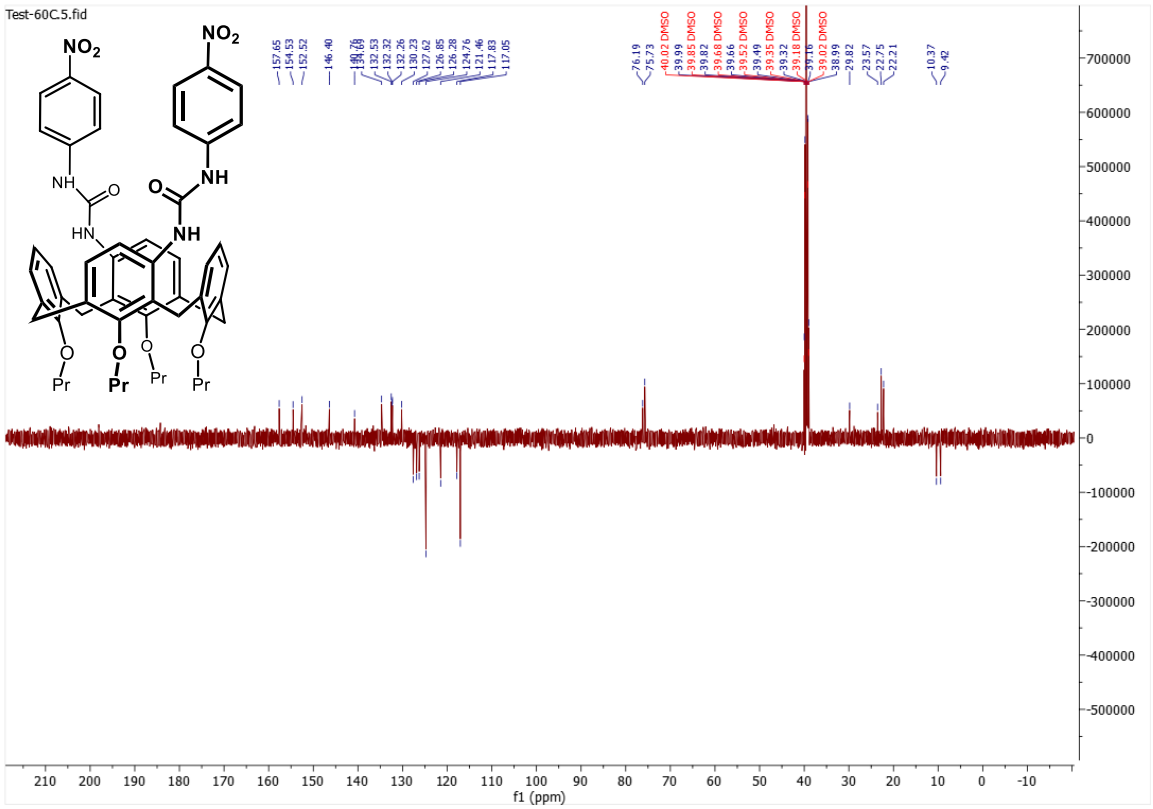

Fig. S28: ^{13}C(APT) NMR of compound **7a** (DMSO, 125 MHz, 333 K)

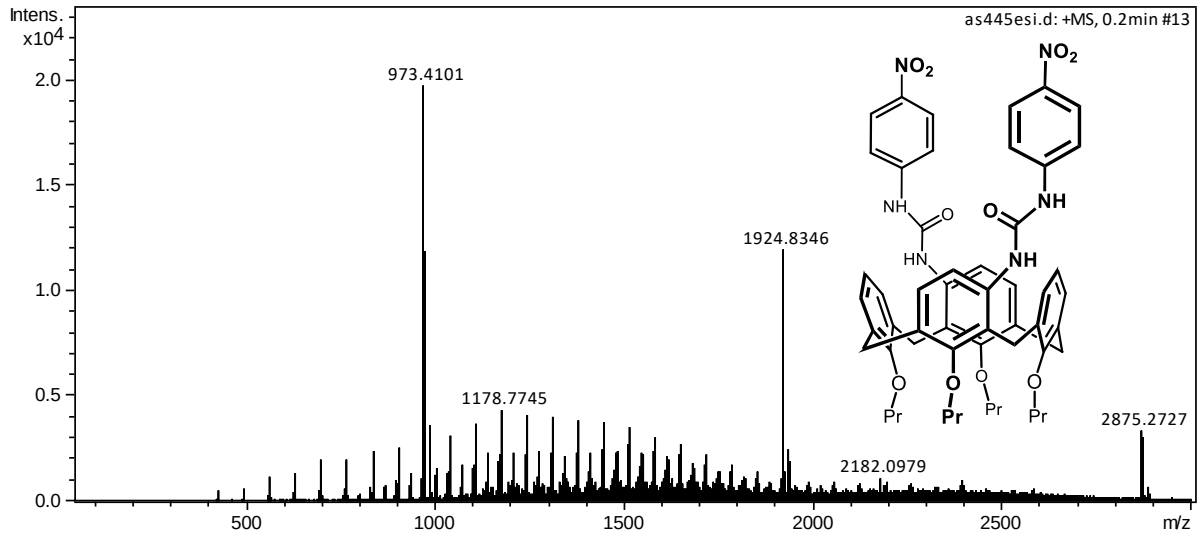

Fig. S29: HRMS (ESI) of compound **7a** calcld. $[C_{54}H_{58}N_6O_{10}+Na]^+$ 973.4106; found *m/z* 973.4101 [M+Na]+.

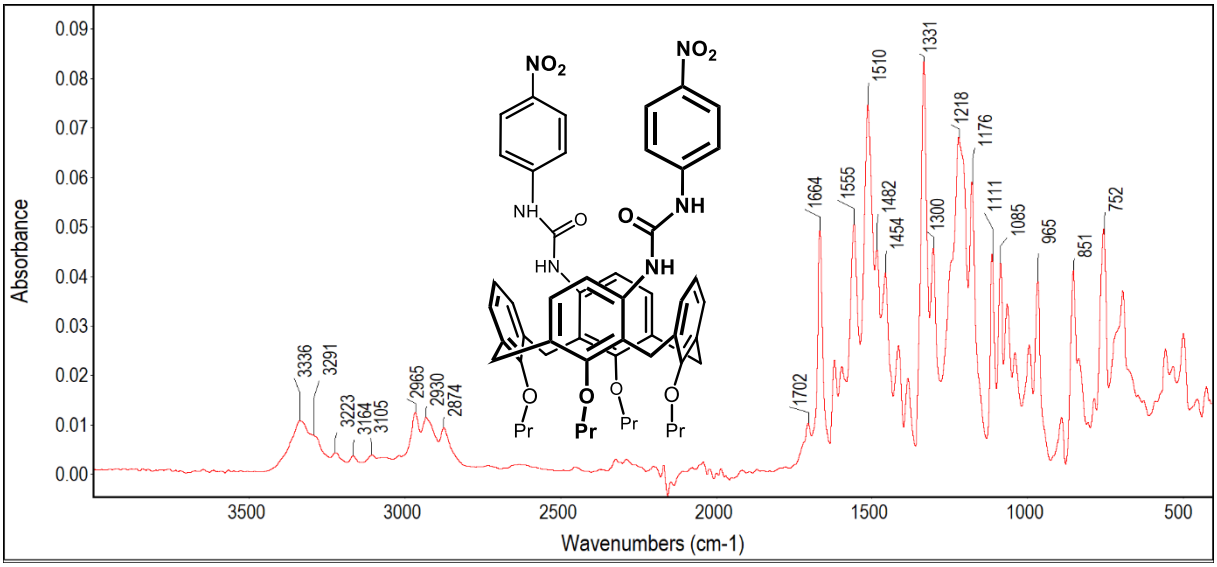

Fig. S30: IR spectrum of compound **7a** (ATR).

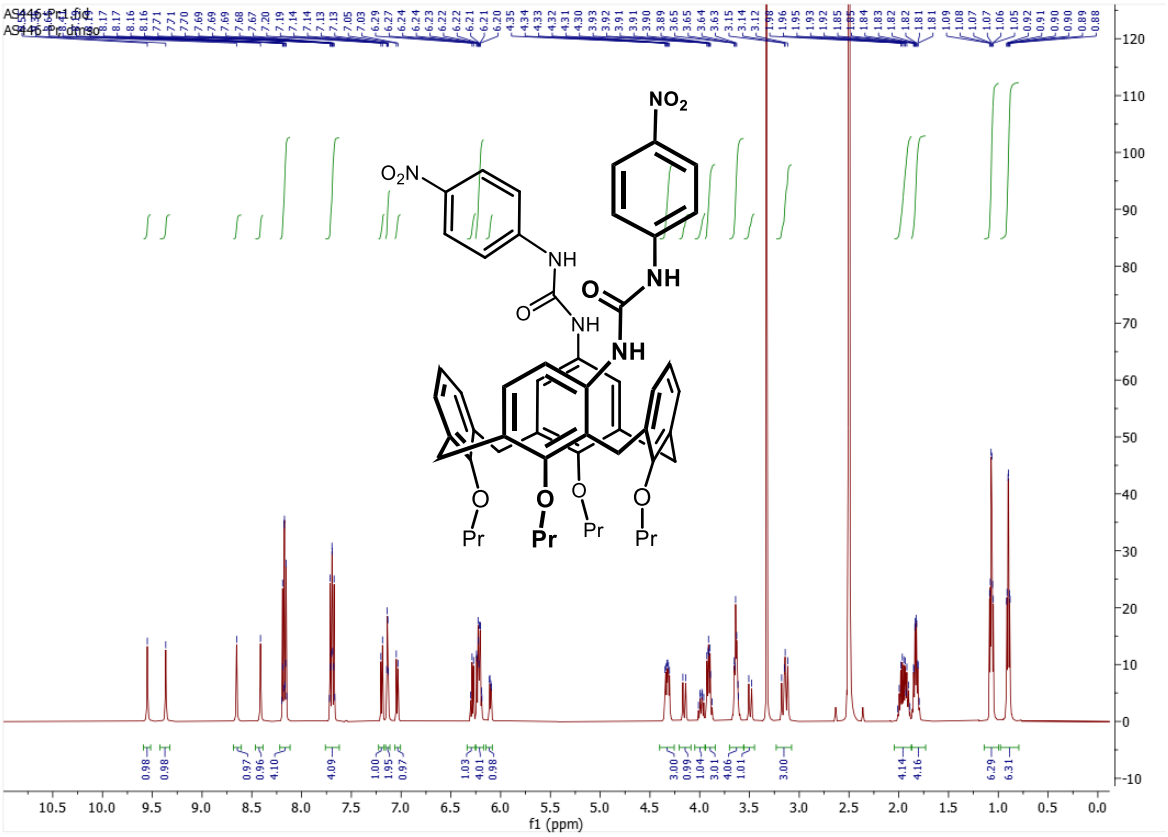

Fig. S31: ^{1}H NMR of compound **8a** (DMSO, 500 MHz, 298 K)

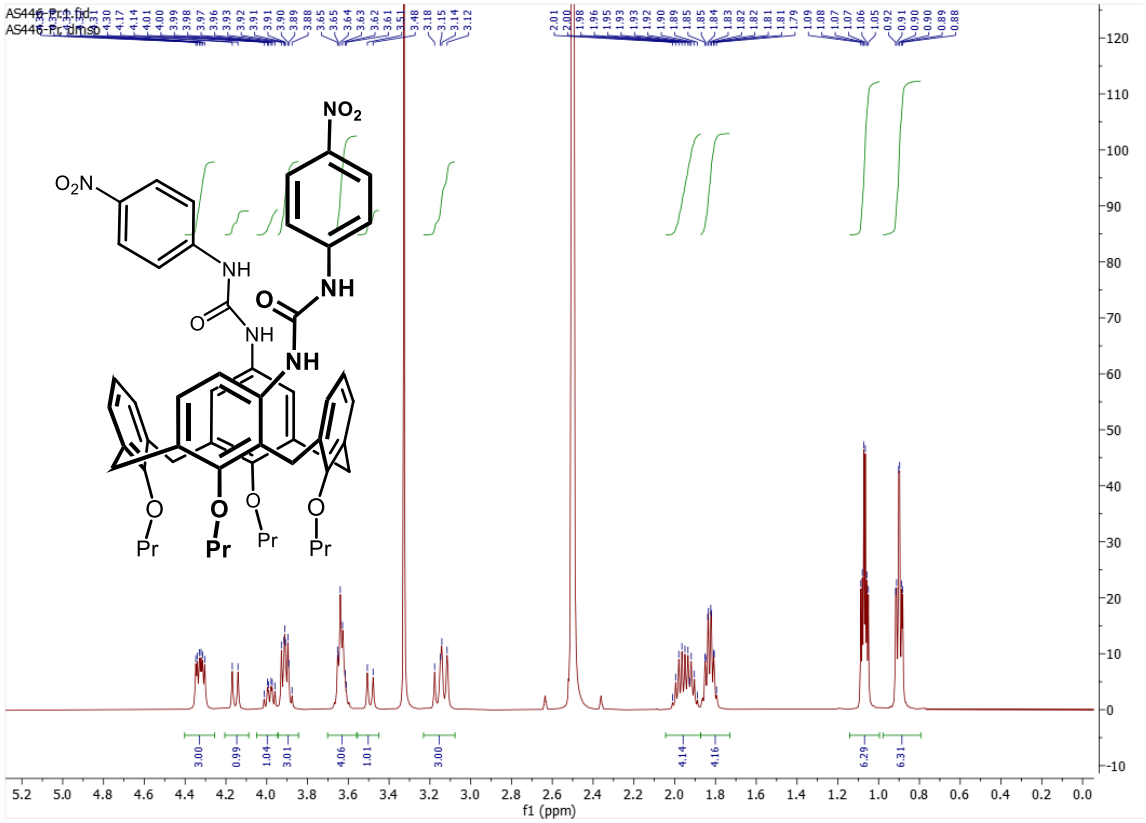

Fig. S32: ^{1}H NMR of compound **8a**, aliphatic region (DMSO, 500 MHz, 298 K)

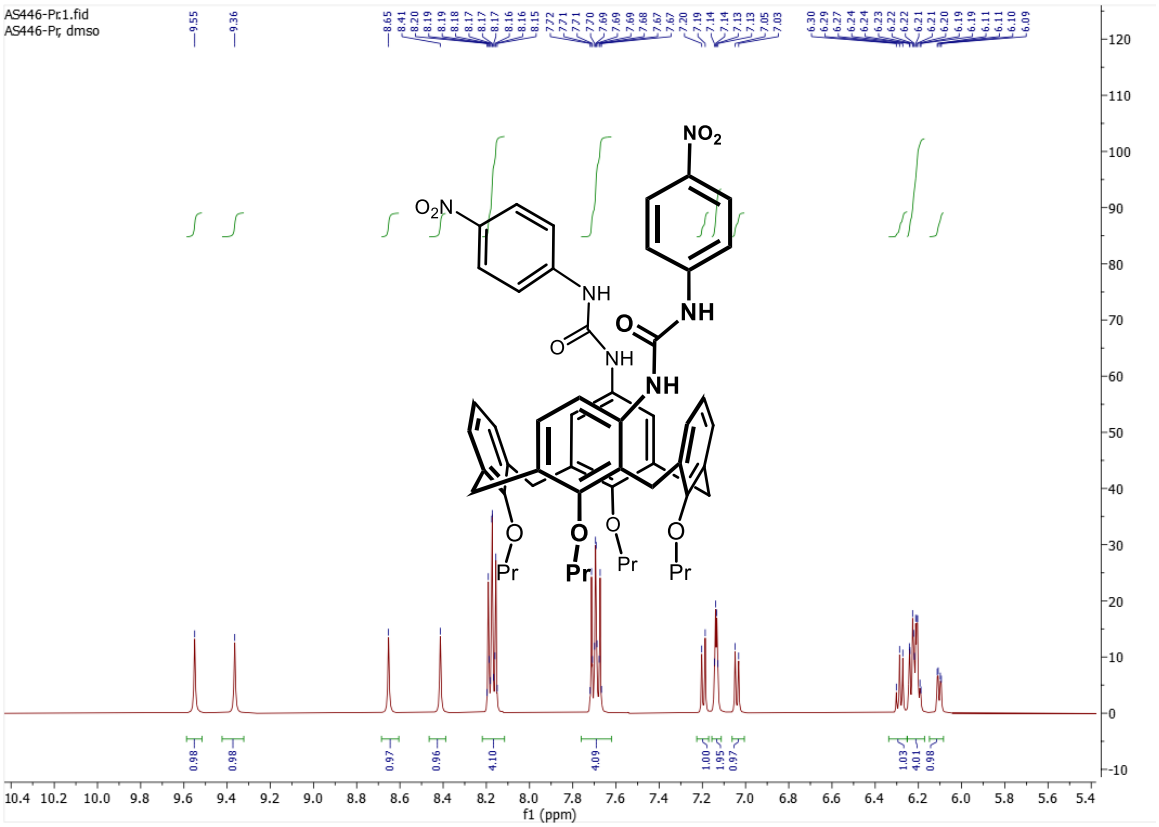

Fig. S33: ^{1}H NMR of compound **8a**, aromatic region (DMSO, 500 MHz, 298 K)

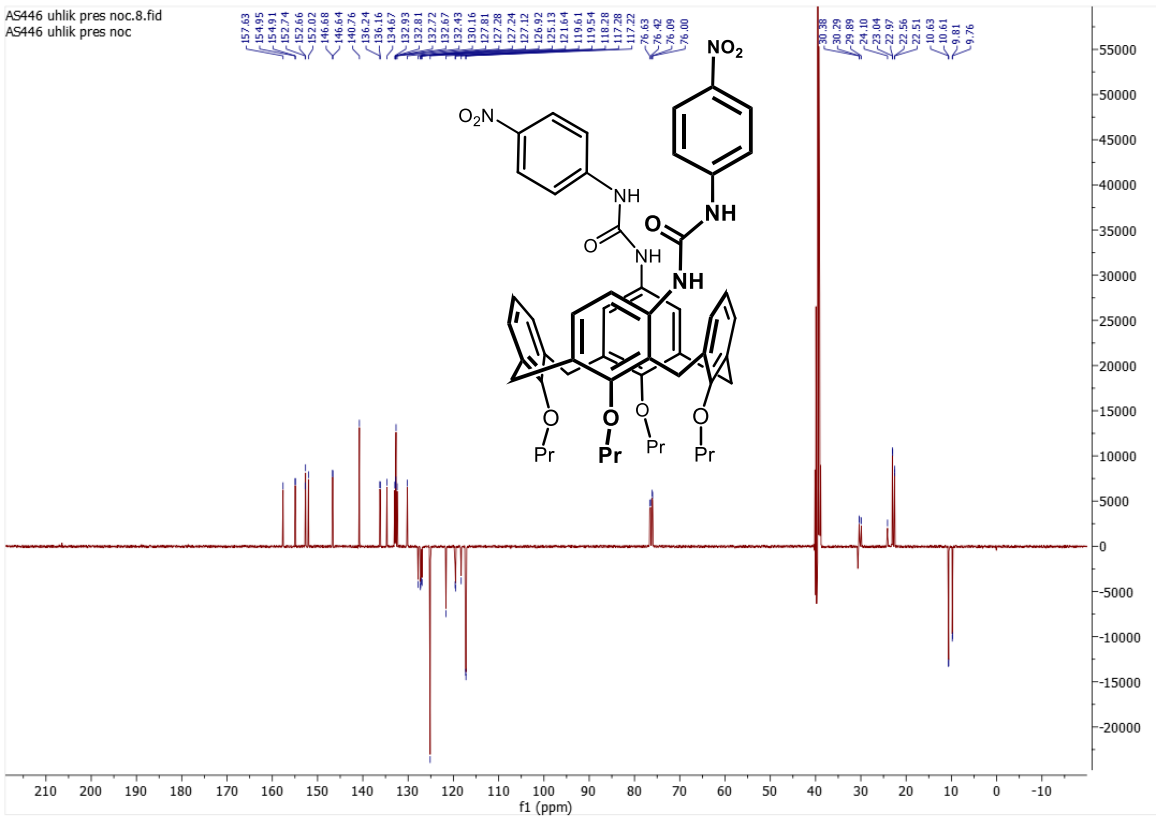

Fig. S34: ^{13}C(APT) NMR of compound **8a** (DMSO, 125 MHz, 298 K)

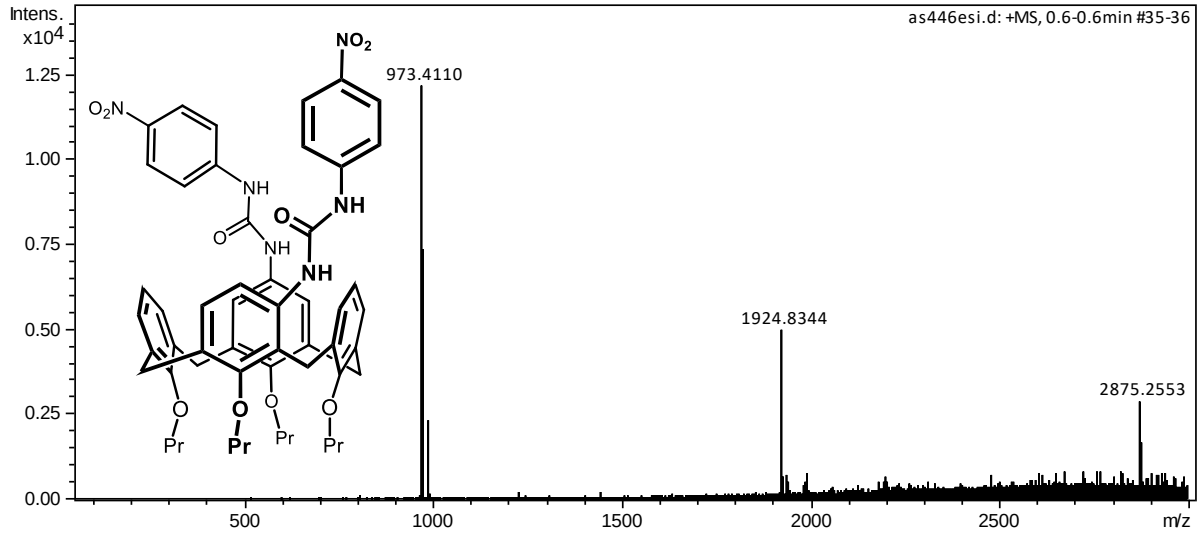

Fig. S35: HRMS (ESI) of compound **8a** calcld. $[C_{54}H_{58}N_6O_{10}+Na]^+$ 973.4106; found *m/z* 973.4110 [M+Na]+.

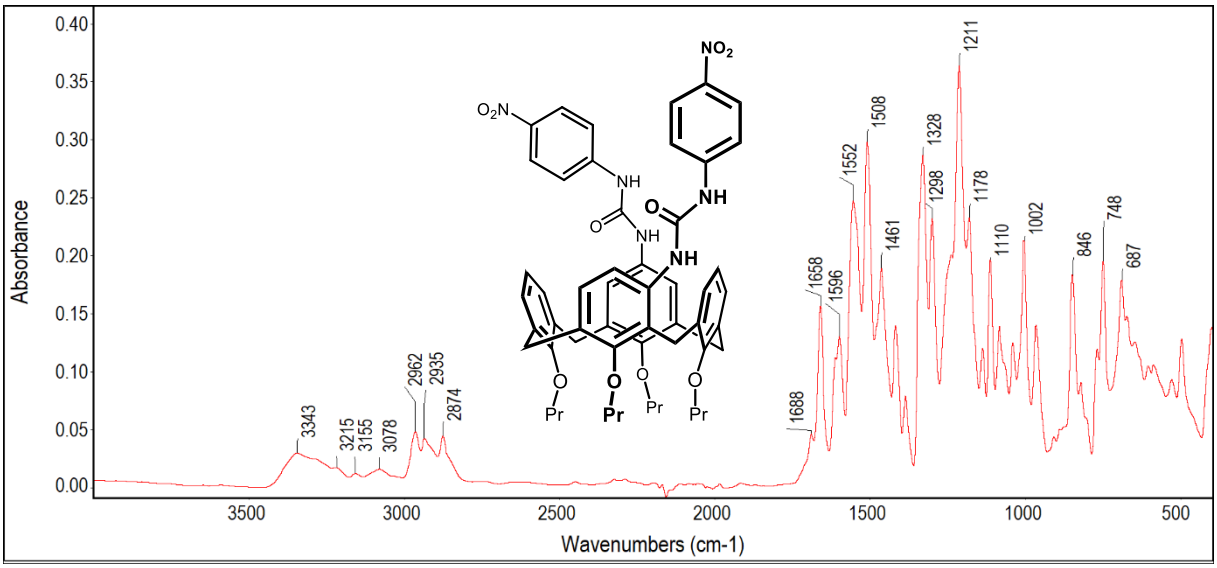

Fig. S36: IR spectrum of compound **8a** (ATR).

2. Association constants K_{As}

Table S1: Comparison of association constants K_{As} for a series of mono *m*- substituted urea receptors **3** during recognition of $TBAH_2PO_4$, determined by UV-Vis[b] (in DMSO) or ^{1}H NMR[c] titrations (in DMSO-d_6) at 25 °C, reported together with chemical shift of receptor urea N*H* proton (highlighted in Fig. 23 by orange colour).

Receptor (R-)	**3a (-NO_2)** [b]	**3b (-CF_3)** [c]	**3c (-*n*Bu)** [c]	**3d (-OCH_3)** [c]
K_{As} [a]	1 060	750	470	300
δ_{NH1} (ppm)	9.56	9.21	8.73	8.61

[a] Error, when estimated, was < 15 %.

Table S2: Comparison of association constants K_{As} (1:1)[a] for nitro-substituted mono-urea receptors **3a** and **4** with a series of anions in the form of TBA salts at 25 °C.

	4 (mono *p*-)	**3a** (mono *m*-)
$H_2PO_4^-$ [c]	2 020	1 060
BzO^-	845 [b]	830 [c]
Cl^- [b]	35	50
HSO_4^- [b]	6	4

[a] Error, when estimated, was < 10 %. [b]Determined by ^{1}H NMR in DMSO-d_6. [c]Determined by UV-Vis in DMSO.

Table S3: Association constants K_{As} (1:1)[a] and overall association constants β of receptors **7a** were determined by ^{1}H NMR with a series of anions in the form of TBA salts in DMSO-d_6 at 25 °C.

Anion/ Constant	K_{As} (1:1) [a]	β
$H_2PO_4^-$	1 660	$6.89 \cdot 10^5$
BzO^-	1 440	$5.18 \cdot 10^5$
AcO^-	1 160	$3.36 \cdot 10^5$

[a] Error, when estimated, was < 5 %. Evaluated by the non-cooperative model: $\beta = K_{As}(1) \times K_{As}(2)$, and $K_{As}(2) = K_{As}(1)/4$.

Table S4: Association constants K_{As} (1:1) and overall association constants β of receptors **8a** were determined by ^{1}H NMR[a] (or UV-Vis[b]) in DMSO-d_6 (DMSO) with a series of anions in the form of TBA salts at 25 °C.

	Utilised stoichiometry	K_{As} **(1:1)** [c]	β
$H_2PO_4^-$ [b]	1:1	13 600	-
BzO^- [b, *]	1:1	2 450	-
AcO^- [b]	1:1	4 170	-
Cl^- [a,d]	1:2	60	900
HSO_4^- [a,d]	1:2	15	56

[c] Error, when estimated, was < 5 %. [d] Were evaluated by the non-cooperative model: : $\beta = K_{As}(1) \times K_{As}(2)$, and $K_{As}(2) = K_{As}(1)/4$. * The results might also be fitted by 1:2 stoichiometry.

3. Dilution study of nitro-substituted ureas in DMSO

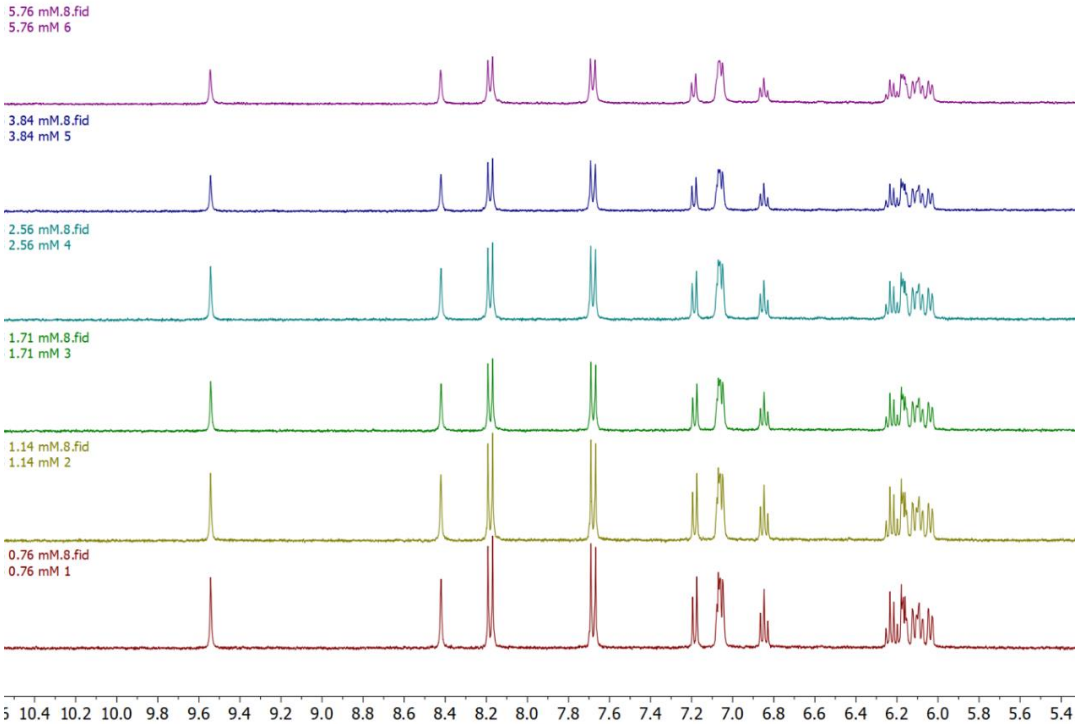

Fig. S37: Part of ^{1}H NMR spectra for urea´s hydrogen N*H* and aromatic region of **3a** in DMSO-d_6. The studied concentration range corresponds to 5.8 - 0.8 mM. The higher concentration was not obtained as the compound did not dissolve.

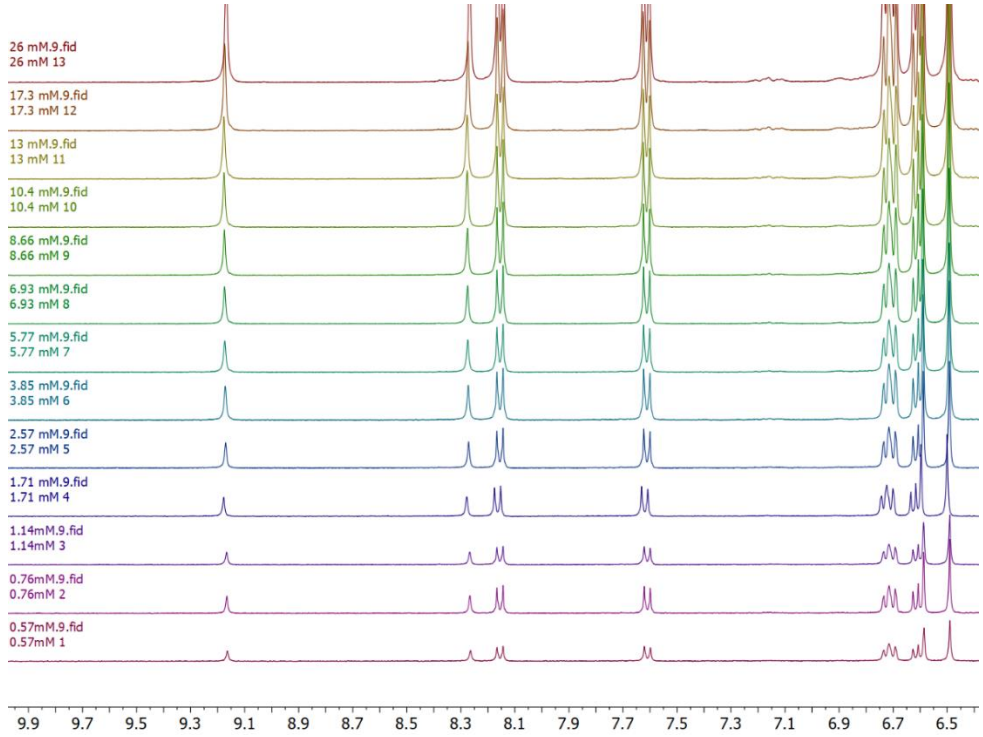

Fig. S38: Part of ^{1}H NMR spectra for urea´s hydrogen N*H* and aromatic region of **4** in DMSO-d_6. The studied concentration range corresponds to 26 - 0.6 mM.

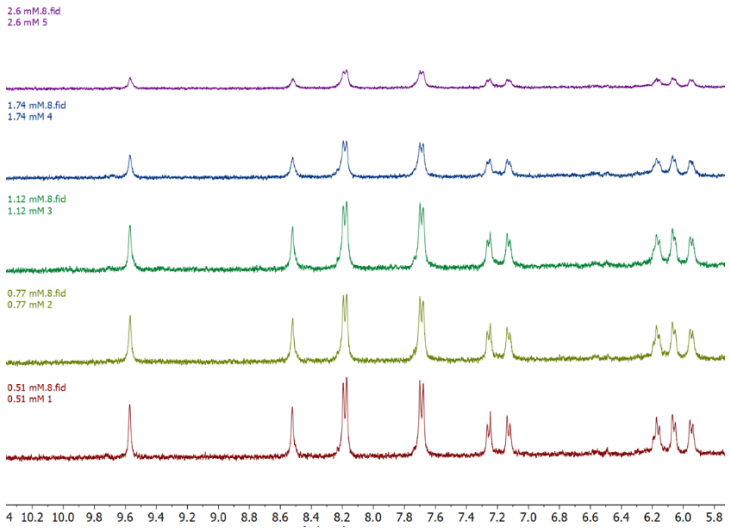

Fig. S39: Part of ^{1}H NMR spectra for urea´s hydrogen N*H* and aromatic region of **7a** in DMSO-d_6. The studied concentration range corresponds to 2.6 - 0.5 mM. The higher concentration was not obtained as the compound did not dissolve.

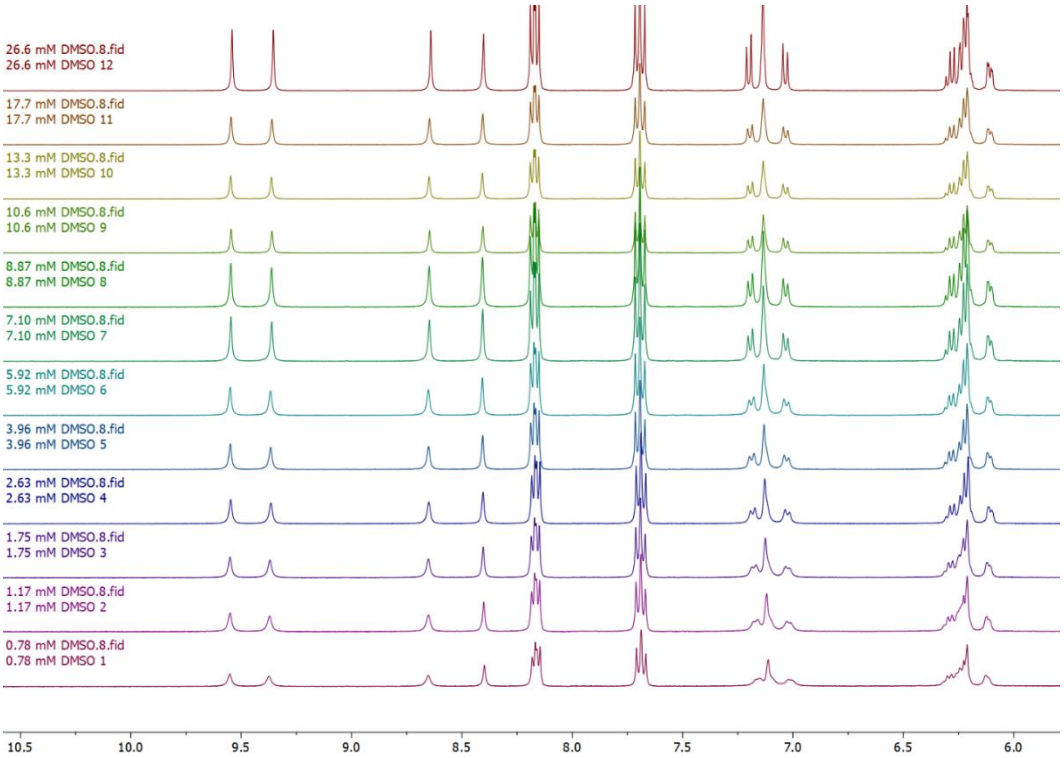

Fig. S40: Part of ^{1}H NMR spectra for urea´s hydrogen N*H* and aromatic region of **8a** in DMSO-d_6. The studied concentration range corresponds to 26.6 - 0.8 mM.

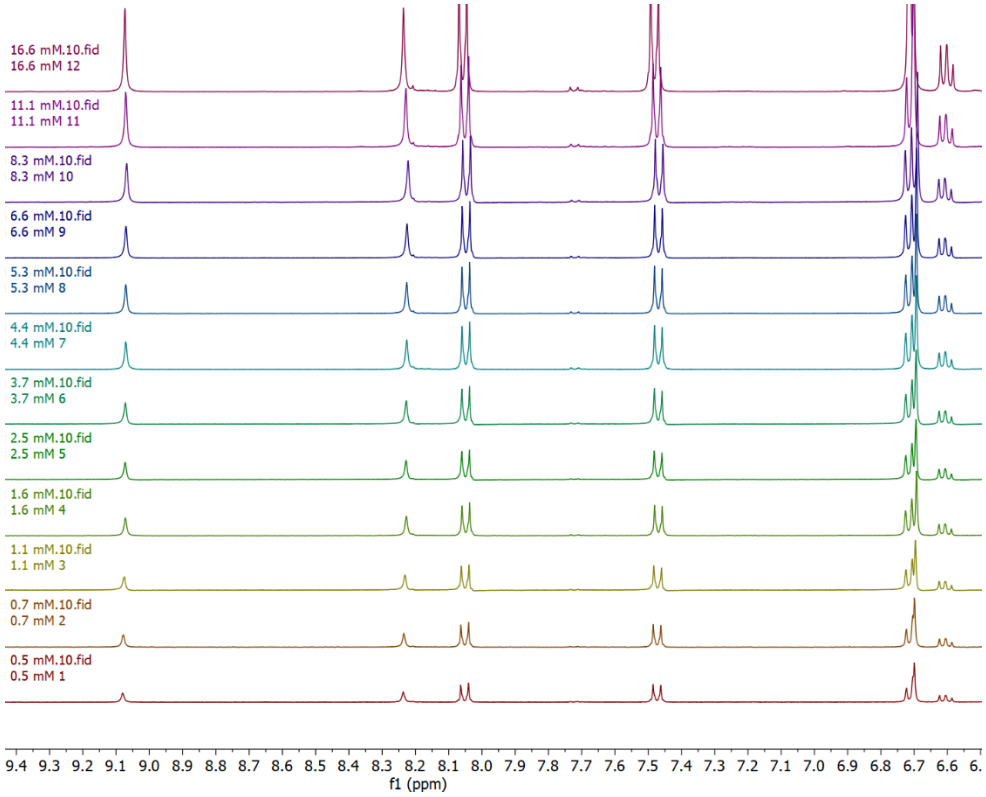

Fig. S41: Part of ^{1}H NMR spectra for urea´s hydrogen N*H* and aromatic region of receptor **9** in DMSO-d_6. The studied concentration range corresponds to 16.6 – 0.5 mM.

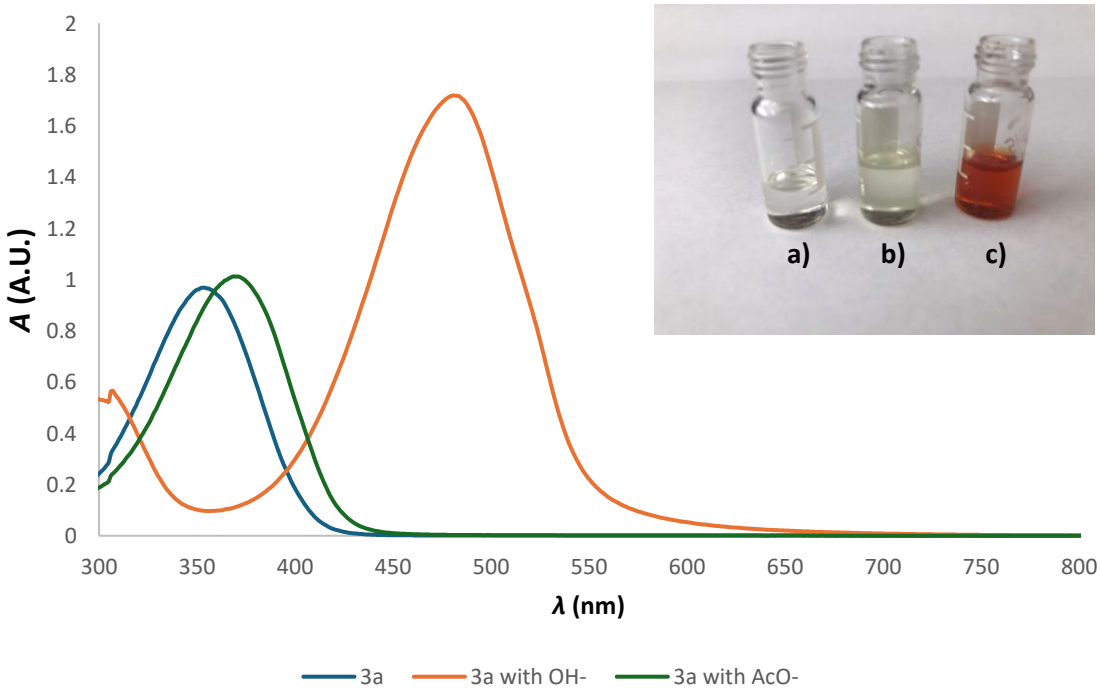

Fig. S42: Records of UV-Vis spectra collected in cuvette with 2-mm pathlength obtained for: **a) blue** nitro substituted urea receptor **3a** (0.31 mM in DMSO); **b) green** nitro substituted urea receptor **3a** (0.31 mM in DMSO) with TBAAcO; **c) orange** nitro substituted urea receptor **3a** (0.31 mM in DMSO) with TBAOH as an example of deprotonation.

4. Job plot analysis

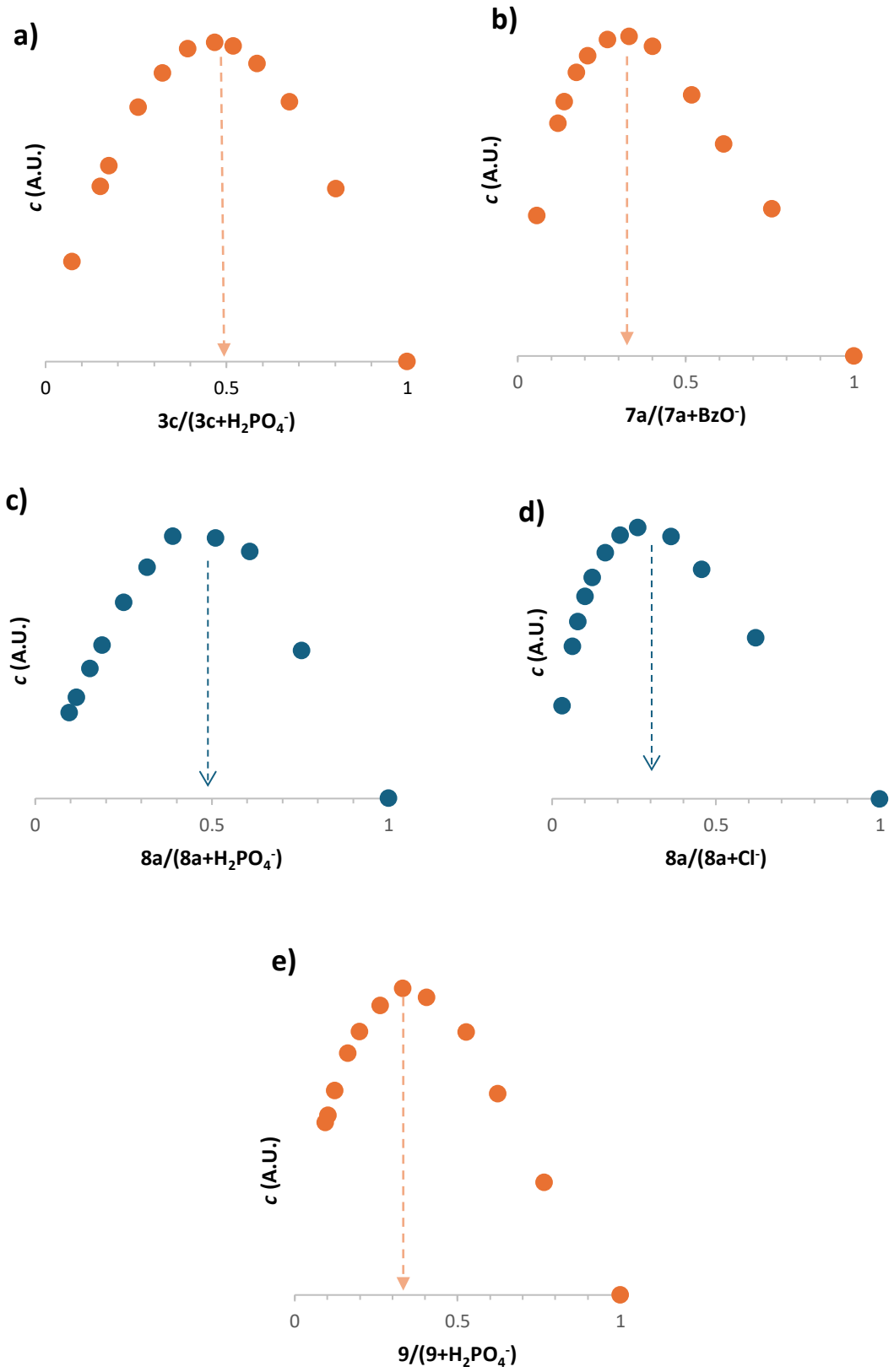

Fig. S43 a-e): Representative Job-plot records, obtained for several different urea-based receptors (built on calix[4]arene skeletons) *via* ^{1}H NMR (400 MHz) titrations with corresponding TBA salts in DMSO-d_6. Arrows indicate the position of their maxima.

5. Titration experiments

c (**3a**) mM	*c* ($H_2PO_4^-$) mM	A_{400} (A.U.)
0.272	0	0.161
0.272	0.0636	0.173
0.272	0.126	0.195
0.272	0.187	0.210
0.272	0.306	0.236
0.272	0.420	0.255
0.272	0.584	0.278
0.272	0.838	0.311
0.272	1.07	0.331
0.272	1.48	0.361
0.272	1.83	0.380
0.272	2.14	0.393

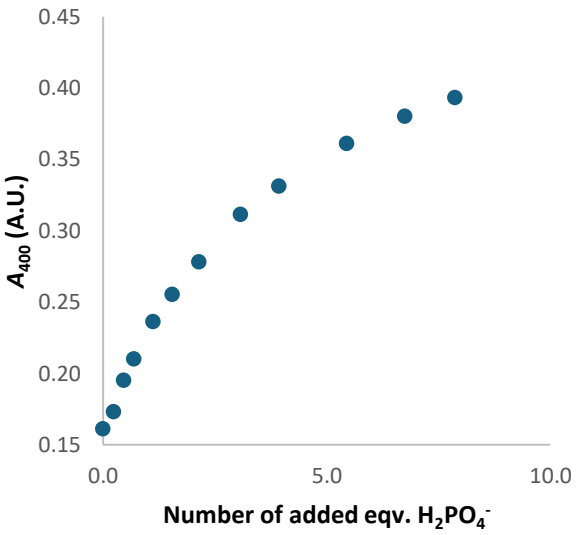

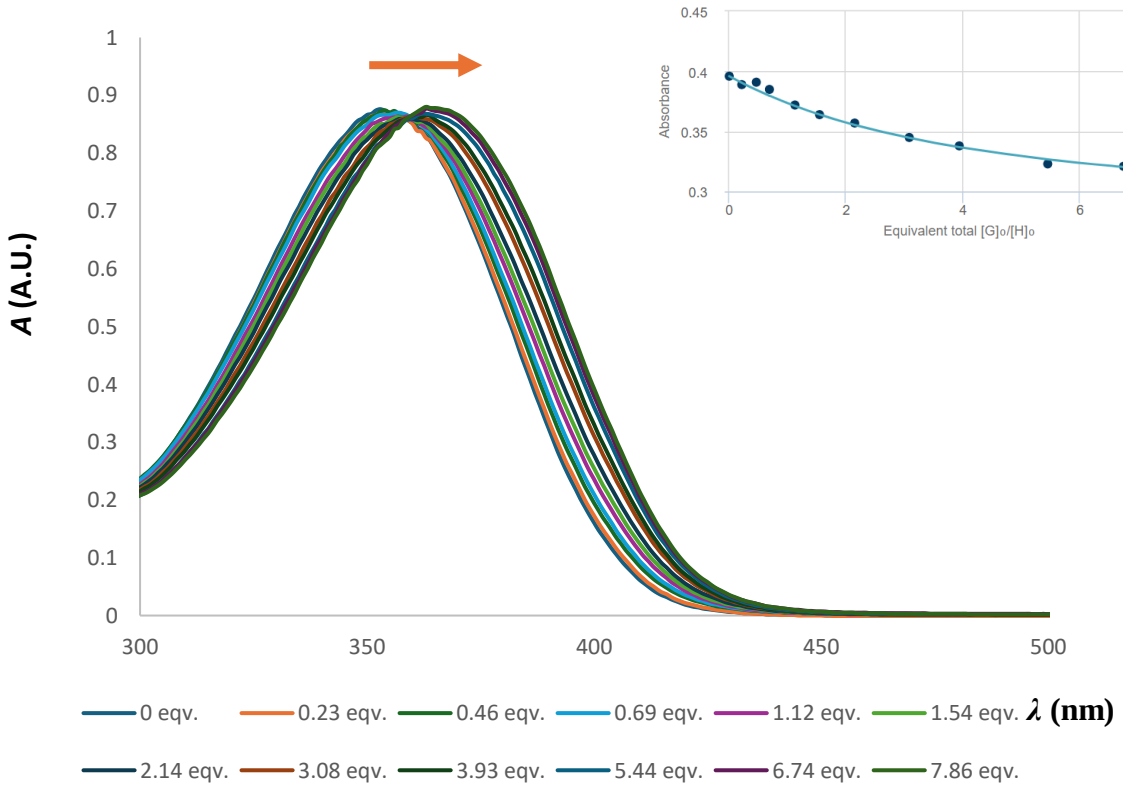

Fig. S44: Records of UV-Vis obtained for nitro substituted urea receptor **3a** (0.27 mM in DMSO) titrated with $TBAH_2PO_4$ (final concentration 2.14 mM) in a cuvette with 2-mm pathlength. The arrow indicates the direction of a bathochromic shift. There is a diagnostic window of representative fit exported from BindFit.

Link: http://app.supramolecular.org/bindfit/view/97cc9d00-1891-4ec4-b5d8-58bb0e96fb5e

c (**3a**) mM	*c* (AcO^-) mM	A_{400} (A.U.)
0.306	0	0.185
0.306	0.197	0.265
0.306	0.390	0.317
0.306	0.580	0.354
0.306	0.948	0.405
0.306	1.30	0.436
0.306	1.81	0.466
0.306	2.60	0.488
0.306	3.32	0.504
0.306	4.59	0.52
0.306	5.69	0.526
0.306	6.18	0.529

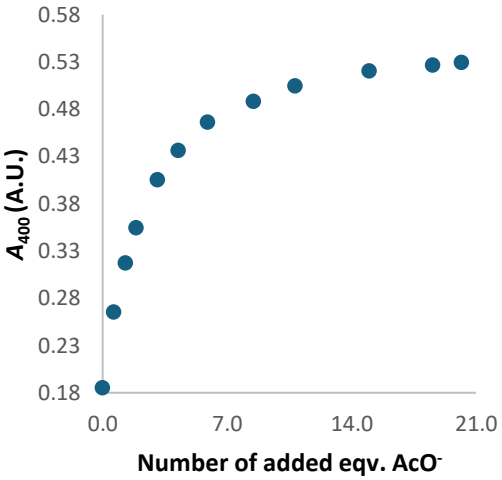

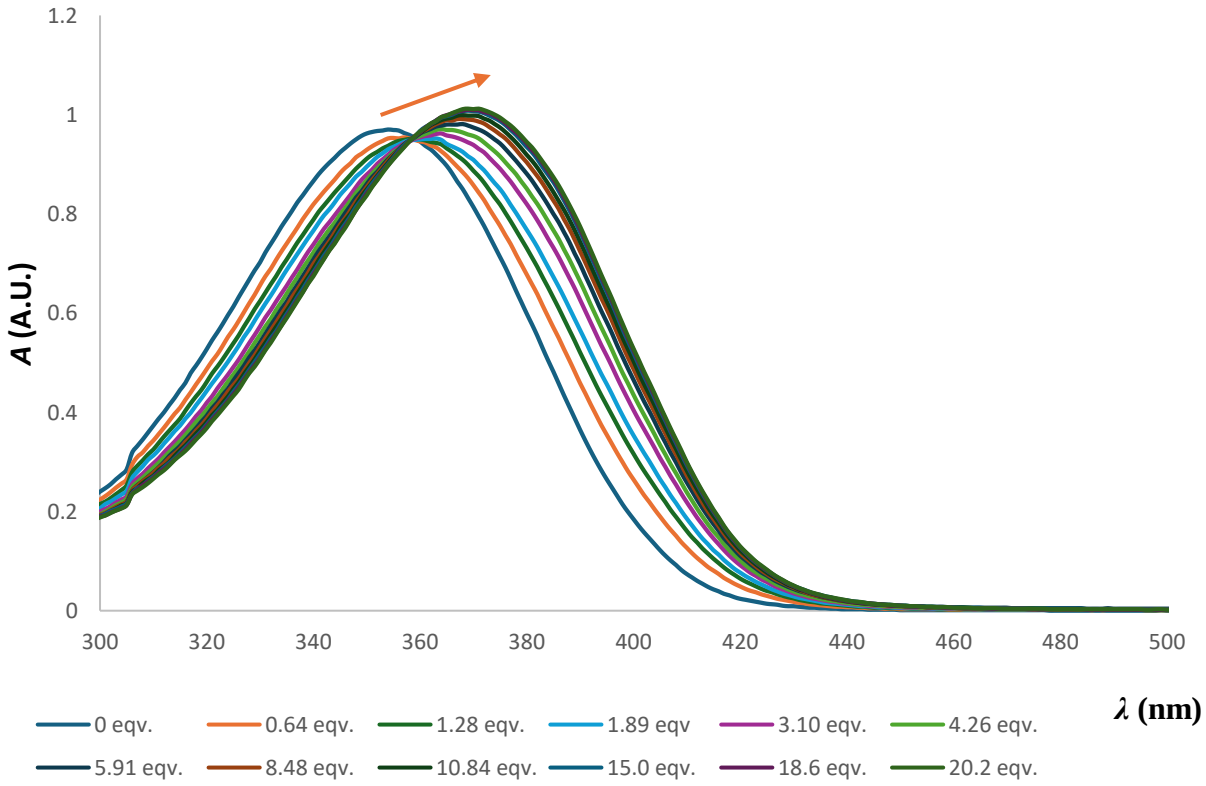

Fig. S45: Records of UV-Vis obtained for nitro substituted urea receptor **3a** (0.31 mM in DMSO) titrated with TBAAcO (final concentration 6.18 mM) in a cuvette with 2-mm pathlength. The arrow indicates the direction of a bathochromic shift.

c (**3a**) mM	*c* (BzO^-) mM	A_{400} (A.U.)
0.272	0	0.161
0.272	0.112	0.181
0.272	0.220	0.200
0.272	0.324	0.215
0.272	0.520	0.242
0.272	0.703	0.265
0.272	0.953	0.285
0.272	1.32	0.311
0.272	1.63	0.326
0.272	2.15	0.348
0.272	2.54	0.362

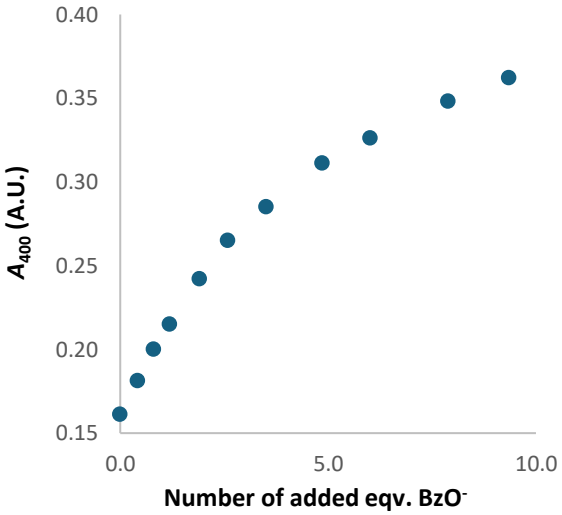

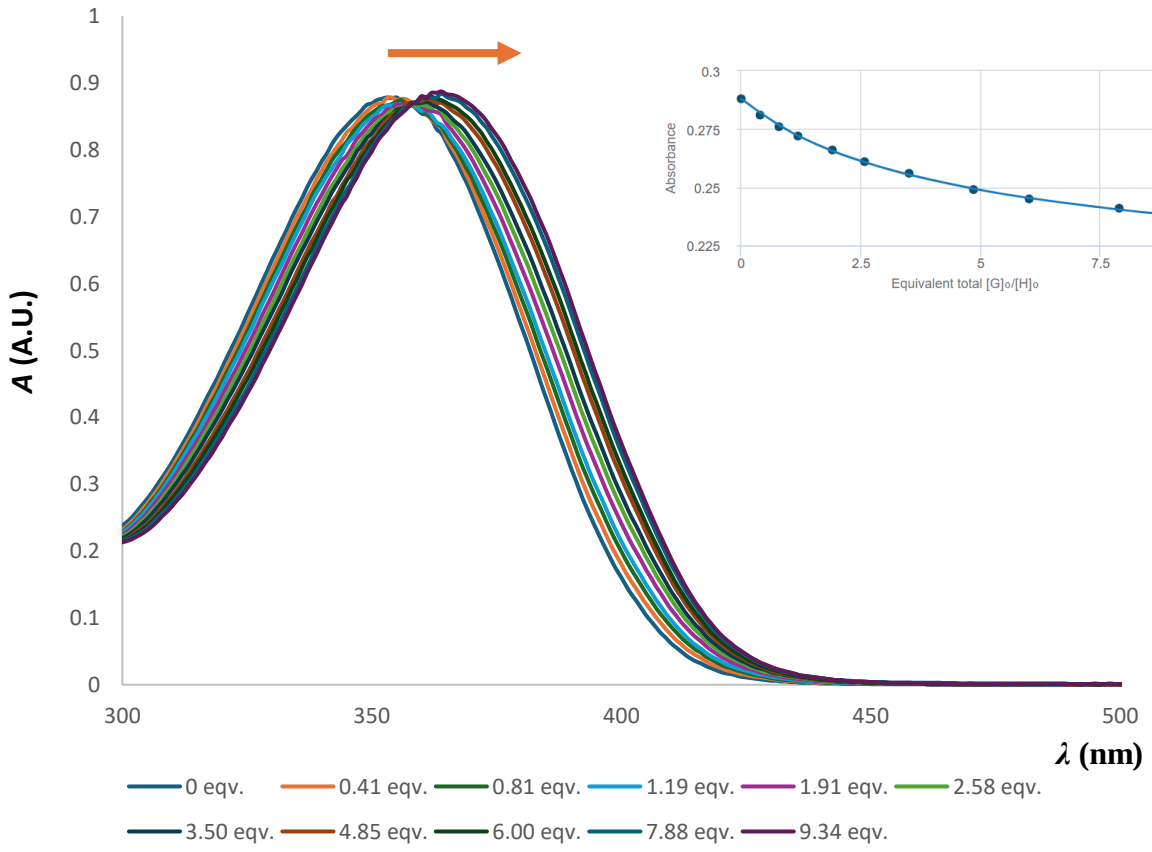

Fig. S46: Records of UV-Vis obtained for nitro substituted urea receptor **3a** (0.27 mM in DMSO) titrated with TBABzO (final concentration 2.54 mM) in a cuvette with 2-mm pathlength. The arrow indicates the direction of a bathochromic shift. There is a diagnostic window of representative fit exported from BindFit.

c (**3a**) mM	*c* (Cl^-) mM	δ_{NH} (ppm)
3.40	0	9.5560
3.40	2.01	9.6924
3.40	3.95	9.8229
3.40	5.82	9.9349
3.40	9.34	10.1142
3.40	12.6	10.2504
3.40	17.1	10.4025
3.40	23.7	10.5688
3.40	29.4	10.6781
3.40	38.5	10.8102
3.40	45.7	10.8858
3.40	103	11.1917

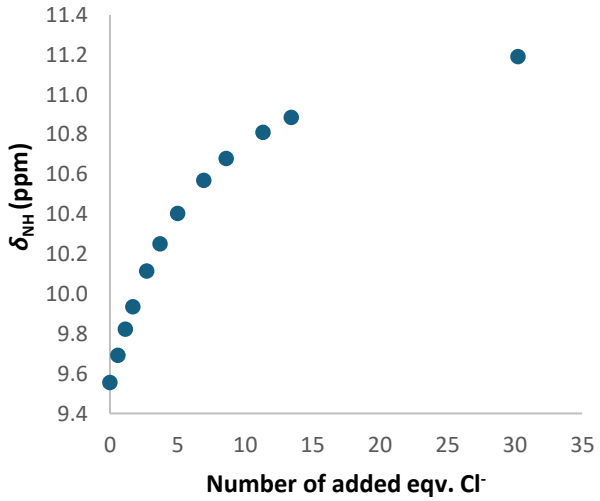

Link:

http://app.supramolecular.org/bindfit/view/cd0ada6e-6738-4fe5-a1ac-877367e024dd

c (**3a**) mM	*c* (HSO_4^-) mM	δ_{NH} (ppm)
4.39	0	9.5494
4.39	5.97	9.5640
4.39	11.7	9.5825
4.39	17.2	9.5964
4.39	27.7	9.6217
4.39	37.4	9.6440
4.39	50.7	9.6733
4.39	70.2	9.7108
4.39	86.9	9.7413
4.39	114	9.7852
4.39	149	9.8294
4.39	304	9.9560

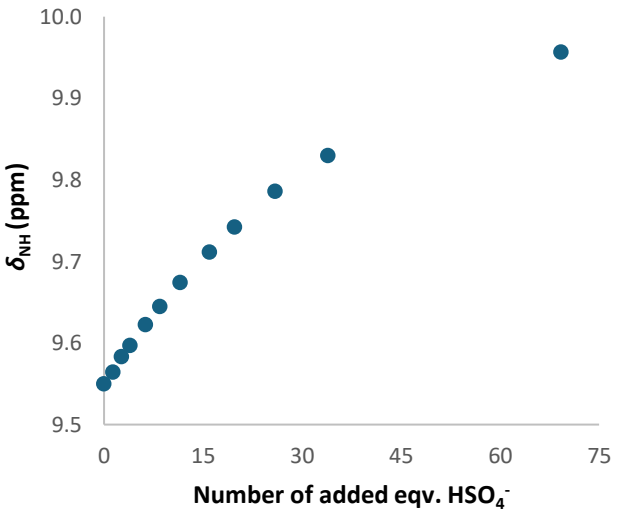

Link:

http://app.supramolecular.org/bindfit/view/1bbdaa74-e561-4c7c-b6e4-c83c8f331828

c (**3b**) mM	*c* ($H_2PO_4^-$) mM	δ_{NH} (ppm)
0.185	0	9.21
0.185	0.0982	9.27
0.185	0.193	9.39
0.185	0.285	9.51
0.185	0.461	9.77
0.185	0.626	9.96
0.185	0.856	10.18
0.185	1.20	10.41
0.185	1.50	10.57
0.185	2.00	10.73
0.185	2.40	10.80
0.185	5.99	11.22

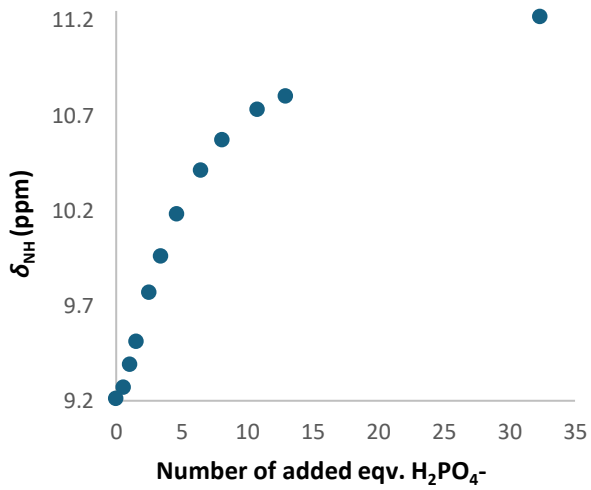

Link:
http://app.supramolecular.org/bindfit/view/b34bd805-645d-4b45-a8a1-7c7d88f7fbee

c (**3c**) mM	*c* ($H_2PO_4^-$) mM	δ_{NH} (ppm)
3.22	0	8.7269
3.22	0.789	9.0108
3.22	1.55	9.235
3.22	2.28	9.399
3.22	2.98	9.5287
3.22	3.66	9.6269
3.22	4.94	9.7737
3.22	6.71	9.9020
3.22	9.29	10.0324
3.22	15.1	10.1992
3.22	17.9	10.2415
3.22	40.3	10.5123

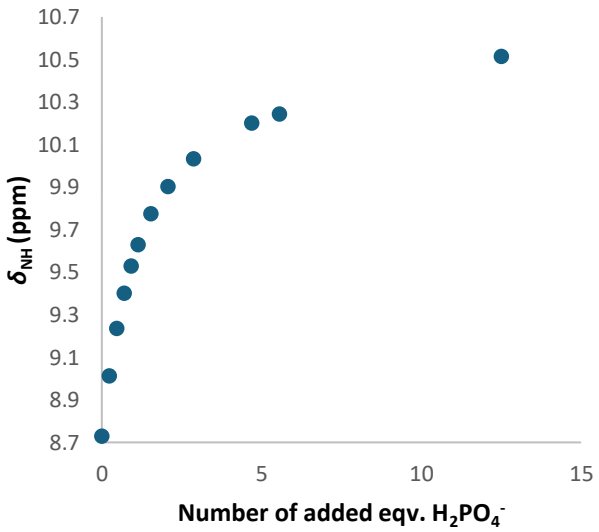

Link:

http://app.supramolecular.org/bindfit/view/d0359634-581a-4003-b650-4933808818a0

c (**3d**) mM	*c* ($H_2PO_4^-$) mM	δ_{NH} (ppm)
4.52	0	8.6105
4.52	2.57	9.1741
4.52	5.04	9.5522
4.52	7.41	9.7774
4.52	9.70	9.9192
4.52	11.9	10.021
4.52	16.1	10.1432
4.52	20.0	10.2294
4.52	25.4	10.296
4.52	33.2	10.364
4.52	45.9	10.4369
4.52	59.8	10.4693
4.52	131	10.5562

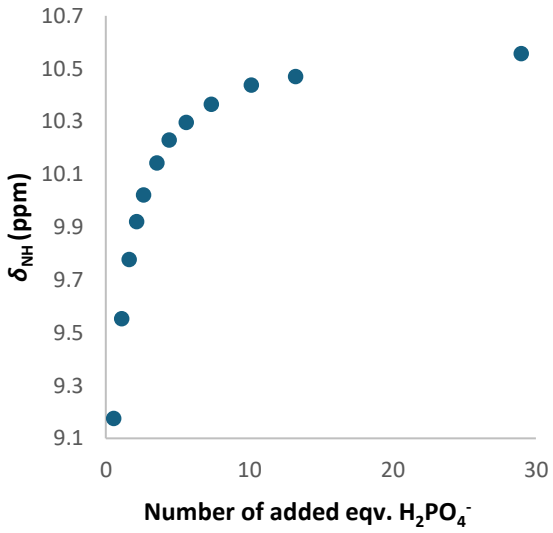

Link:

http://app.supramolecular.org/bindfit/view/f674b4d1-562f-4dab-8311-a163b6b3e6e0

c (**4**) mM	*c* (AcO^-) mM	A_{400} (A.U.)
0.276	0	0.180
0.276	0.083	0.200
0.276	0.165	0.219
0.276	0.246	0.236
0.276	0.404	0.265
0.276	0.559	0.29
0.276	0.783	0.316
0.276	1.14	0.346
0.276	1.47	0.366
0.276	2.09	0.388
0.276	2.64	0.399

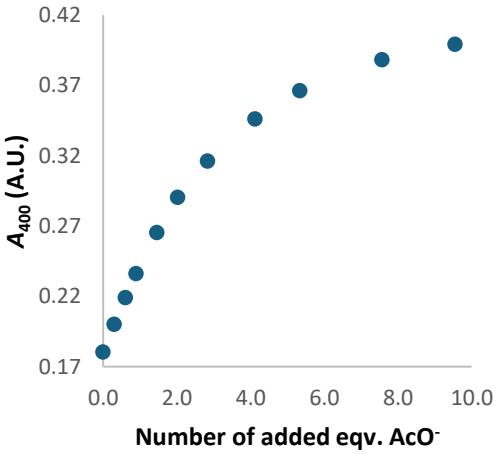

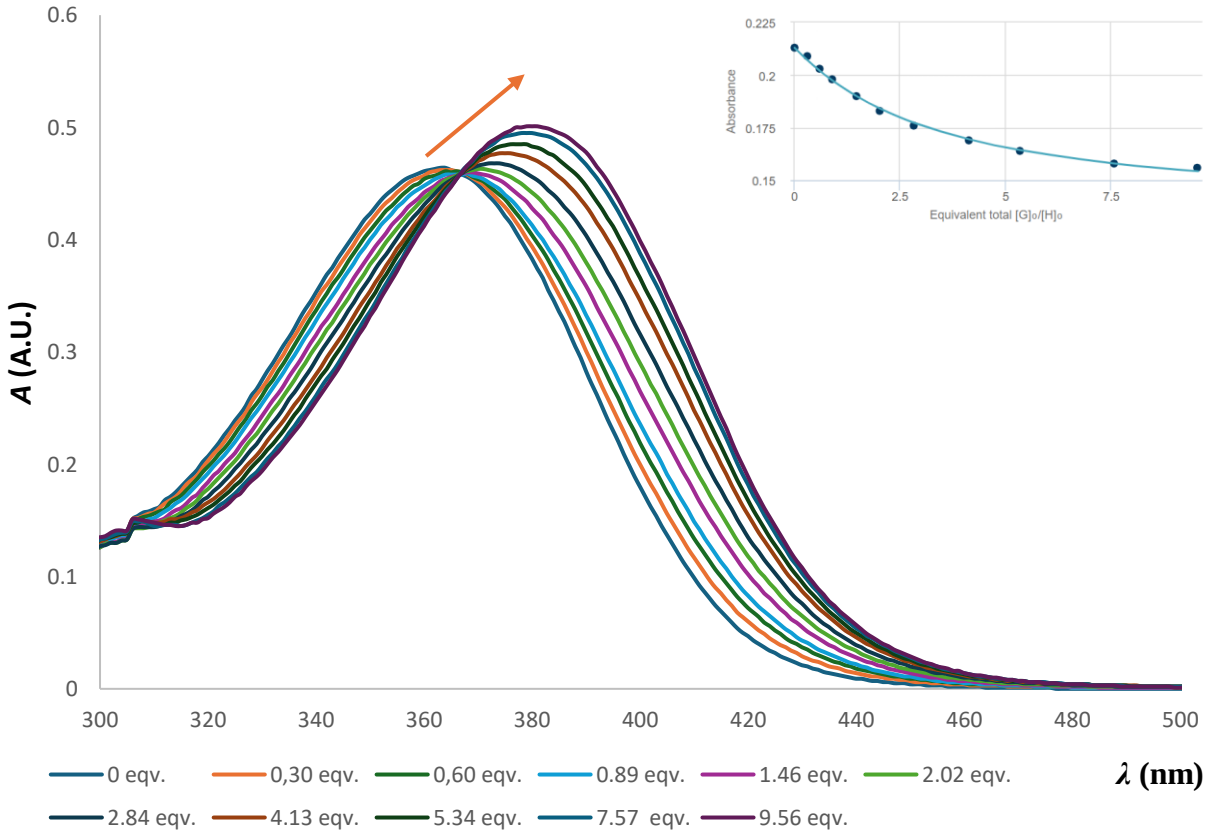

Fig. S47: Records of UV-Vis obtained for nitro substituted urea receptor **4** (0.28 mM in DMSO) titrated with TBABzO (final concentration 2.64 mM) in a cuvette with 1-mm pathlength. The arrow indicates the direction of a bathochromic shift. There is a diagnostic window of representative fit exported from BindFit.

c (**4**) mM	*c* (BzO^-) mM	A_{400} (A.U.)
0.276	0	0.170
0.276	0.113	0.189
0.276	0.222	0.207
0.276	0.327	0.222
0.276	0.525	0.246
0.276	0.709	0.261
0.276	0.963	0.280
0.276	1.33	0.302
0.276	1.65	0.315
0.276	2.17	0.328
0.276	5.78	0.391

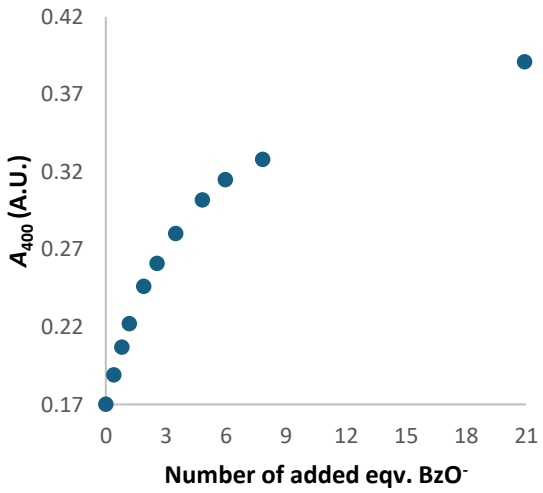

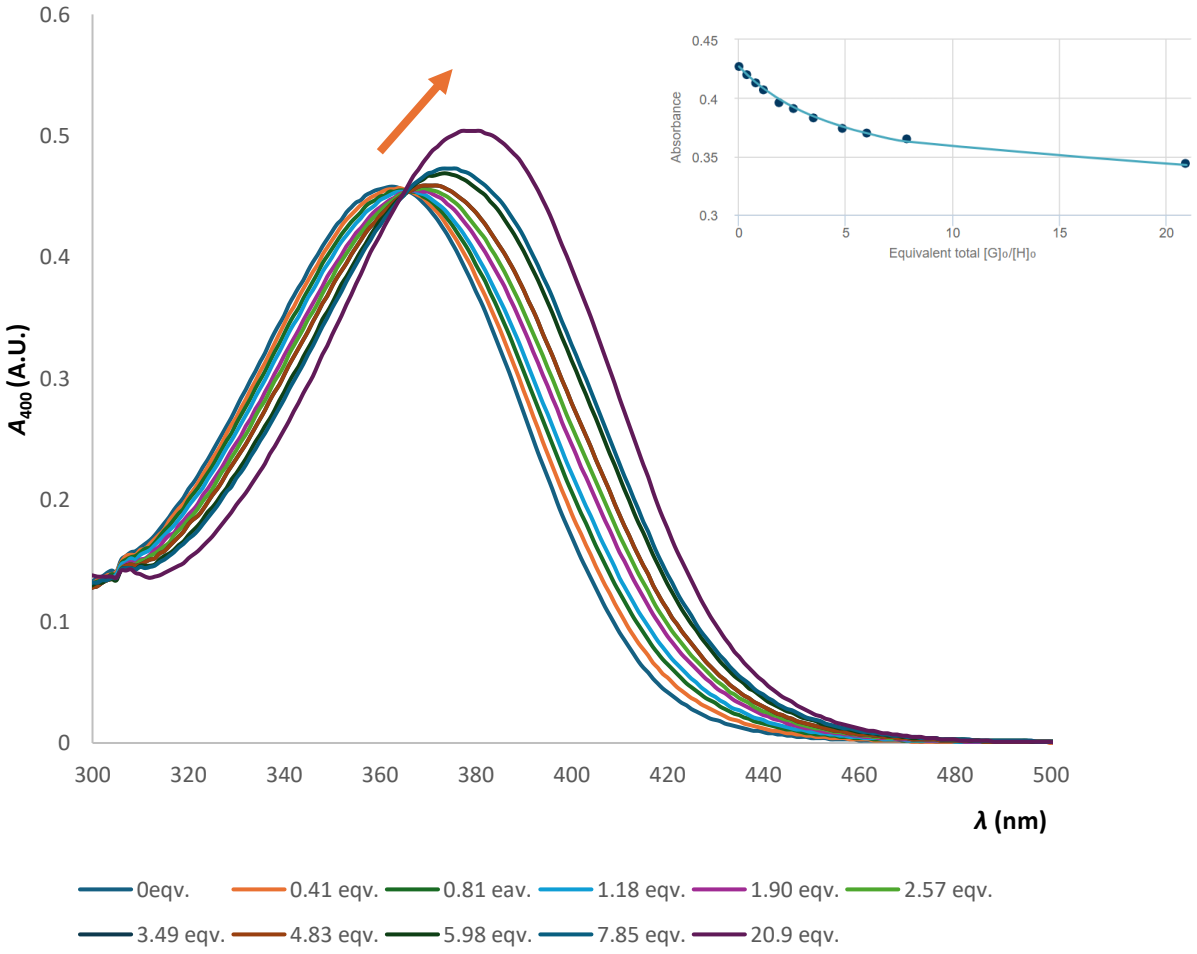

Fig. S48: Records of UV-Vis obtained for nitro substituted urea receptor **4** (0.28 mM in DMSO) titrated with TBABzO (final concentration 5.78 mM) in a cuvette with 1-mm pathlength. The arrow indicates the direction of a bathochromic shift. There is a diagnostic window of representative fit exported from BindFit.

c (**4**) mM	*c* (Cl^-) mM	δ_{NH} (ppm)
3.47	0	9.1715
3.47	2.05	9.3010
3.47	4.03	9.4165
3.47	5.93	9.5093
3.47	9.52	9.6663
3.47	12.9	9.7905
3.47	17.5	9.9344
3.47	24.2	10.1001
3.47	29.9	10.2091
3.47	39.3	10.3474
3.47	49.6	10.4481
3.47	105	10.7969

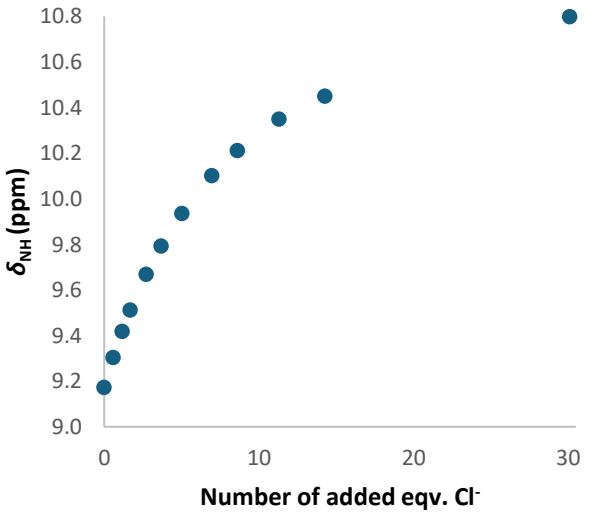

Link:

http://app.supramolecular.org/bindfit/view/35659b87-a2e3-4083-aaa1-970faff60cb0

c (**4**) mM	*c* (HSO_4^-) mM	δ_{NH} (ppm)
5.87	0	9.1686
5.87	5.72	9.2203
5.87	11.2	9.2549
5.87	16.5	9.2843
5.87	26.5	9.3313
5.87	35.9	9.3706
5.87	48.7	9.4223
5.87	67.4	9.4889
5.87	83.4	9.5423
5.87	109	9.6177
5.87	144	9.7004
5.87	292	9.9040

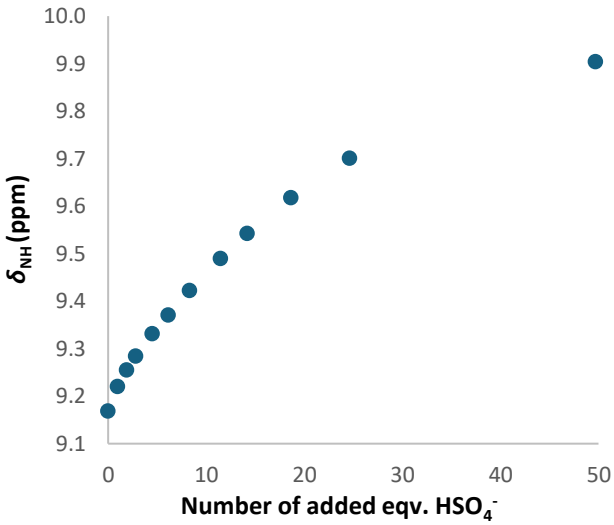

Link:

http://app.supramolecular.org/bindfit/view/bbd1e8d0-59a5-4d73-9579-d464e7405564

c (**7a**) mM	*c* ($H_2PO_4^-$) mM	δ_{NH} (ppm)
0.229	0	9.6069
0.229	0.118	9.8349
0.229	0.231	10.0231
0.229	0.340	10.180
0.229	0.546	10.489
0.229	0.738	10.708
0.229	1.00	10.934
0.229	1.39	11.166
0.229	1.72	11.318
0.229	2.25	11.450
0.229	2.67	11.560
0.229	6.01	11.849

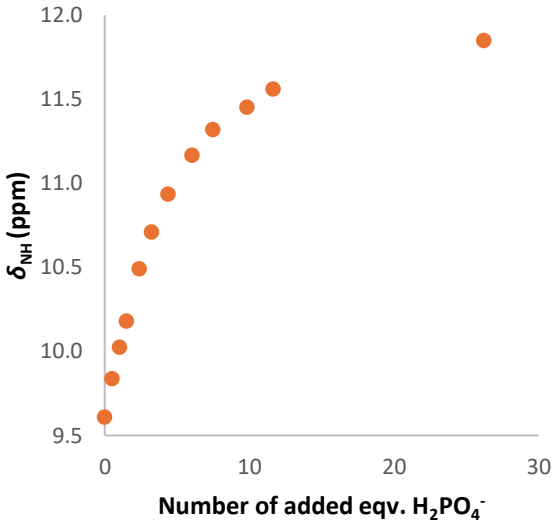

Link:

http://app.supramolecular.org/bindfit/view/a332e095-ef92-499b-a074-dd18aa318dc9

c (**7a**) mM	*c* (BzO^-) mM	δ_{NH} (ppm)
0.344	0	9.5989
0.344	0.133	9.8239
0.344	0.260	9.9989
0.344	0.383	10.1819
0.344	0.615	10.4920
0.344	0.831	10.7139
0.344	1.13	10.9677
0.344	1.56	11.2622
0.344	1.93	11.4650
0.344	2.54	11.7044
0.344	3.01	11.8315
0.344	6.77	12.4318

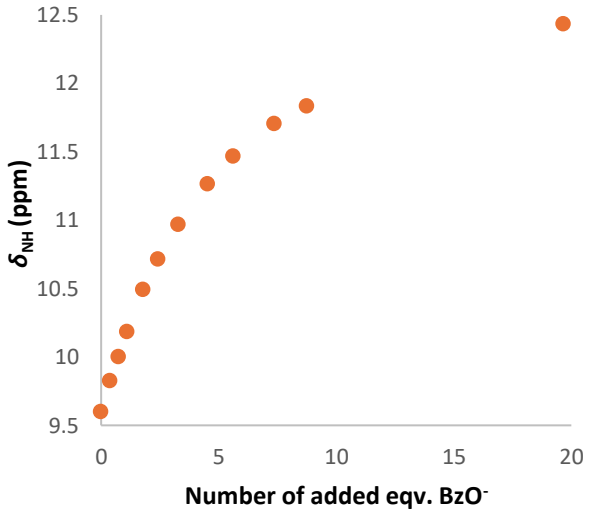

Link:

http://app.supramolecular.org/bindfit/view/32b2bbd9-4e94-49f7-ba0b-b95f207b116c

c (**7a**) mM	*c* (AcO^-) mM	δ_{NH} (ppm)
0.229	0	9.6305
0.229	0.163	10.0071
0.229	0.319	10.3405
0.229	0.469	10.6211
0.229	0.754	11.1409
0.229	1.02	11.4883
0.229	1.38	11.8202
0.229	1.91	12.0981
0.229	2.37	12.2701
0.229	3.11	12.4516
0.229	3.69	12.5395
0.229	8.29	12.8357

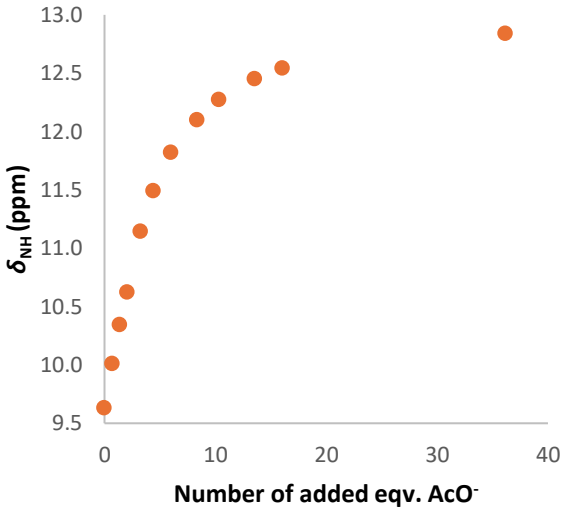

Link:

http://app.supramolecular.org/bindfit/view/a086255e-be72-43c2-a274-ca5c4e64690c

c (**8a**) mM	*c* ($H_2PO_4^-$) mM	A_{390} (A.U.)
0.214	0	0.368
0.214	0.0700	0.434
0.214	0.139	0.505
0.214	0.206	0.54
0.214	0.337	0.595
0.214	0.463	0.614
0.214	0.643	0.632
0.214	0.922	0.642
0.214	1.18	0.652
0.214	1.63	0.661
0.214	2.02	0.668
0.214	2.19	0.670

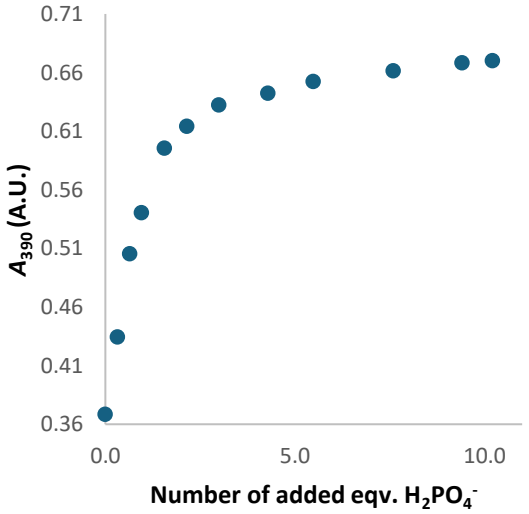

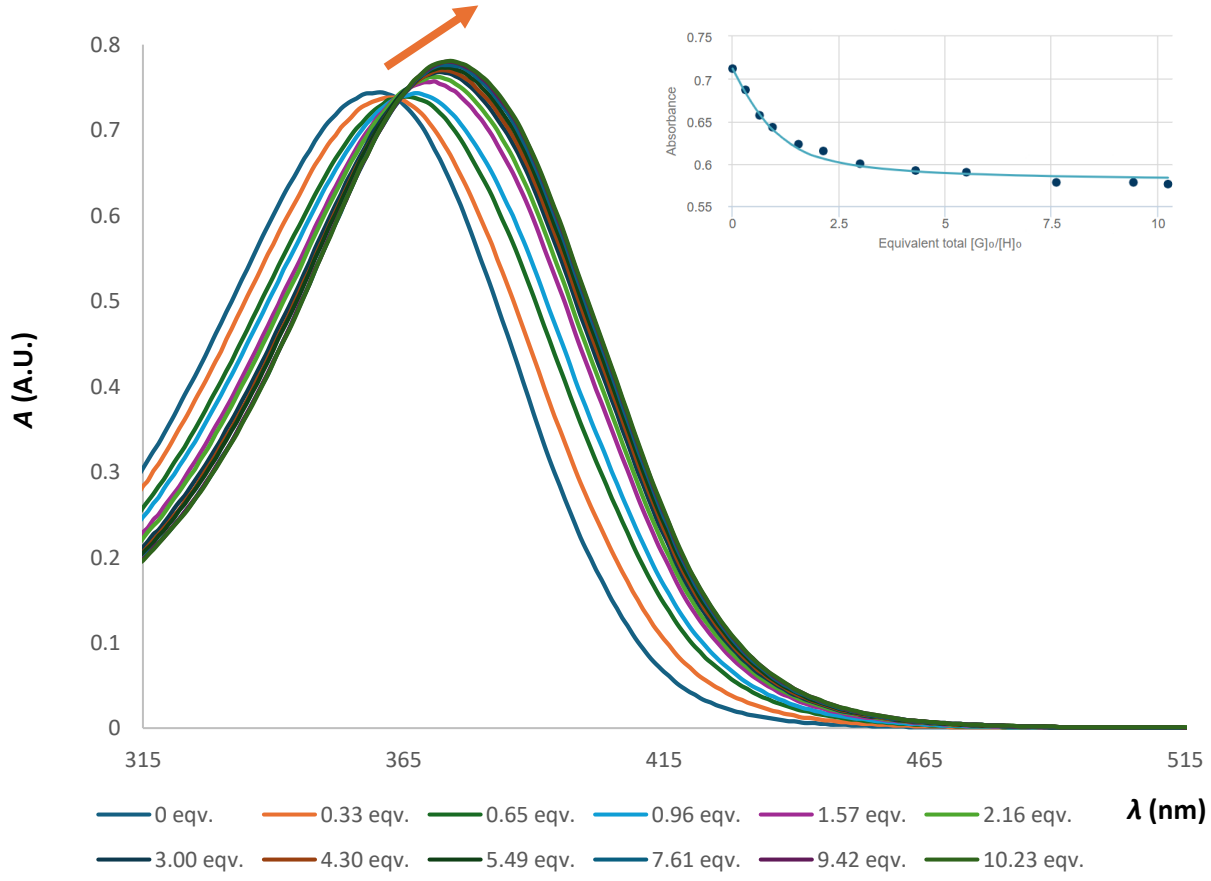

Fig. S49: Records of UV-Vis obtained for nitro substituted urea receptor **8a** (0.21 mM in DMSO) titrated with $TBAH_2PO_4$ (final concentration 2.19 mM) in a cuvette with 1-mm pathlength. The arrow indicates the direction of a bathochromic shift. There is a diagnostic window of representative fit exported from BindFit.

c (**8a**) mM	*c* (AcO^-) mM	A_{390} (A.U.)
0.214	0	0.369
0.214	0.0653	0.416
0.214	0.130	0.458
0.214	0.194	0.494
0.214	0.320	0.539
0.214	0.444	0.568
0.214	0.625	0.596
0.214	0.859	0.617
0.214	1.19	0.642
0.214	1.41	0.656
0.214	1.71	0.668
0.214	1.91	0.672
0.214	2.19	0.683
0.214	2.63	0.693

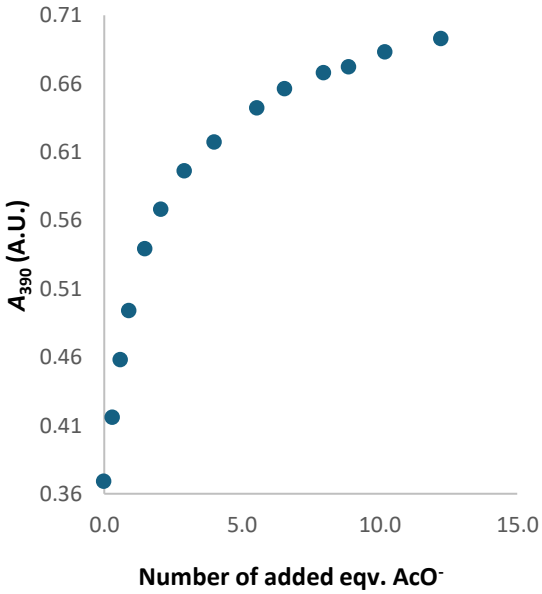

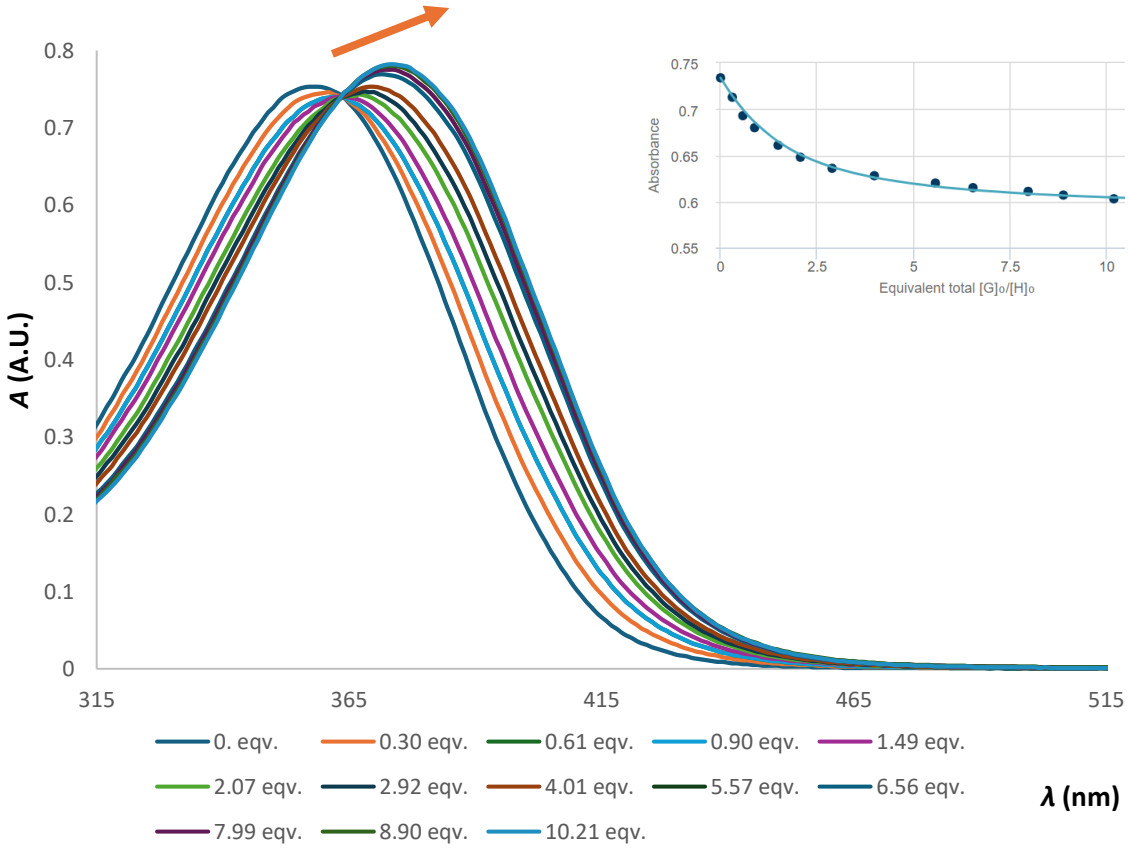

Fig. S50: Records of UV-Vis obtained for nitro substituted urea receptor **8a** (0.21 mM in DMSO) titrated with TBAAcO (final concentration 2.63 mM) in a cuvette with 1-mm pathlength. The arrow indicates the direction of a bathochromic shift. There is a diagnostic window of representative fit exported from BindFit.

c (**8a**) mM	*c* (BzO^-) mM	A_{390} (A.U.)
0.208	0	0.357
0.208	0.0599	0.39
0.208	0.119	0.412
0.208	0.176	0.428
0.208	0.288	0.456
0.208	0.396	0.478
0.208	0.550	0.499
0.208	0.789	0.528
0.208	1.01	0.545
0.208	1.40	0.570
0.208	1.73	0.584
0.208	1.88	0.590

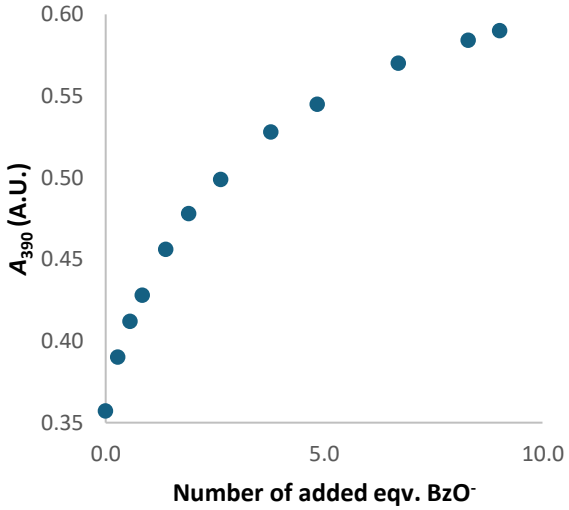

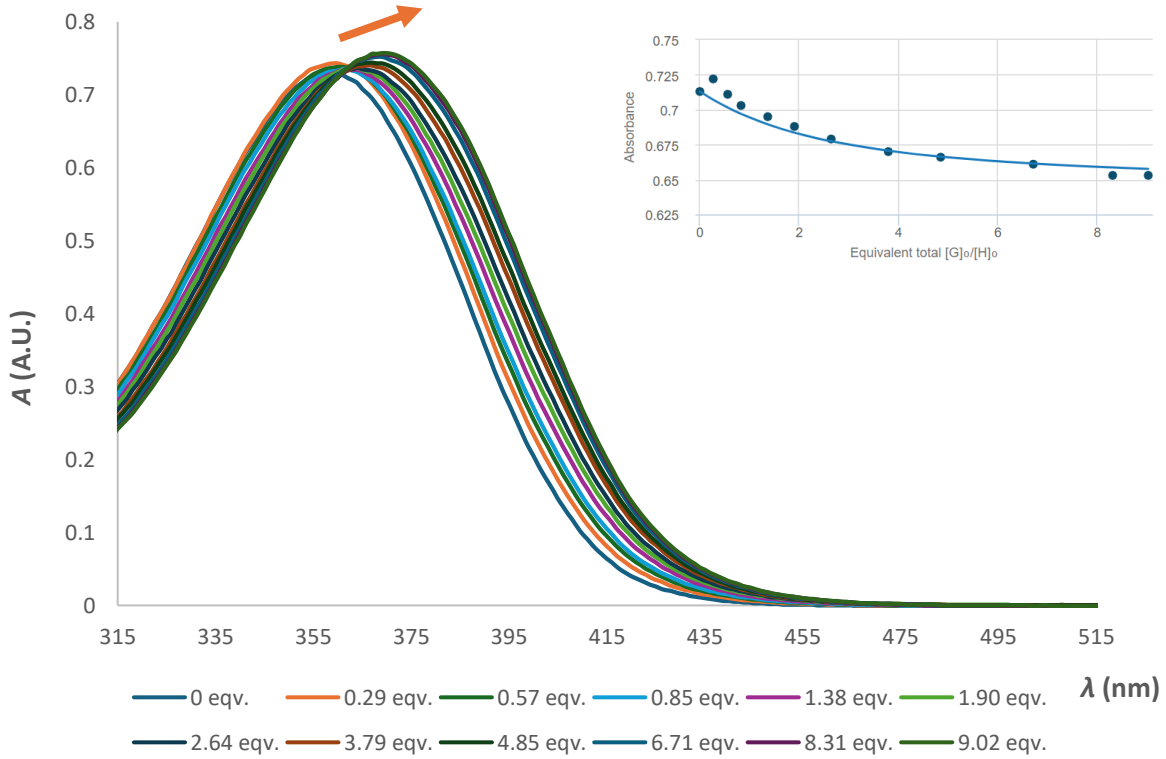

Fig. S51: Records of UV-Vis obtained for nitro substituted urea receptor **8a** (0.21 mM in DMSO) titrated with TBABzO (final concentration 1.88 mM) in a cuvette with 1-mm pathlength. The arrow indicates the direction of a bathochromic shift. There is a diagnostic window of representative fit exported from BindFit.

c (**8a**) mM	*c* (Cl^-) mM	δ_{NH} (ppm)
5.85	0	9.5559
5.85	3.55	9.7047
5.85	6.97	9.8449
5.85	10.3	9.9711
5.85	16.5	10.1512
5.85	22.3	10.2839
5.85	30.2	10.4275
5.85	41.8	10.5931
5.85	51.8	10.7029
5.85	68.0	10.8422
5.85	87.8	10.9573
5.85	181	11.2648

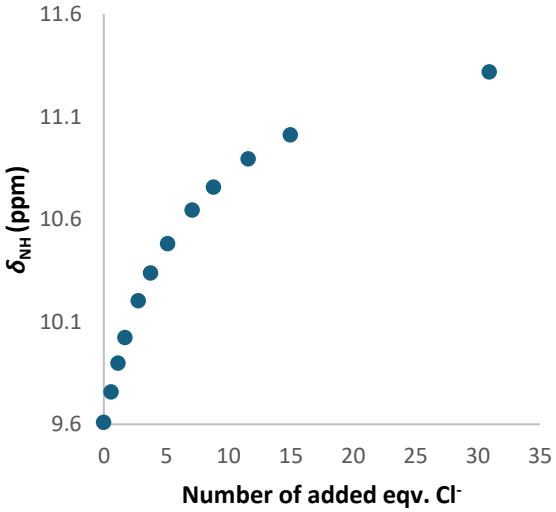

Link:

http://app.supramolecular.org/bindfit/view/21850989-9fe4-4348-a105-814e830ff6c1

c (**8a**) mM	*c* (HSO_4^-) mM	δ_{NH} (ppm)
7.18	0	9.5555
7.18	3.24	9.5676
7.18	6.36	9.5789
7.18	9.36	9.5883
7.18	15.0	9.6032
7.18	20.3	9.6157
7.18	27.5	9.6322
7.18	38.1	9.6491
7.18	47.2	9.6674
7.18	62.0	9.6859
7.18	73.5	9.6995
7.18	81.0	9.7202
7.18	165	9.8060

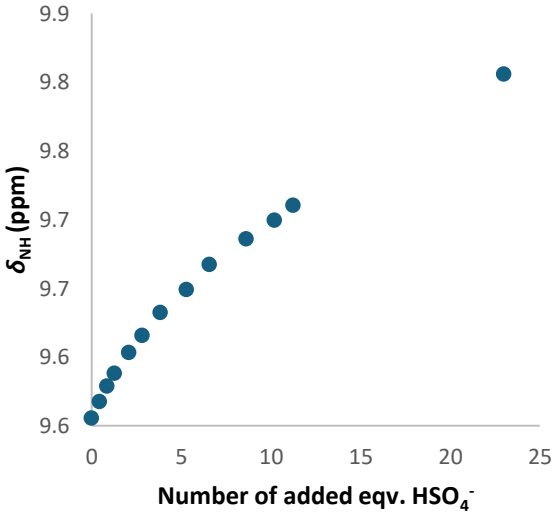

Link:

http://app.supramolecular.org/bindfit/view/c7d6567f-0cfe-4084-904b-0d9162ea38c4

c (**9**) mM	*c* ($H_2PO_4^-$) mM	A_{390} (A.U.)
0.210	0.000	0.399
0.210	0.0642	0.409
0.210	0.127	0.421
0.210	0.189	0.433
0.210	0.309	0.449
0.210	0.424	0.462
0.210	0.589	0.474
0.210	0.845	0.489
0.210	1.08	0.500
0.210	1.50	0.512
0.210	1.85	0.519
0.210	2.01	0.523

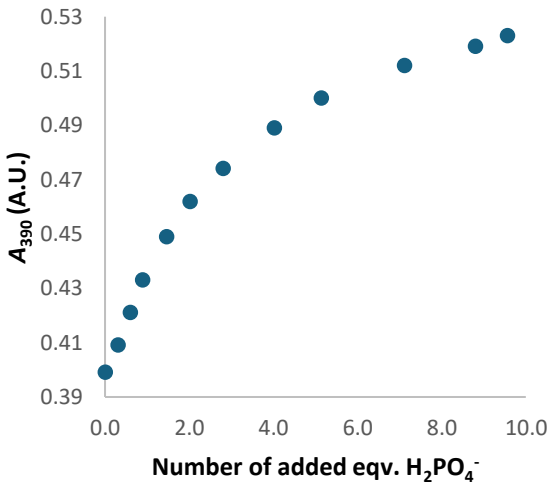

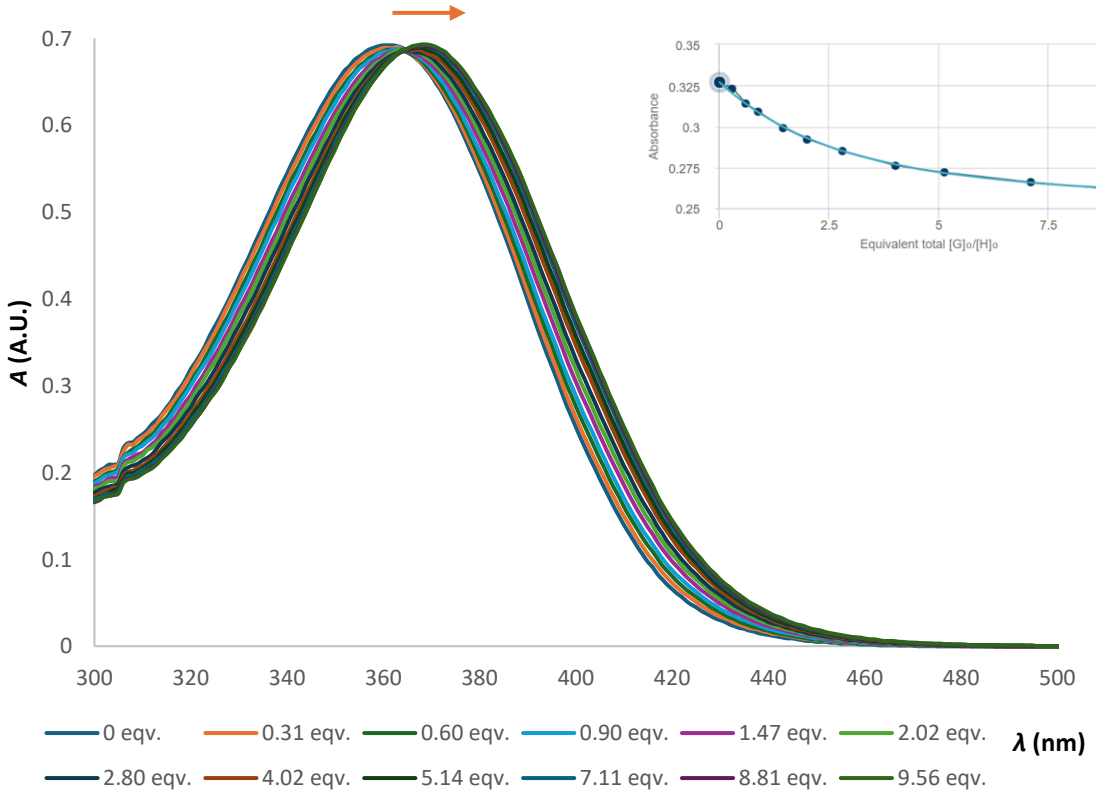

Fig. S52: Records of UV-Vis obtained for nitro substituted urea receptor **9** (0.21 mM in DMSO) titrated with $TBAH_2PO_4$ (final concentration 2.01 mM) in a cuvette with 1-mm pathlength. The arrow indicates the direction of a bathochromic shift.

6. Electrochemistry

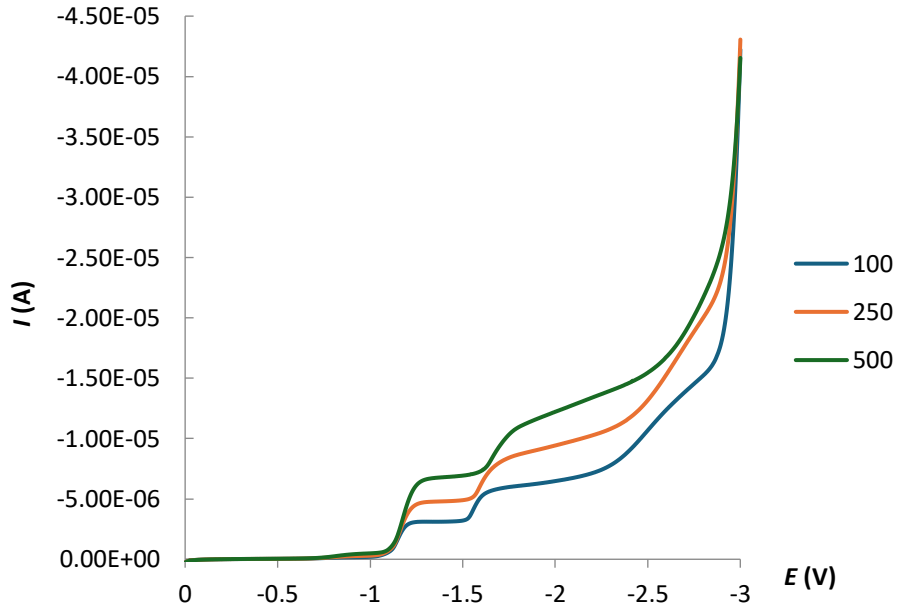

Fig. S53: Linear sweep voltammetry of receptor **4** ($1.1 \cdot 10^{-3}$ M) in DMSO (0.1 M $TBAPF_6$) (W = RDE = glassy carbon - ⌀ 1 mm, Ref = SCE, Aux = Pt) was recorded with a scan rate of 10 $mV \cdot s^{-1}$ using several rotating rates.

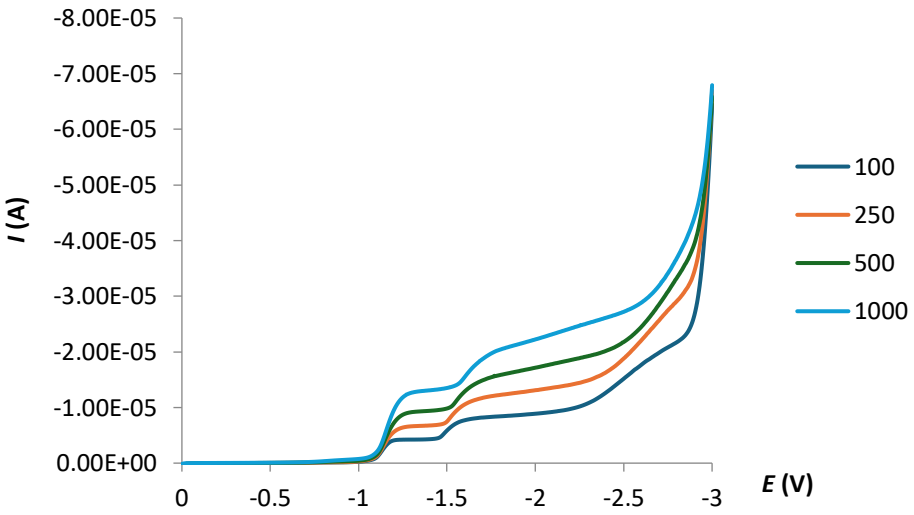

Fig. S54: Linear sweep voltammetry of **7a** ($8.6 \cdot 10^{-4}$ M) in DMSO (0.1 M $TBAPF_6$) (W = RDE = glassy carbon - ⌀ 1 mm, Ref = SCE, Aux = Pt) was recorded with a scan rate of 10 $mV \cdot s^{-1}$ using several rotating rates.

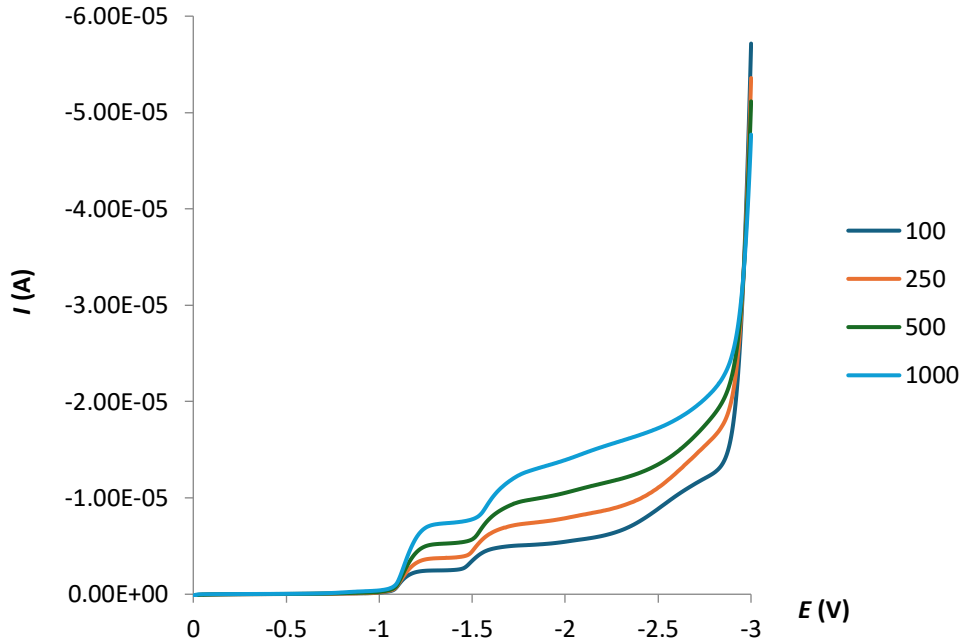

Fig. S55: Linear sweep voltammetry of **8a** ($4.9 \cdot 10^{-4}$ M) in DMSO (0.1 M $TBAPF_6$) (W = RDE = glassy carbon - ⌀ 1 mm, Ref = SCE, Aux = Pt) was recorded with a scan rate of 10 $mV \cdot s^{-1}$ using several rotating rates.

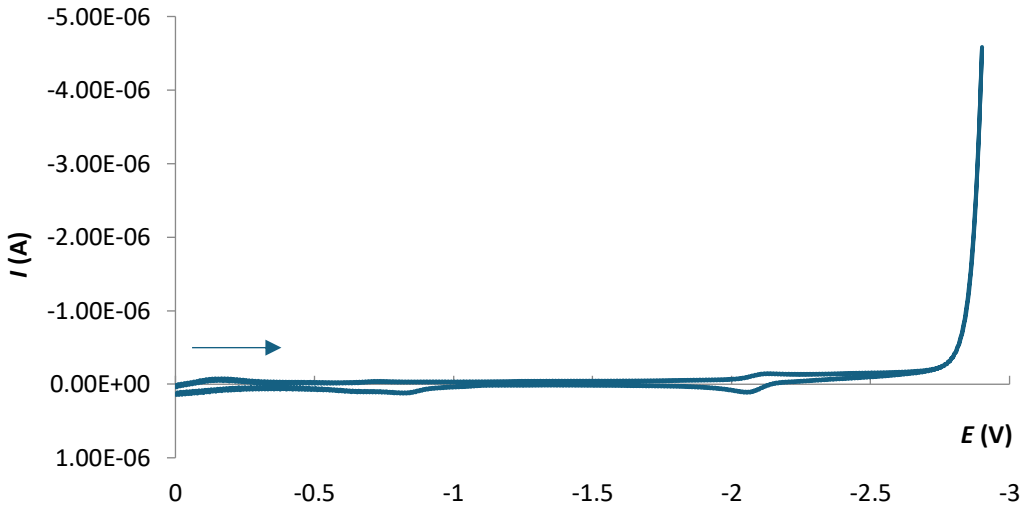

Fig. S56: Cyclic voltammogram (W = HMDE) of typical blank of DMSO (0.1 M $TBAPF_6$) with scan rate 100 $mV \cdot s^{-1}$ (gradually increasing potential range).

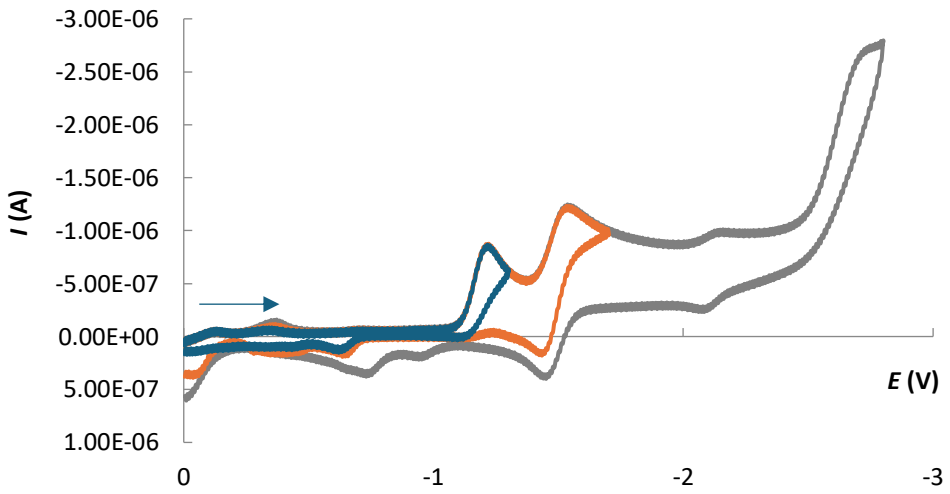

Fig. S57: Cyclic voltammogram (W = HMDE) of compound **3a** ($8.9 \cdot 10^{-4}$ M) in DMSO (0.1 M $TBAPF_6$) with scan rate 100 $mV \cdot s^{-1}$ (gradually increasing potential range).

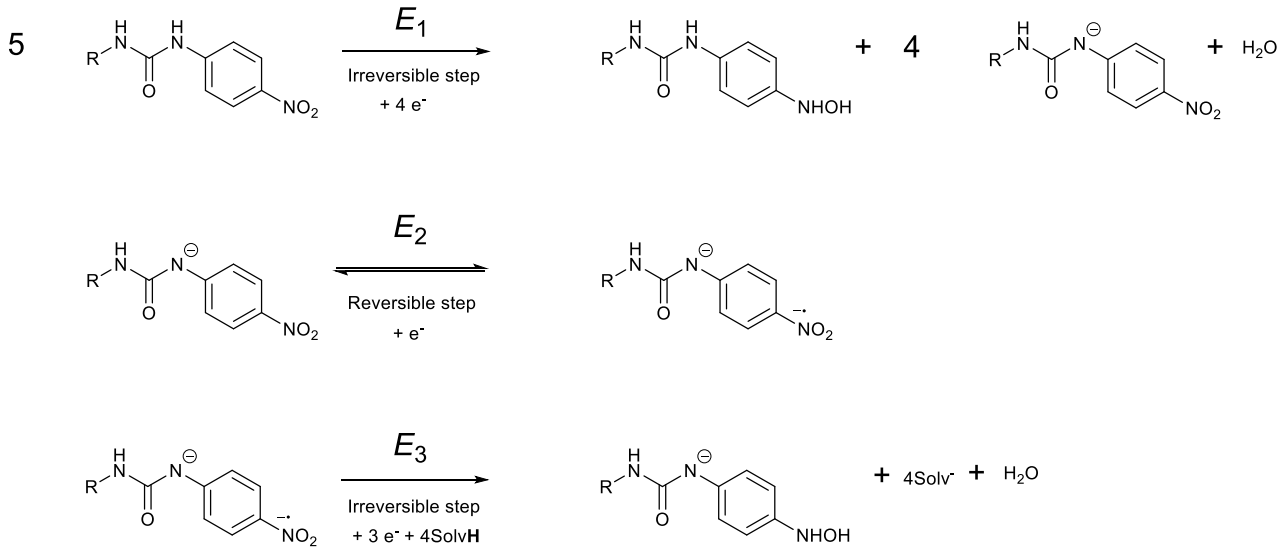

Scheme S58: Self-protonation reduction mechanism describing the reduction of nitro derivatives. The potentials of three reduction steps might be obtained from the cyclic voltammogram above (e.g. Fig. S57).

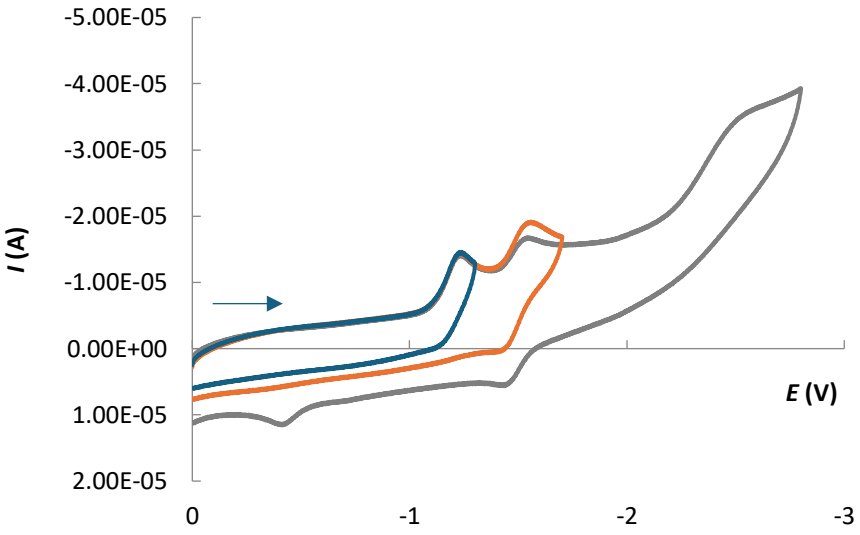

Fig. S59: Cyclic voltammogram (W = GC) of compound **3a** ($8.9 \cdot 10^{-4}$ M) in DMSO (0.1 M $TBAPF_6$) with scan rate 200 $mV \cdot s^{-1}$ (gradually increasing potential range).

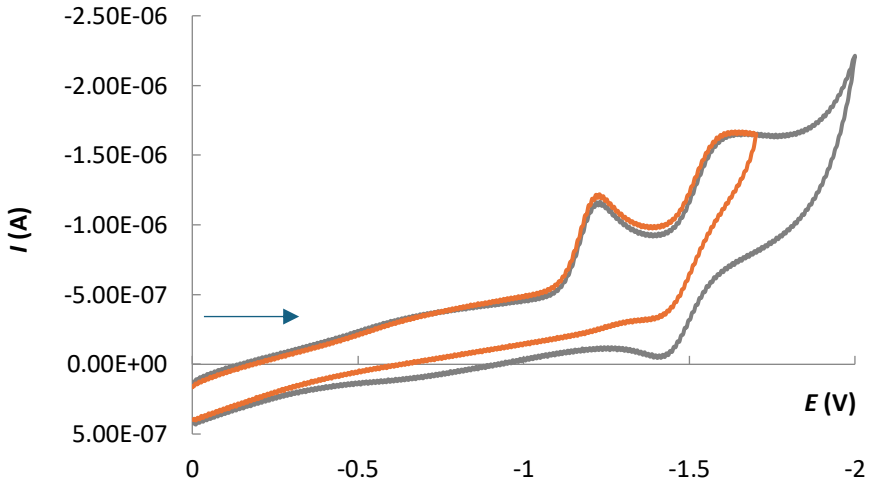

Fig. S60: Cyclic voltammogram (W = Pt) of compound **3a** ($8.9 \cdot 10^{-4}$ M) in DMSO (0.1 M $TBAPF_6$) with scan rate 100 $mV \cdot s^{-1}$ (gradually increasing potential range).

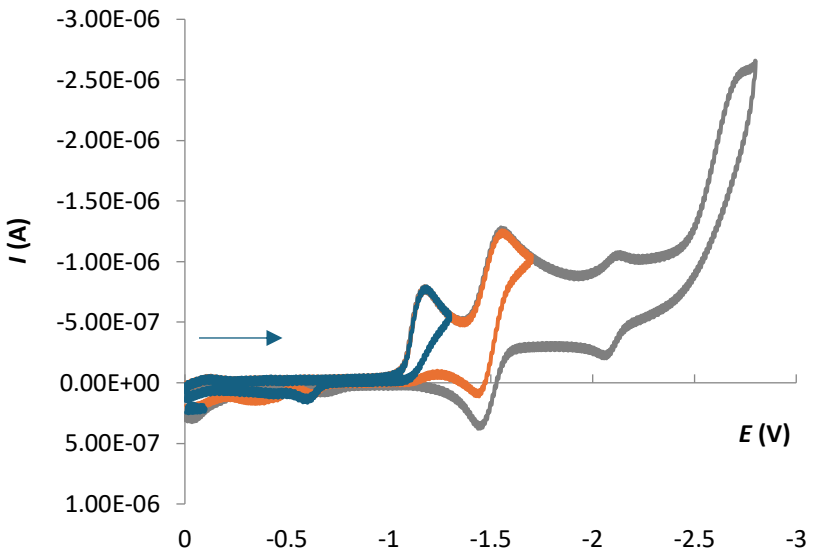

Fig. S61: Cyclic voltammogram (W = HMDE) of compound **4** ($1.1 \cdot 10^{-3}$ M) in DMSO (0.1 M $TBAPF_6$) with scan rate 100 $mV \cdot s^{-1}$ (gradually increasing potential range).

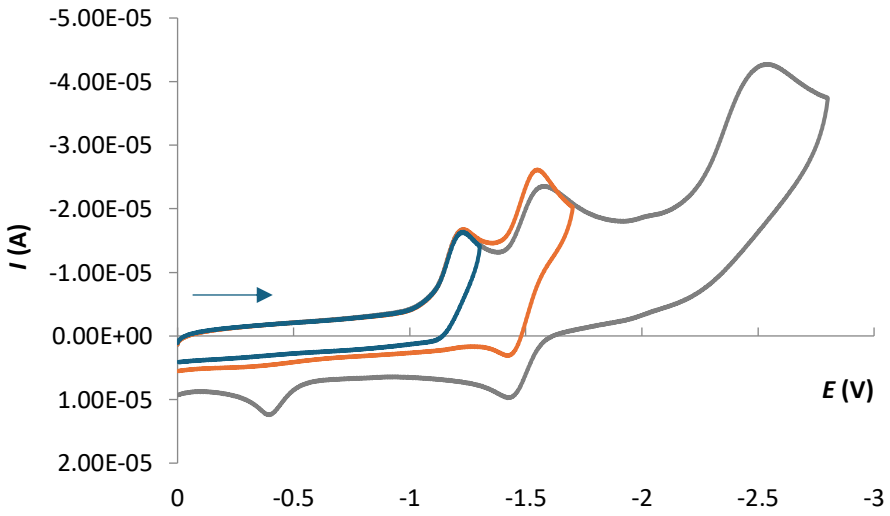

Fig. S62: Cyclic voltammogram (W = GC) of compound **4** ($1.1 \cdot 10^{-3}$ M) in DMSO (0.1 M $TBAPF_6$) with scan rate 200 $mV \cdot s^{-1}$ (gradually increasing potential range).

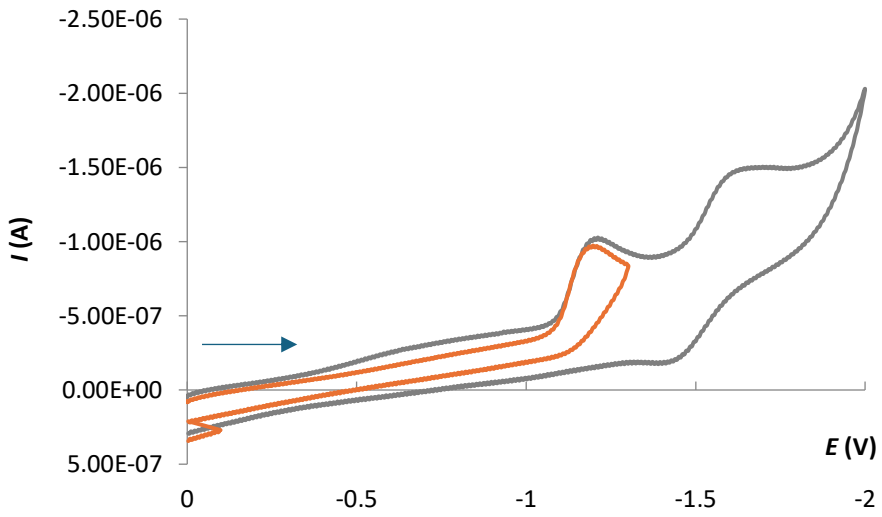

Fig. S63: Cyclic voltammogram (W = Pt) of compound **4** ($1.1 \cdot 10^{-3}$ M) in DMSO (0.1 M $TBAPF_6$) with scan rate 100 $mV \cdot s^{-1}$ (gradually increasing potential range).

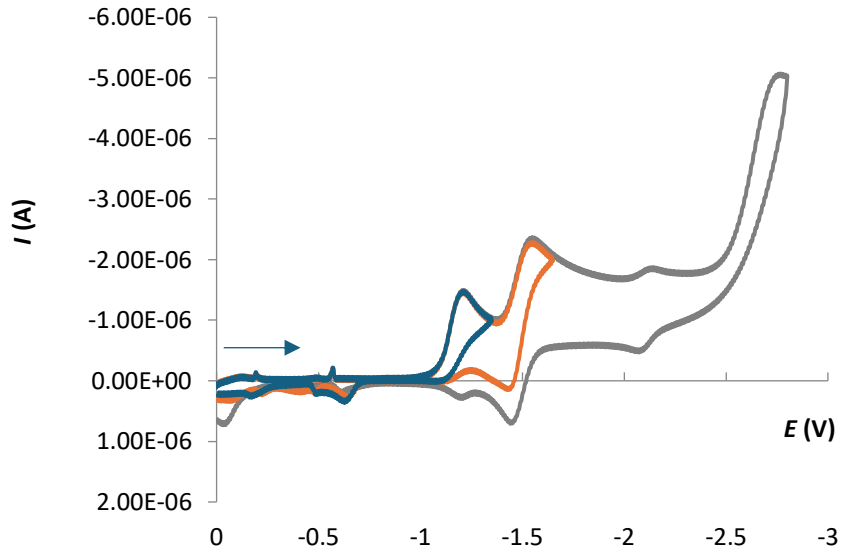

Fig. S64: Cyclic voltammogram (W = HMDE) of compound **7a** ($8.6 \cdot 10^{-4}$ M) in DMSO (0.1 M $TBAPF_6$) with scan rate 100 $mV \cdot s^{-1}$ (gradually increasing potential range).

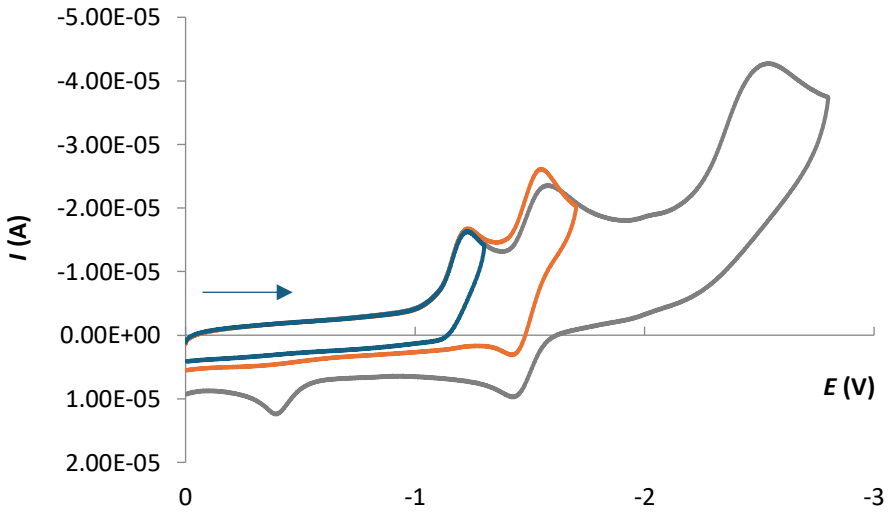

Fig. S65: Cyclic voltammogram (W = GC) of compound **7a** ($8.6 \cdot 10^{-4}$ M) in DMSO (0.1 M $TBAPF_6$) with scan rate 200 $mV \cdot s^{-1}$ (gradually increasing potential range).

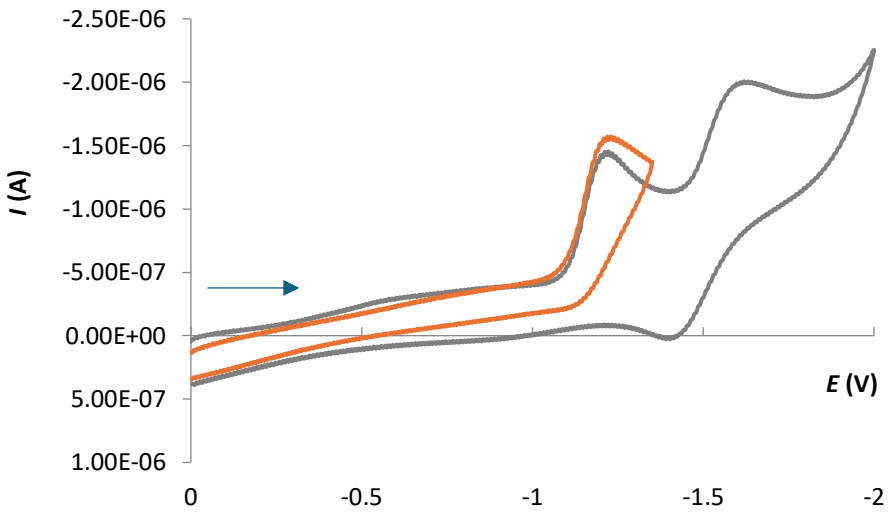

Fig. S66: Cyclic voltammogram (W = Pt) of compound **7a** ($8.6 \cdot 10^{-4}$ M) in DMSO (0.1 M $TBAPF_6$) with scan rate 100 $mV \cdot s^{-1}$ (gradually increasing potential range).

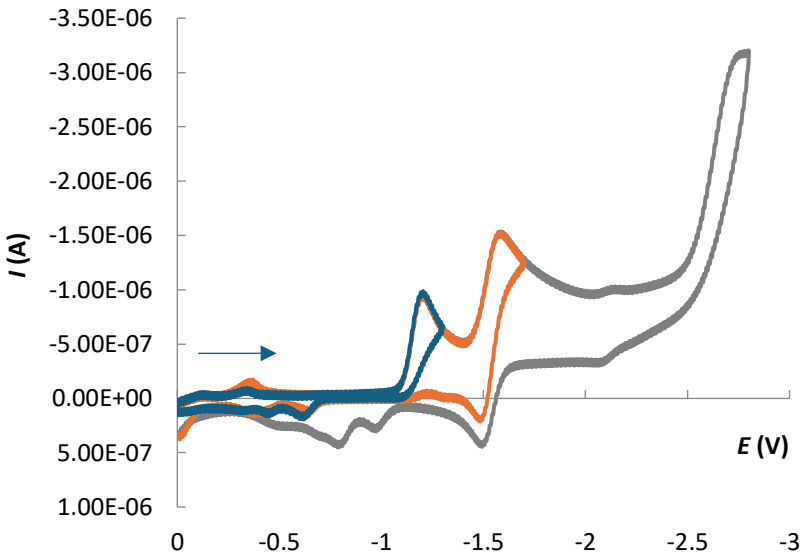

Fig. S67: Cyclic voltammogram (W = HMDE) of compound **8a** ($4.9 \cdot 10^{-4}$ M) in DMSO (0.1 M $TBAPF_6$) with scan rate 100 $mV \cdot s^{-1}$ (gradually increasing potential range).

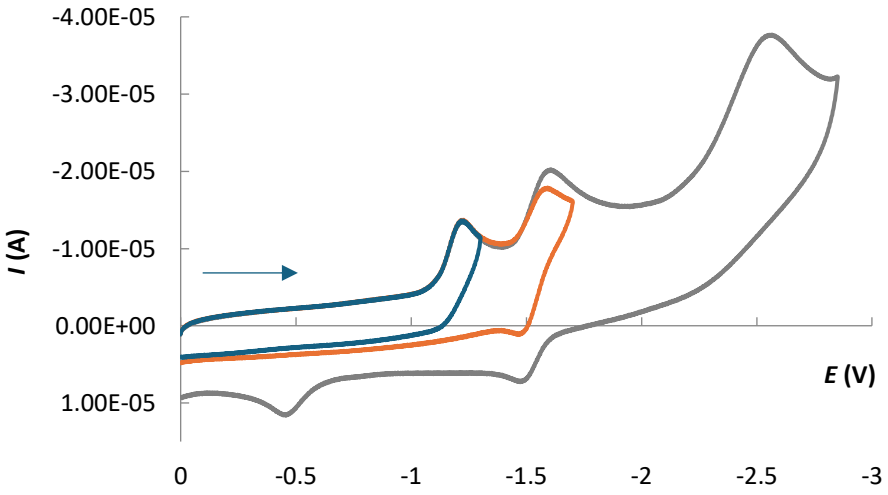

Fig. S68: Cyclic voltammogram (W = GC) of compound **8a** ($4.9 \cdot 10^{-4}$ M) in DMSO (0.1 M $TBAPF_6$) with scan rate 200 $mV \cdot s^{-1}$ (gradually increasing potential range).

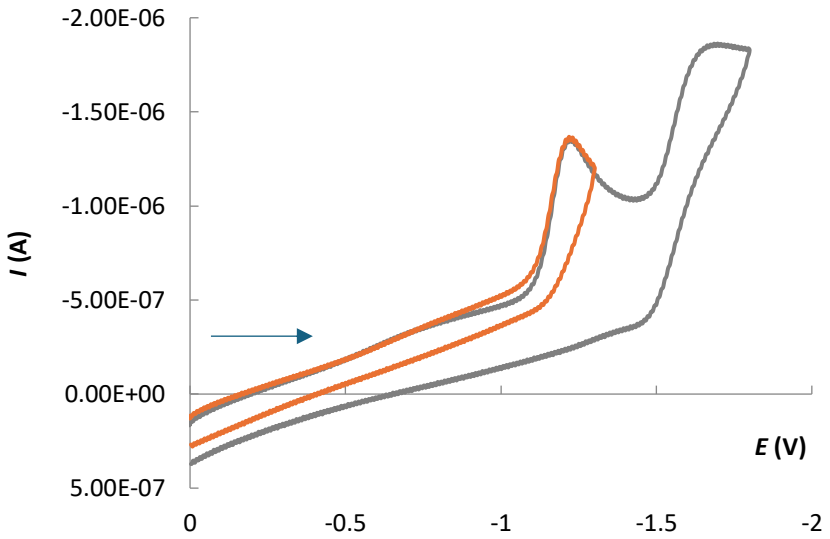

Fig. S69: Cyclic voltammogram (W = Pt) of compound **8a** ($4.9 \cdot 10^{-4}$ M) in DMSO (0.1 M $TBAPF_6$) with scan rate 100 $mV \cdot s^{-1}$ (gradually increasing potential range).

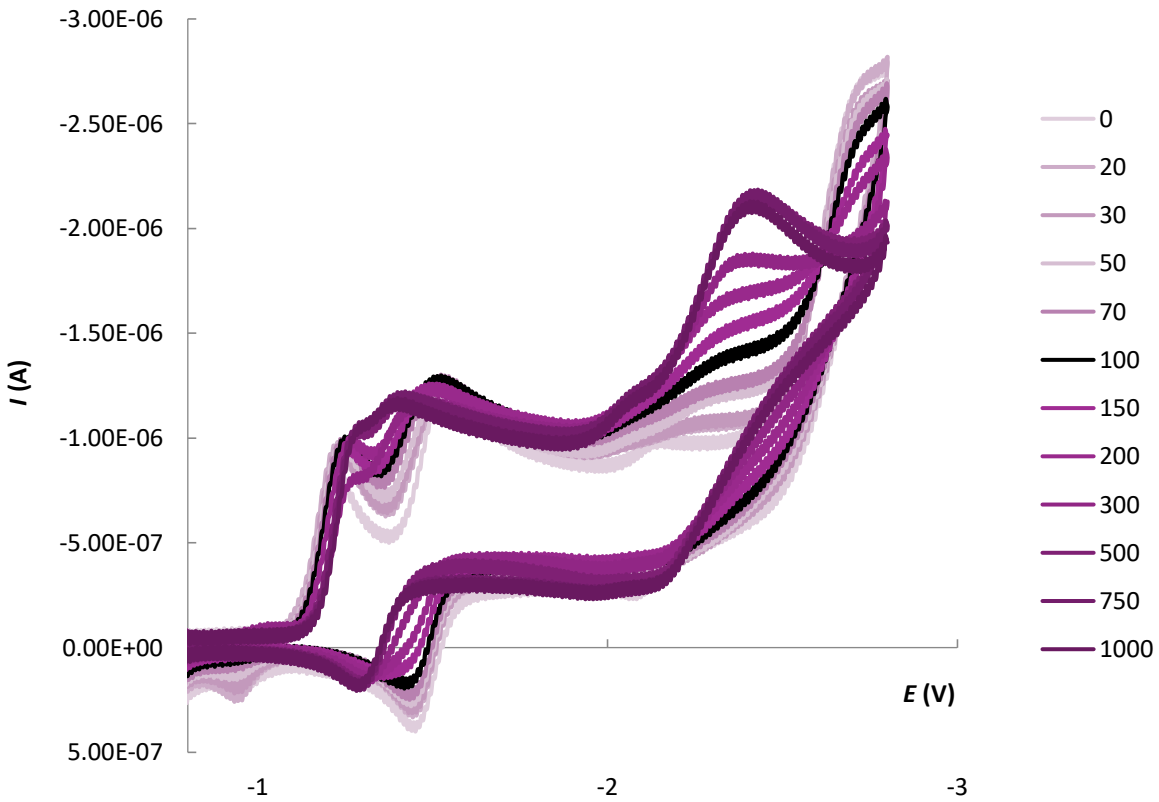

Fig. S70: Titration of **3a** ($8.9 \cdot 10^{-4}$ M) by $TBAH_2PO_4$ (final concentration 9.41 mM) in DMSO (0.1M TBAHPF) monitored by CV (W = HMDE) with scan rate 100 $mV \cdot s^{-1}$; black - with 1 molar equiv. of $H_2PO_4^-$.

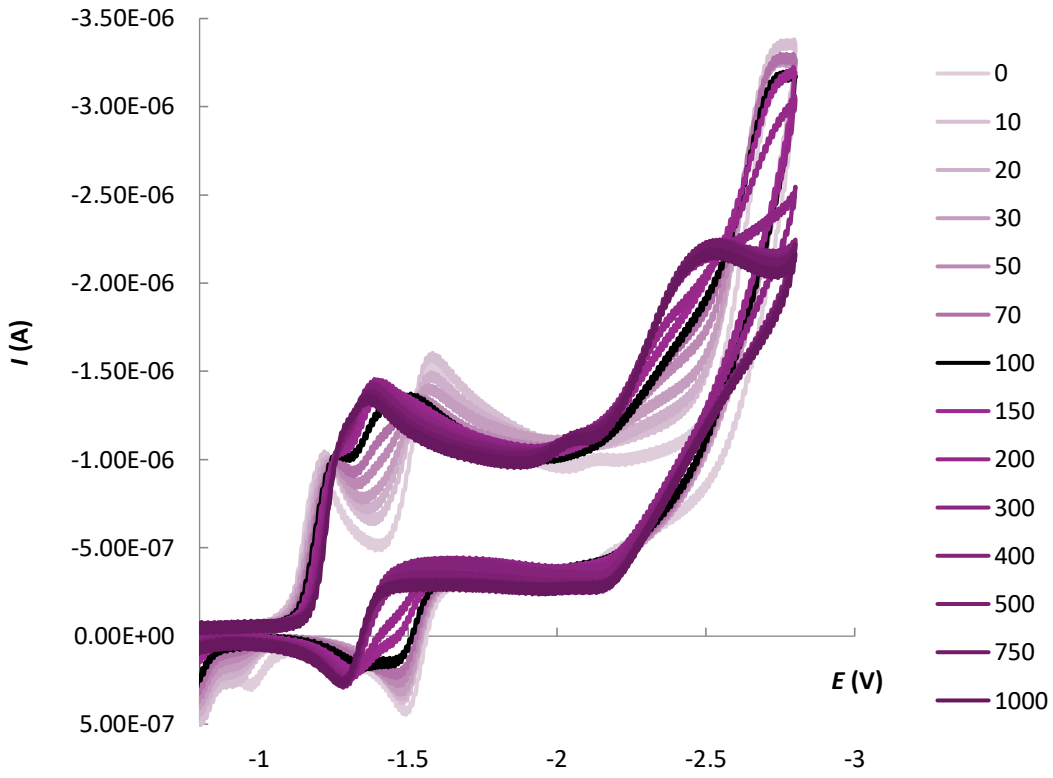

Fig. S71: Titration of **4** ($1.1 \cdot 10^{-3}$ M) by $TBAH_2PO_4$ (final concentration 11.8 mM) in DMSO (0.1M TBAHPF) monitored by CV (W = HMDE) with scan rate 100 $mV \cdot s^{-1}$; black - with 1 molar equiv. of $H_2PO_4^-$.

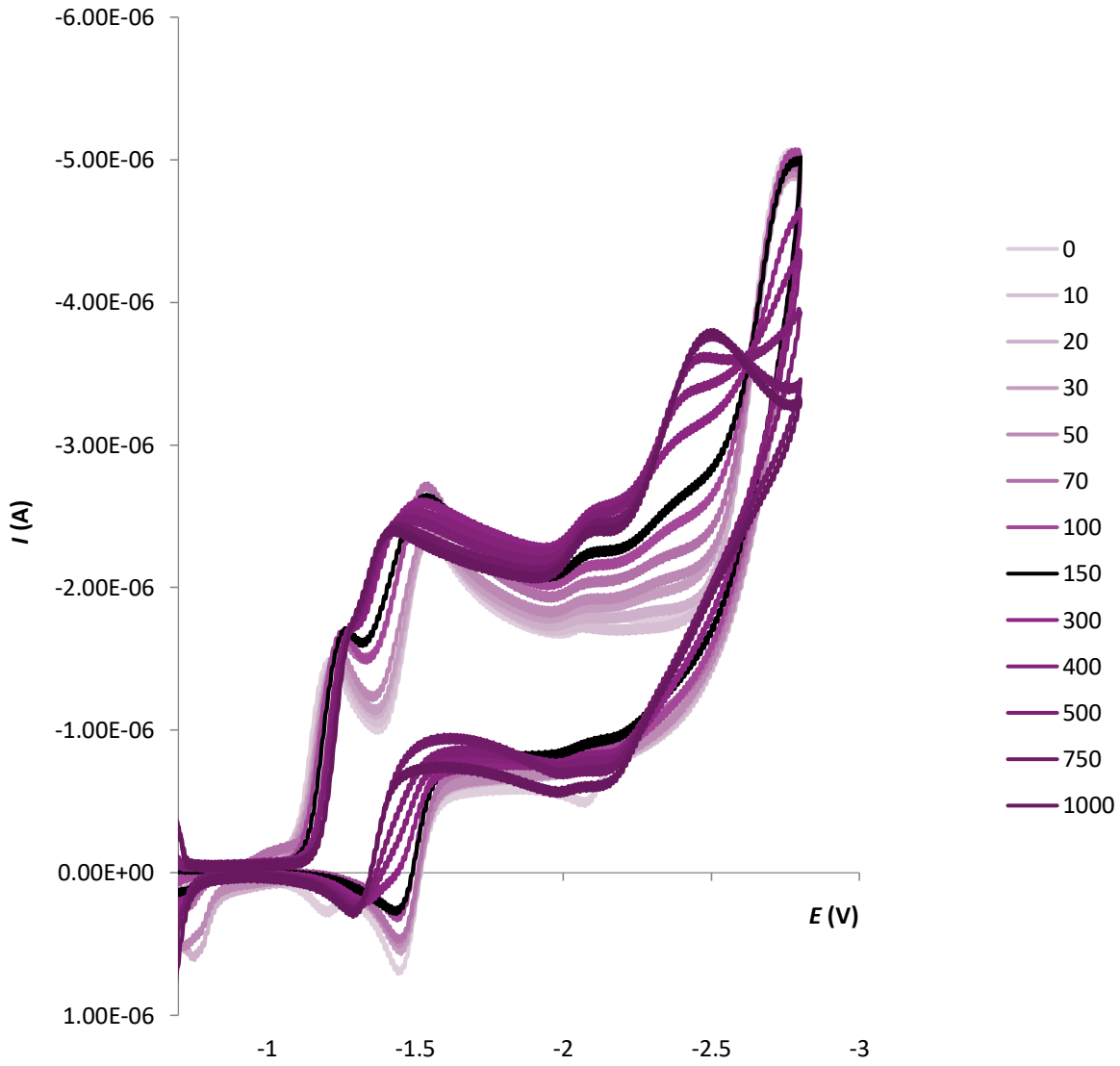

Fig. S72: Titration of **8a** ($8.6 \cdot 10^{-4}$ M) by $TBAH_2PO_4$ (final concentration 11.7 mM) in DMSO (0.1M TBAHPF) monitored by CV (W = HMDE) with scan rate 100 $mV \cdot s^{-1}$; black - with 2 molar equiv. of $H_2PO_4^-$.

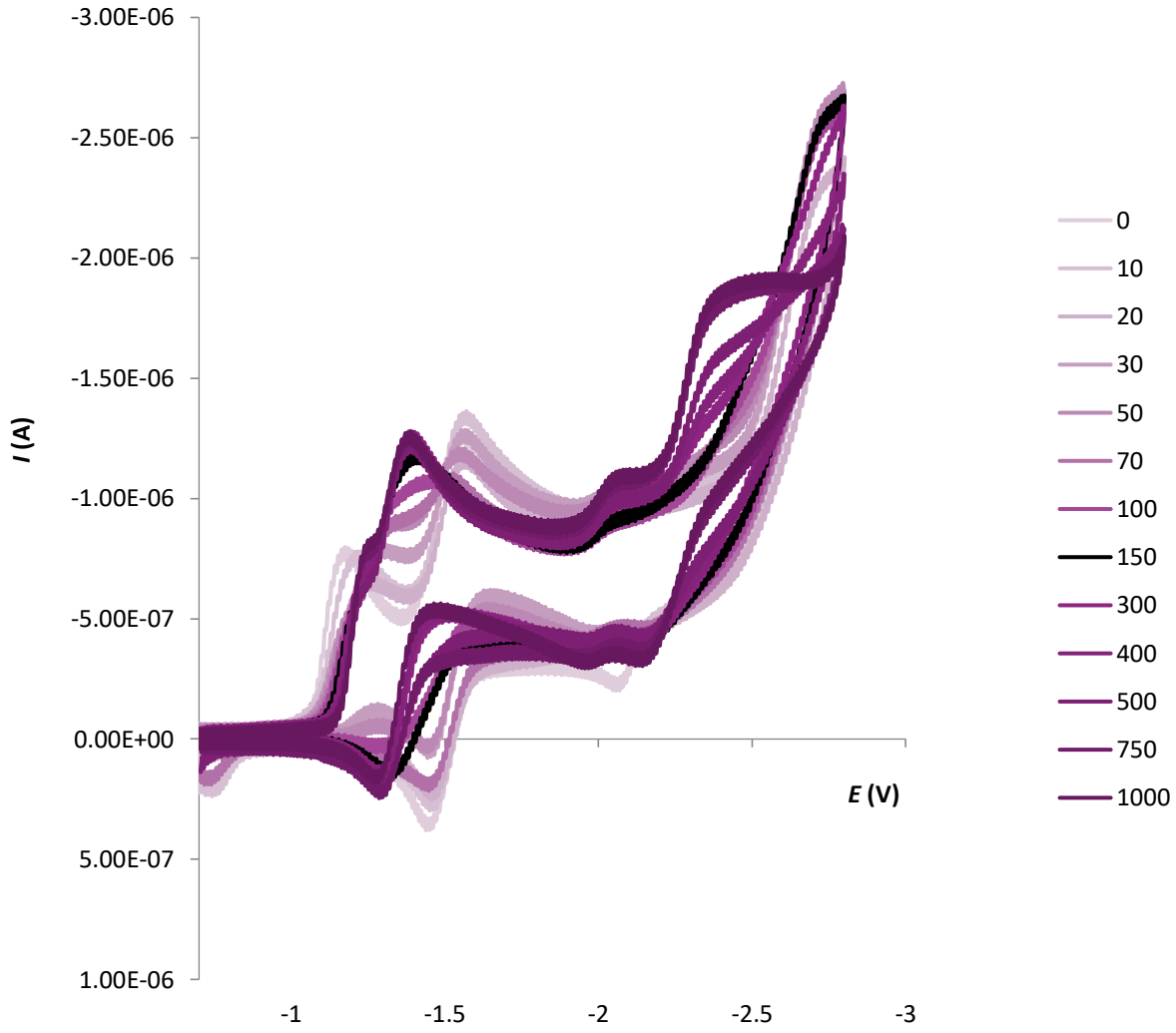

Fig. S73: Titration of **8a** ($4.9 \cdot 10^{-4}$ M) by $TBAH_2PO_4$ (final concentration 5.89 mM) in DMSO (0.1M TBAHPF) monitored by CV (W = HMDE) with scan rate 100 $mV \cdot s^{-1}$; black - with 2 molar equiv. of $H_2PO_4^-$.

7. Crystallographic data

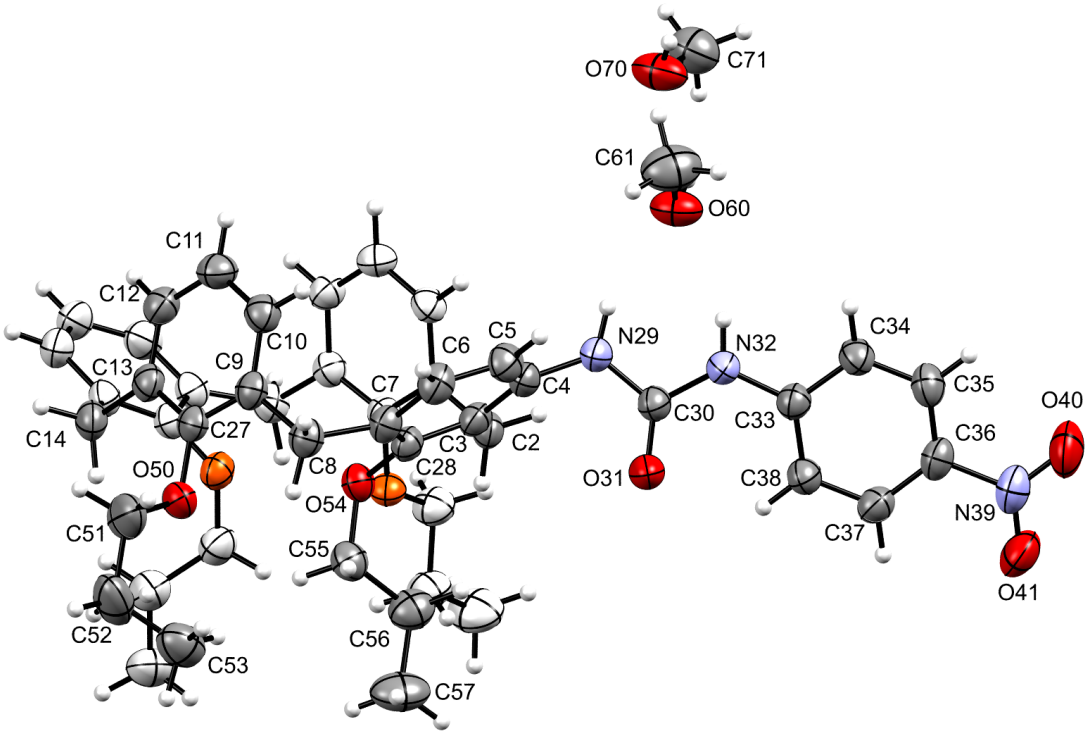

Fig. S74: Thermal ellipsoid plot (50% probability level) of compound **3a**.

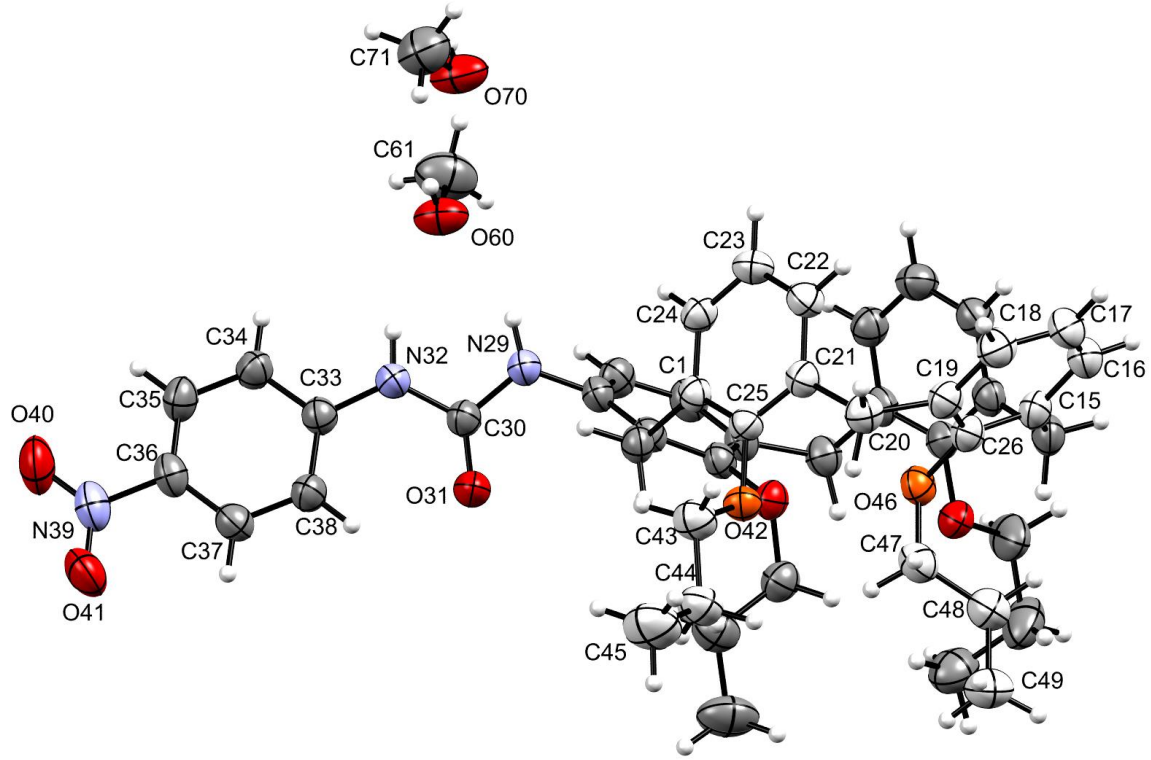

Fig. S75: Thermal ellipsoid plot (50% probability level) of compound **3a** - view from the opposite side (180 ° rotation).